

- I. THE CRYSTAL STRUCTURE OF POTASSIUM
BIS-(TRICYANOVINYL)AMINE
- II. NUCLEAR MAGNETIC RESONANCE STUDIES
OF ALKALI HALIDE SOLUTIONS
- III. ELUCIDATION OF THE INTRAMOLECULAR
HYDROGEN BOND IN ACETYLACETONE BY
THE DEUTERIUM ISOTOPE EFFECT ON THE
CHEMICAL SHIFT OF THE BRIDGE HYDROGEN

Thesis by

Leroy Lin

In Partial Fulfillment of the Requirements

For the Degree of

Doctor of Philosophy

California Institute of Technology

Pasadena, California

1968

(Submitted November 21, 1967)

ACKNOWLEDGEMENTS

This thesis would never have taken form without the generous assistance of many people. In particular, I should like to acknowledge my deep indebtedness to Dr. E. W. Hughes for his patient guidance of the first part of this thesis and to Dr. S. I. Chan for his help and guidance in the second and third part of this thesis. A number of valuable discussions were held with D. R. Dyroff, T. A. Beineke, R. E. Marsh, and R. T. Iwamasa. Financial support in various forms given to me by the California Institute of Technology, the National Science Foundation, and Shell Companies Foundation are gratefully acknowledged. Mention should also be made of the assistance of T. E. Burke, R. T. Iwamasa, J. H. Prestegard, J. H. Nelson, L. Lynds, B. W. Bangerter, D. Duchamp, and those people who wrote the Caltech CRYRM system. Finally, I would like to thank Mrs. E. McKoy for typing this thesis for me.

ABSTRACT

Part I

Potassium bis-(tricyanovinyl) amine, $K^+N[C(CN)=C(CN)_2]_2^-$, crystallizes in the monoclinic system with the space group Cc and lattice constants, $a = 13.346 \pm 0.003 \text{ \AA}$, $b = 10.191 \pm 0.001 \text{ \AA}$, $c = 8.992 \pm 0.003 \text{ \AA}$, $B = 114.42 \pm 0.02^\circ$, and $Z = 4$. Three dimensional intensity data were collected by layers perpendicular to b^* and c^* axes. The crystal structure was refined by the least squares method with anisotropic temperature factor to an R value of 0.064.

The average carbon-carbon and carbon-nitrogen bond distances in $-C-C\equiv N$ are $1.441 \pm 0.016 \text{ \AA}$ and $1.146 \pm 0.014 \text{ \AA}$ respectively. The bis-(tricyanovinyl) amine anion is approximately planar. The coordination number of the potassium ion is eight with bond distances from 2.890 \AA to 3.408 \AA . The bond angle C—N—C of the amine nitrogen is $132.4 \pm 1.9^\circ$. Among six cyano groups in the molecule, two of them are bent by what appear to be significant amounts (5.0° and 7.2°). The remaining four are linear within the experimental error. The bending can probably be explained by molecular packing forces in the crystals.

Part II

The nuclear magnetic resonance of ^{81}Br and ^{127}I in aqueous solutions were studied. The cation-halide ion interactions were studied by studying the effect of the Li^+ , Na^+ , K^+ , Mg^{++} , Cs^+ upon the line width of the halide ions. The solvent-halide ion interactions were studied by studying the effect of methanol, acetonitrile, and acetone upon the line width of ^{81}Br and ^{127}I in the aqueous solutions. It was found that the viscosity plays a very important role upon the halide ions line width. There is no specific cation-halide ion interaction for those ions such as Mg^{++} , Li^+ , Na^+ , and K^+ , whereas the Cs^+ - halide ion interaction is strong. The effect of organic solvents upon the halide ion line width in aqueous solutions is in the order acetone > acetonitrile > methanol. It is suggested that halide ions do form some stable complex with the solvent molecules and the reason Cs^+ has an unusually large effect upon the halide ion line width is mainly due to the effect that Cs^+ can replace one of the ligands in the solvent-halide ion complex.

Part III

An unusually large isotope effect on the bridge hydrogen chemical shift of the enol form of pentanedione-2, 4 (acetylacetone) and 3-methylpentanedione-2, 4 has been observed. An attempt has been made to interpret this effect. It is suggested from the deuterium isotope effect studies, temperature dependence of the bridge hydrogen chemical shift studies, IR studies in the OH, OD, and C=O stretch regions, and the HMO calculations, that there may probably be two structures for the enol form of acetylacetone. The difference between these two structures arises mainly from the electronic structure of the π -system. The relative population of these two structures at various temperatures for normal acetylacetone and at room temperature for the deuterated acetylacetone were calculated.

TABLE OF CONTENTS

PART	TITLE	PAGE
I	THE CRYSTAL STRUCTURE OF POTASSIUM BIS(TRICYANOVINYL)AMINE	1
	Introduction	2
	Experimental	3
	Determination and refinements of the structure	7
	Discussion	11
	References	23
	Appendix	24
II	NUCLEAR MAGNETIC RESONANCE STUDIES OF ALKALI HALIDE SOLUTIONS	27
	Introduction	28
	Experimental	37
	Results	39
	Discussion	64
	References	75
III	ELUCIDATION OF THE INTRAMOLECULAR HYDROGEN BOND IN ACETYLACETONE BY THE DEUTERIUM ISOTOPE EFFECT ON THE CHEMICAL SHIFT OF THE BRIDGE HYDROGEN	77
	Introduction	78
	Experimental	82

PART	TITLE	PAGE
	Materials	82
	Preparation	83
	Results and Discussions	84
	Deuterium isotope effect	84
	Temperature studies	96
	IR results	99
	Summary	106
	Model	108
	Estimation of ΔE_H^0 from temperature dependence of the bridge hydrogen chemical shift	111
	Potential function for the two enol structures and the estimation of isotope effect on the zero point energy	115
	Calculation of the deuterium isotope effect	123
	Molecular orbital calculations	124
	Conclusions	128
	References	129
PROPOSITIONS	131

PART I

The Crystal Structure of Potassium bis-(tricyanovinyl) amine

INTRODUCTION

Bis-(tricyanovinyl)amine, $\text{NH}[\text{C}(\text{CN})=\text{C}(\text{CN})_2]_2$, is a strong acid comparable in strength with the common inorganic acids. The configuration of the ion $\text{N}[\text{C}(\text{CN}=\text{C}(\text{CN})_2]_2^-$ is unknown and has been the subject of speculation. The $-\text{C}(\text{CN})=\text{C}(\text{CN})_2$ groups themselves are closely related to the interesting series of recently prepared compounds in which most or all of the hydrogen atoms of the parent compounds have been replaced by the cyano groups. It has therefore seemed desirable to determine the structure of a salt of the above acid.

EXPERIMENTAL

Crystals of the potassium salt of bis-(tricyanovinyl)amine were kindly supplied by Dr. D. W. Wiley of the Central Research Department, E. I. du Pont de Nemours & Company Incorporated. The material is dark brown in color and crystallizes in lathlike needles. The longest needle axis is the crystallographic c and the shortest needle thickness is the crystallographic a . Rotation and equi-inclination Weissenberg photographs taken with Cu K_{α} radiation showed the crystals to be monoclinic. A primitive unit cell was chosen with approximate parameters $a = 13.36 \text{ \AA}$, $b = 10.27 \text{ \AA}$, $c = 9.01 \text{ \AA}$, and $B = 114^{\circ}$. The values were later refined by least squares with data primarily from photographs of crystals rotated about the b and c axes, taken with copper radiation and using a precision Straumanis type Weissenberg camera. The final cell parameters, based on least squares fitting to 37 and 40 equatorial reflection from photographs of crystals rotated about the b and c axes respectively, are:

$$a = 13.346 \pm 0.003 \text{ \AA}$$

$$b = 10.191 \pm 0.001 \text{ \AA}$$

$$c = 8.992 \pm 0.003 \text{ \AA}$$

$$B = 114.42 \pm 0.02^{\circ}$$

The wavelengths used in the calculations are: $\text{Cu K}_{\alpha_1} = 1.54051 \text{ \AA}$, $\text{Cu K}_{\alpha_2} = 1.54433 \text{ \AA}$, $\text{Cu K}_{\alpha(\text{weighted average})} = 1.5418 \text{ \AA}$. The observed extinctions; hkl when $h + k$ is odd, $h0l$ when l is odd,

showed that the space group is either Cc or C2/c. Intensity statistics (1) indicated that the space group is Cc (see Figure 1). The density of the crystal was measured by a floatation method with mixtures of chloroform and bromoform solution. The measured density is 1.543 g/cm³ and the calculated density is 1.543 g/cm³ with Z = 4.

Multiple-film equi-inclination Weissenberg photographs were taken with Cu K_α radiation for layer lines 0 through 9 about the b axis and for layer lines 0 through 2 about the c axis. The intensities were estimated visually by comparison with intensity strips prepared from the same two crystals. The film factor k of any set of films with equi-inclination angle μ is related to the film factor k_0 at normal incidence by

$$k = (k_0)^{\sec \mu} \quad (1)$$

Empirical film factors were obtained by averaging estimated intensities for each pair of adjacent films in all sets and were corrected to normal incidence of the x-ray beam by equation (1). The weighted average of these factors gave a film factor for normal incidence of 3.657. This factor, raised to $\sec \mu$ power for any layer line set, was then used to relate the intensities on all films within the set to the first film of the set.

The crystals used in the structure determination had all cross sections less than 0.15 mm in maximum dimension. Only Lorentz and polarization corrections are necessary (in the later refinement it was found that the extinction correction was negligible). The

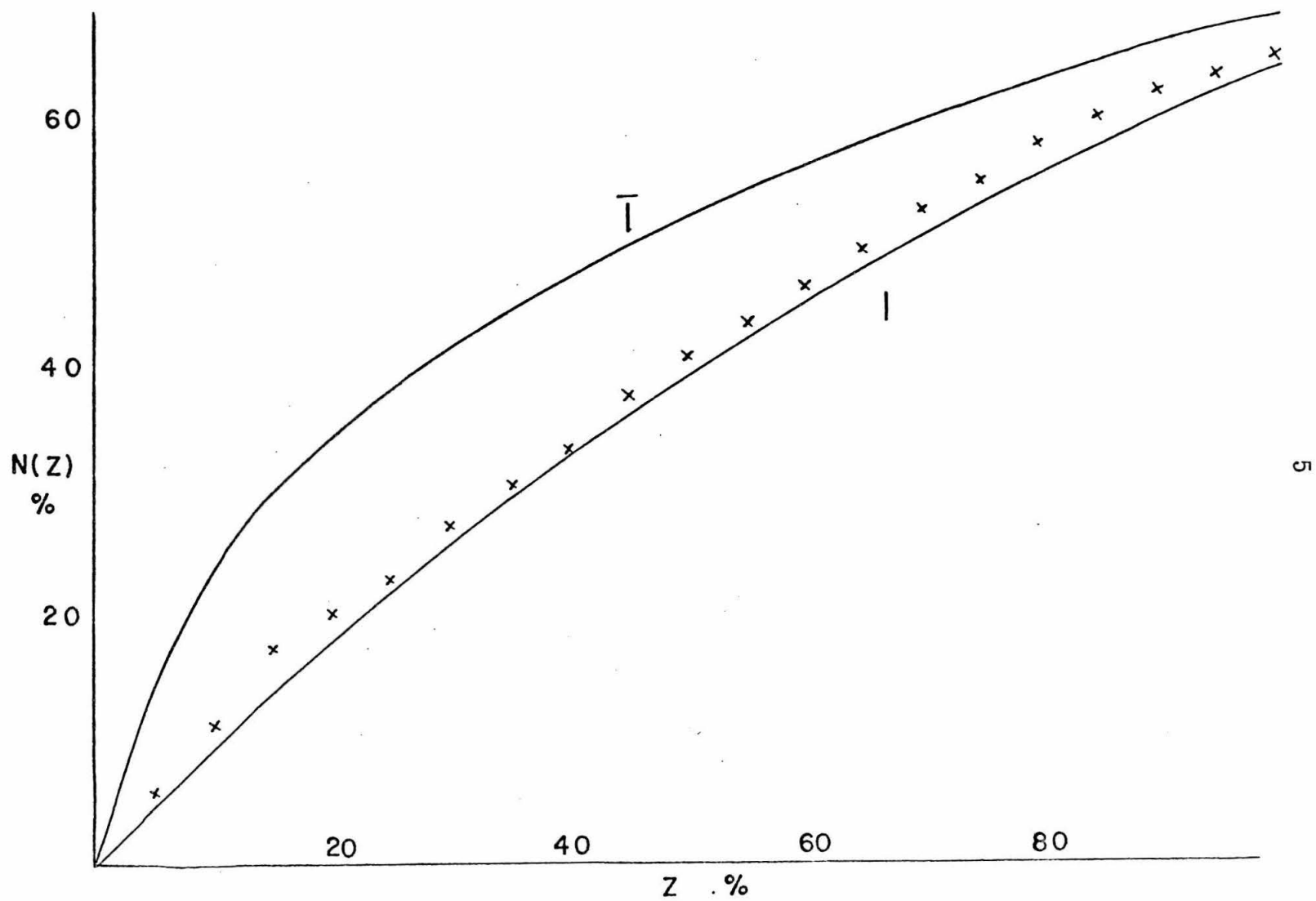


Fig. 1 Intensity distribution curve

intensities were corrected for L. P. effects and compared with values obtained by oscillation about the other axis to obtain correction factors for the various exposure times. Finally, F^2 values were obtained on an arbitrary scale by taking weighted averages of the values observed about the two axes. Altogether, 953 reflections were collected from the possible 1400 reflections; of these, eight may need extinction corrections, 77 were too faint to observe and only 868 reflections entered into the least squares cycles in the final refinement (see notes in the appendix). The final results are listed in the appendix.

DETERMINATION AND REFINEMENT OF THE STRUCTURE

The x and z coordinates of potassium ion were arbitrarily assigned to be 0.5000 and 1.0000 respectively. The y coordinate of the potassium ion was readily determined from a three-dimensional unsharpened Patterson function. But the positions of light atoms (carbons and nitrogens) could not be deduced in this way. A sharpened three-dimensional Patterson with the origin removed was then calculated. Atomic positions of one $-\text{C}(\text{CN})=\text{C}(\text{CN})_2$ group were found. With these atomic positions structure factors and a three-dimensional electron density map were calculated. The remaining atomic positions became apparent; the anion was indeed approximately planar and the ionic plane was approximately parallel to $(\bar{2}10)$.

The trial structure was first refined through five least squares cycles on the 7094 computer with individual isotropic temperature factors. The R value was then 0.138. (The R value is given by

$$R = \frac{\sum ||F_{\text{obs}}| - |F_{\text{cal}}||}{\sum |F_{\text{obs}}|} \quad \text{the sum being over the observed reflections,}$$

The quantity minimized in the least squares calculations is

$$\sum w (|F_{\text{obs}}|^2 - |F_{\text{cal}}|^2)^2 \quad \text{with weights given from the initial data}$$

processing program. The values of atomic scattering factors used in the calculations are listed in the International Table for X-ray Crystallography (2). Five least squares cycles with anisotropic temperature factors

$$\exp [- (B_{11}h^2 + B_{22}k^2 + B_{33}\ell^2 + B_{12}hK + B_{13}h\ell + B_{23}k\ell)]$$

included in the refinement, were calculated next. Only the real part of the dispersion correction of potassium ion was considered ($\Delta f' = 0.3$)². The R value dropped from 13.8% to 6.78%. Finally, the weighting function was changed to

$$\sqrt{w} = \frac{1}{R + S |F_{\text{obs}}| + T |F_{\text{obs}}|^2 + U |F_{\text{obs}}|^3}$$

where R, S, T, and U were obtained by fitting the curve

$$|F_{\text{obs}}|^2 - |F_{\text{cal}}|^2 = R + S |F_{\text{obs}}| + T |F_{\text{obs}}|^2 + U |F_{\text{obs}}|^3$$

using the values of F_{obs} and F_{cal} from the last least squares calculation. They are: $R = 3882$, $S = 716.0$, $T = 756.8$, $U = -7.046$.

Seven more least squares were run. The final R value was 0.064 for a total of 868 reflections. The mean shift in the last cycle for coordinates and anisotropic temperature B_{ij} were 0.0004 Å and 0.00004 Å respectively. The maximum shift in the last cycle for coordinates and temperature factors, B_{ij} , were 0.0013 Å and 0.00036 respectively. The coordinates and anisotropic temperature factors as well as their standard deviations are listed in Tables I and II respectively. The calculated and observed $|F|$ values are listed in the appendix.

Table I. Atomic Coordinates $\times 10^4$

Atom	x/a	σ_x/a	y/b	σ_y/b	z/c	σ_z/c	σ^{**}
N(1)	4978	09	0248	10	7298	13	19
N(2)	5809	10	3318	13	8436	15	23
N(3)	8000	12	0640	12	12437	15	23
N(4)	6330	12	-2358	13	10048	18	26
N(5)	4365	11	-3113	11	6361	17	24
N(6)	2030	11	-1129	13	2314	19	26
N(7)	3585	12	2514	13	4527	21	28
C(8)	6403	09	1039	10	9667	13	19
C(9)	6079	09	2305	11	8971	16	22
C(10)	7300	10	0799	14	11203	16	24
C(11)	5805	08	-0011	11	8720	13	20
C(12)	6096	09	-1294	11	9425	14	20
C(13)	3508	08	0028	09	4780	13	18
C(14)	7507	09	1426	10	4604	16	21
C(15)	2702	11	-0688	15	3453	17	26
C(16)	4289	09	-0512	10	6148	14	20
C(17)	4320	10	-1982	13	6271	17	24
K ⁺ (18)*	5000		-4657	01	10000		

* Coordinates x and z of K⁺ were arbitrarily assigned to be 0.5000 and 1.0000 respectively.

** Standard deviations of atomic positions in Å

Table II. Final Thermal Parameters*

Atom	B_{11}^*	B_{22}	B_{33}	B_{12}	B_{13}	B_{23}
N(1)	.0060(04)	.0117(14)	.0166(16)	-.0047(13)	.0030(14)	-.0099(23)
N(2)	.0091(08)	.0121(12)	.0173(16)	.0032(14)	.0026(19)	-.0005(21)
N(3)	.0106(09)	.0133(13)	.0190(20)	-.0052(17)	-.0074(23)	.0065(24)
N(4)	.0104(09)	.0133(13)	.0241(25)	-.0085(17)	.0095(24)	-.0002(27)
N(5)	.0097(09)	.0096(11)	.0244(21)	.0024(13)	.0054(22)	.0100(23)
N(6)	.0090(09)	.0162(16)	.0209(19)	-.0007(17)	-.0035(22)	-.0111(28)
N(7)	.0113(10)	.0113(12)	.0295(28)	-.0059(17)	.0155(28)	.0004(27)
C(8)	.0068(06)	.0087(09)	.0128(14)	-.0014(12)	.0031(17)	.0022(19)
C(9)	.0074(08)	.0090(11)	.0164(17)	.0014(13)	.0073(19)	.0028(22)
C(10)	.0055(07)	.0117(12)	.0156(17)	-.0018(14)	-.0038(20)	-.0021(22)
C(11)	.0057(06)	.0079(10)	.0146(15)	-.0029(11)	.0028(18)	-.0022(19)
C(12)	.0075(08)	.0089(10)	.0148(17)	-.0031(12)	.0045(19)	-.0016(20)
C(13)	.0069(06)	.0077(08)	.0151(13)	-.0009(10)	.0059(16)	.0002(17)
C(14)	.0065(06)	.0092(11)	.0186(17)	-.0036(12)	.0060(18)	.0030(22)
C(15)	.0076(09)	.0115(11)	.0194(20)	-.0040(15)	.0111(23)	-.0073(23)
C(16)	.0069(07)	.0077(09)	.0148(14)	-.0011(13)	.0076(16)	-.0040(20)
C(17)	.0074(08)	.0125(14)	.0184(19)	.0041(14)	.0095(22)	.0047(25)
K ⁺ (18)	.0077(01)	.0055(01)	.0172(03)	-.0003(02)	.0046(03)	-.00007(05)

*The figures in parentheses are standard deviations multiplied by 10^4

DISCUSSION

Bond distances and bond angles of bis-(tricyanovinyl)amine ion are shown in Figure 2 and given in Tables III and IV. The standard deviation of a bond distance between atoms 1 and 2 (σ_{12}) and the standard deviation of a bond angle between atoms 2, 1, and 3 (σ_{213}) were calculated from the following equations (3):

$$\sigma_{12}^2 = \sigma_1^2 + \sigma_2^2$$

$$\sigma_{213}^2 = \frac{\sigma_2^2}{S_{12}^2} + \frac{\sigma_3^2}{S_{13}^2} + \sigma_1^2 \left(\frac{1}{S_{12}^2} + \frac{1}{S_{13}^2} - \frac{2}{S_{12}S_{13}} \cos \angle 213 \right)$$

where σ_n is the standard deviation of atom n

S_{mn} is the bond distance between atoms m and n.

The normal of the mean ionic plane has direction cosines -0.8985, 0.0682, and 0.7661 with respect to the real crystallographic axes a, b, and c. The distances between atoms and the mean ionic plane are given in parentheses in Figure 2.

Bond angles and distances of some compounds containing the $-\text{C}\equiv\text{N}$ group are given in Table V. The average carbon-carbon and carbon-nitrogen bond distances in $-\text{C}-\text{C}\equiv\text{N}$ in this compound are 1.441 Å and 1.146 Å respectively. These values check well with the values found by Kornblau and Hughes for hexacrylonitrile (see Table V).

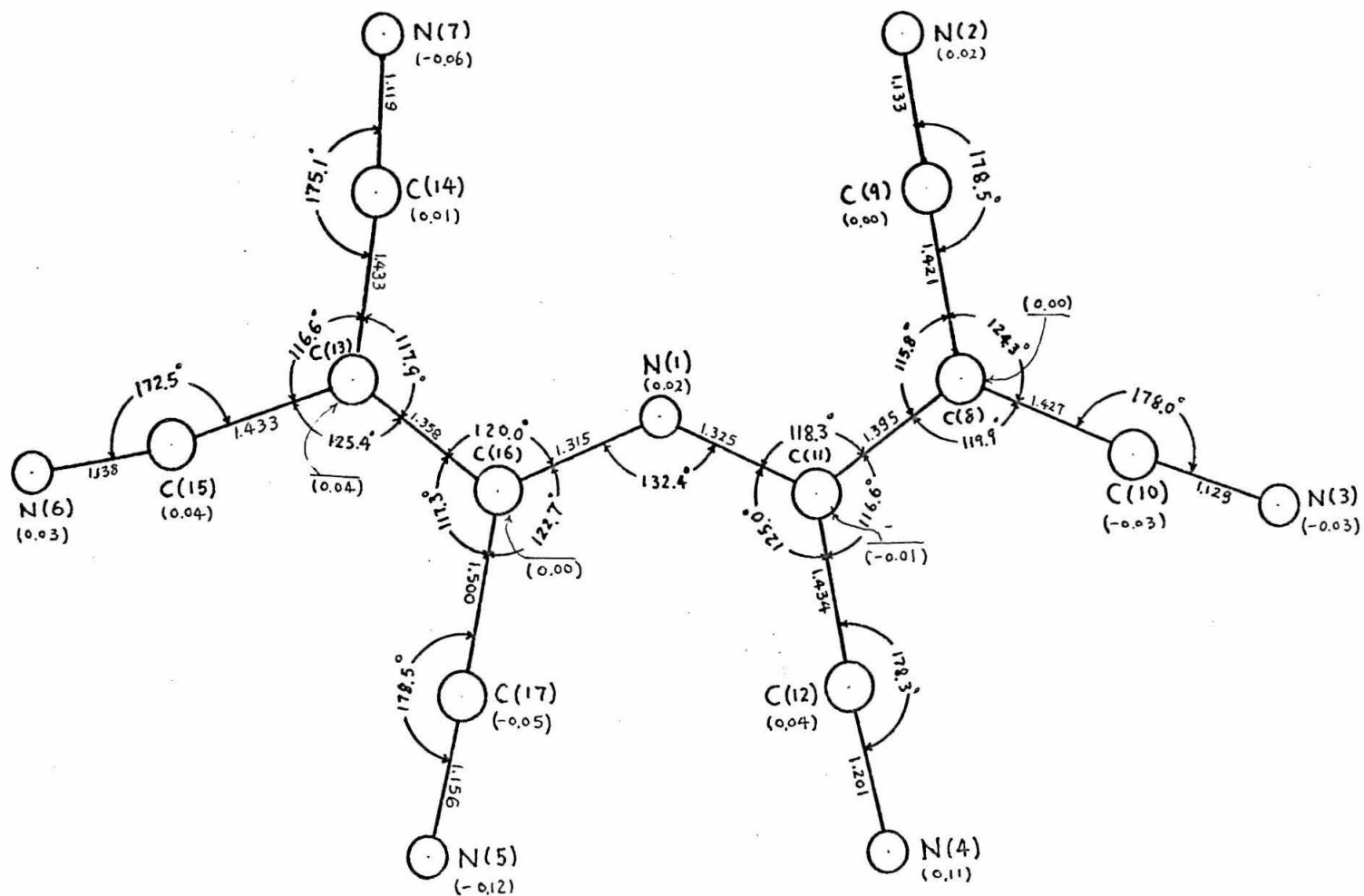


Fig. 2 Projection of the ion on the mean anionic plane
(Figures in parentheses are heights in Å of atoms above the plane.)

Table III. Some Intraionic Bond Distances in $N[C_2(CN)_3]_2^-$

Atom	Atom	value(\AA)*	Atom	Atom	Value(\AA)**
N(1)	C(11)	1.325(27)	N(1)	C(9)	2.643
N(1)	C(16)	1.315(30)	N(1)	C(14)	2.689
N(2)	C(9)	1.133(32)	C(10)	C(12)	2.750
N(3)	C(10)	1.129(35)	C(12)	C(17)	2.931
N(4)	C(12)	1.201(33)	C(15)	C(17)	2.881
N(5)	C(17)	1.155(34)	N(5)	N(6)	4.203
N(6)	C(15)	1.138(37)	N(4)	N(5)	3.358
N(7)	C(14)	1.119(36)	N(3)	N(4)	3.868
C(8)	C(9)	1.421(29)	N(1)	N(2)	3.335
C(8)	C(10)	1.427(31)	N(1)	N(7)	3.342
C(8)	C(11)	1.395(27)	N(4)	C(10)	3.463
C(11)	C(12)	1.434(28)	N(4)	C(17)	3.368
C(13)	C(14)	1.433(28)	N(5)	C(12)	3.332
C(13)	C(15)	1.433(32)	N(6)	C(14)	3.398
C(13)	C(16)	1.358(27)	N(7)	C(16)	3.374
C(16)	C(17)	1.501(31)	C(12)	C(16)	3.043

* The figures in parentheses are standard deviations multiplied by 10^3 .

** The standard deviation for the non-bonded distances is about 0.03 \AA .

Table IV. Some Bond Angles in $\text{N}[\text{C}_2(\text{CN})_3]_2^-$

Atom	Atom	Atom	Value	Standard deviation
C(11)	N(1)	C(16)	132.4 ^o	1.9 ^o
C(9)	C(8)	C(10)	124.3	1.9
C(10)	C(8)	C(11)	119.9	1.8
N(2)	C(9)	C(8)	178.5	3.2
N(3)	C(10)	C(8)	178.0	2.5
C(12)	C(11)	N(1)	125.0	1.8
C(12)	C(11)	C(8)	116.0	1.7
N(1)	C(11)	C(8)	118.3	1.8
N(4)	C(12)	C(11)	178.3	2.3
C(14)	C(13)	C(15)	116.6	1.8
C(14)	C(13)	C(16)	117.9	1.8
C(15)	C(13)	C(16)	125.4	1.9
N(7)	C(14)	C(13)	175.1	2.2
N(6)	C(15)	C(13)	172.5	2.9
C(17)	C(16)	N(1)	122.7	1.9
C(17)	C(16)	C(13)	117.3	1.8
N(1)	C(16)	C(13)	120.0	1.9
N(5)	C(17)	C(16)	178.5	2.5

Table V. Bond Angles and Distances of Some
Compounds Containing Cyano Group

Reference	Compound	$\text{-C}\equiv\text{N}$	C—C in ($\text{-C-C}\equiv\text{N}$)	Bond Angle $\text{X-C}\equiv\text{N}$
4	$\text{N}\equiv\text{C-C}\equiv\text{N}$	$1.13. \overset{\circ}{\text{A}}$		179.4°
5	$\text{P}(\text{CN})_3$	1.124		170.7
		1.165		171.9
		1.158		172.2
6	$\text{Pb}(\text{CN}_2)$	1.25		
		1.17		
7		1.158	1.45-1.46	
8	$(\text{CO})_4(\text{CH}_2=\text{CH-CN})\text{Fe}$	1.20	1.45	178
9	Hexacrylonitrile	1.110	1.503	177.7
		1.146	1.458	178.8
		1.112	1.471	178.5
10	Potassium dicyano guanidine	1.158		175.0
		1.186		175.9
11	Dicyandiamide (cyanoguanidine)	1.22		180
	This work	1.146 ± 0.014	1.441 ± 0.016	

Figures 3 and 4 show how the ions are packed. There are six potassium ions around the bis-(tricyanovinyl)amine anion. The eight shortest bond distances between the potassium ion and atoms of the anions are shown in Figure 3 and Figure 5. The average van der Waals bond distances between potassium ion and nitrogen atoms is 3.00 Å. This value checks well with the values found by Takie and Hughes (10) (3.07 Å, 2.93 Å, 3.19 Å, and 2.91 Å) for potassium dicyanoguanidine. But it is a little larger than the value as given by Pauling (12) (van der Waals radii for nitrogen atom and potassium ion are 1.5 Å and 1.33 Å respectively). The interionic bond distances are given in Table VI. Some interesting bond angles of the anion are qualitatively explained as follows: (1) Two cyano groups, [C(12)≡N(4) and C(17)≡N(5)], are twisted out of the ionic plane in opposite directions by very significant amounts. This reduces the repulsive forces between the groups, which are chiefly those between atoms C(12) and C(17). The same repulsive forces also make angles N(1)-C(16)-C(17), N(1)-C(11)-C(12), and C(16)-N(1)-C(11) larger than 120°. (2) Forces acting upon atom N(6) from atoms C(9)^I, C(10)^I, N(4)^G, and K⁺(18)^H push it towards the +y direction and make the bond angle N(6)≡C(15)-C(13) 7.5° less than 180°, and the angle C(15)-C(13)-C(16) larger than 120°. (3) Forces acting upon atoms N(7) and C(14) from atoms N(2)^H, C(9)^H, C(8)^H, C(10)^H, and K⁺(18) push atom N(7) away from the ionic plane and make the bond angle N(7)≡C(14)-C(13) 4.9° less than 180°. (4) Forces acting upon atoms N(2) and C(9) from atoms N(6)^F, N(7)^D, C(14)^D, and K⁺(18) push atoms N(2) and C(9) towards

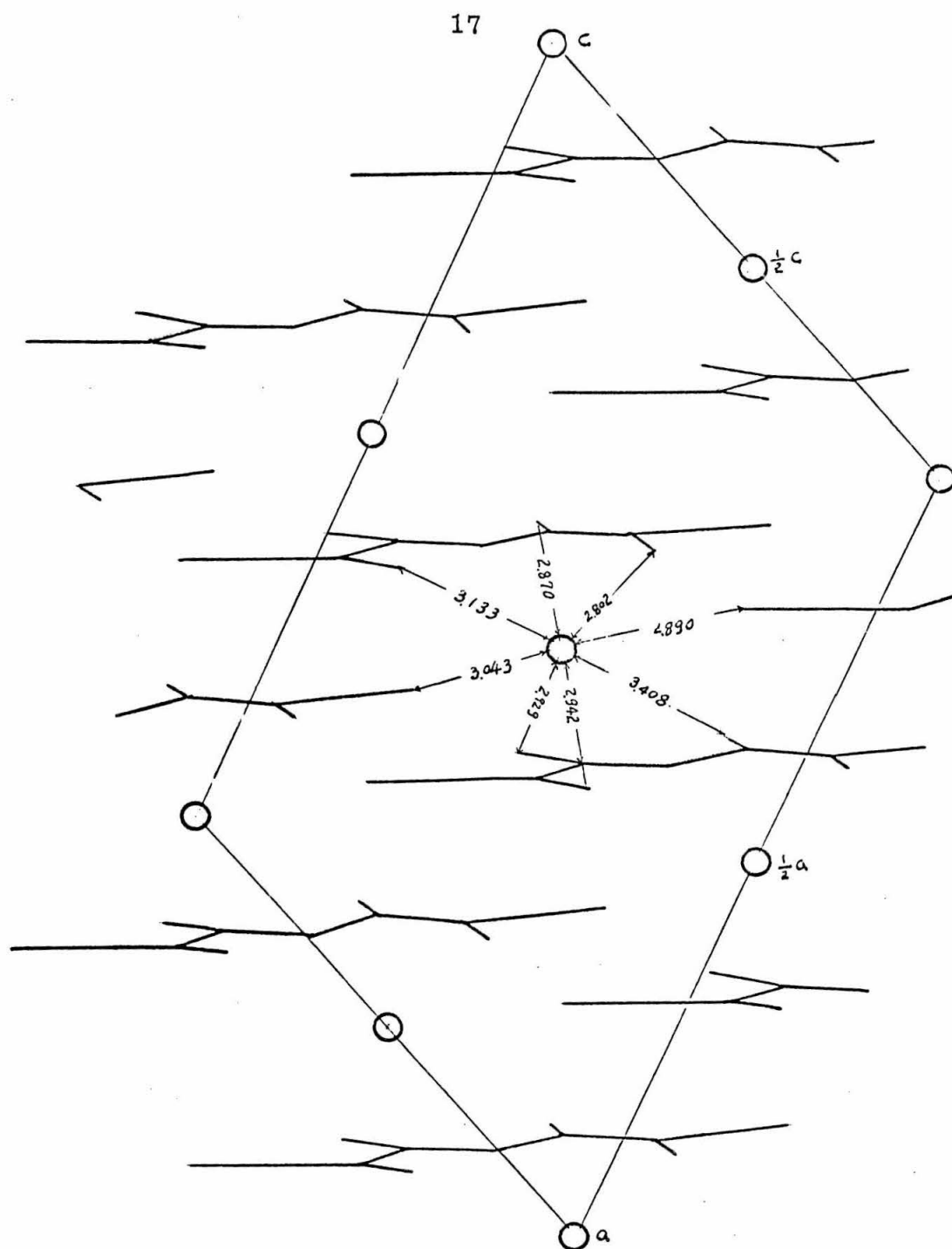


Fig. 3 Structure viewed along the b axis

○ indicates the potassium ion

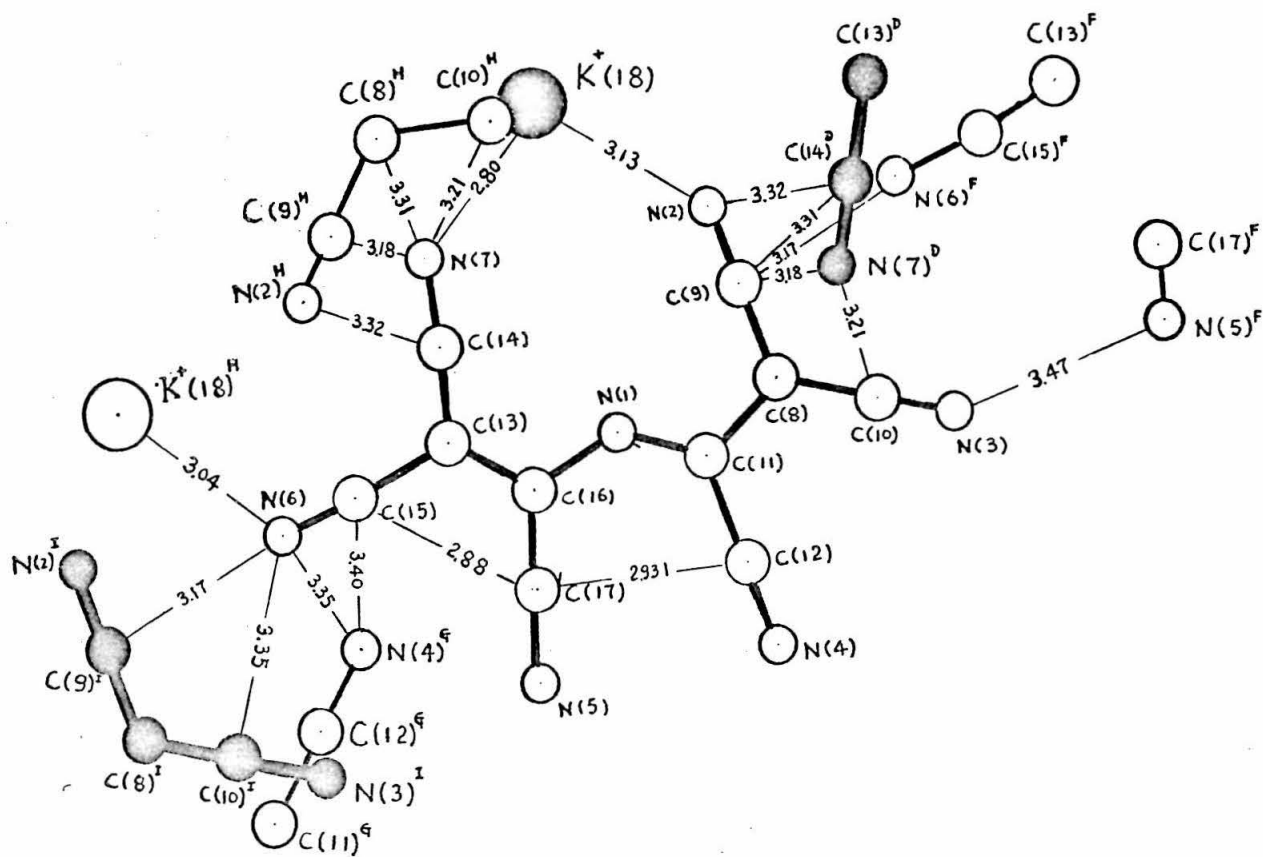


Fig. 4 Perpendicular projection onto the plane of the central anion

- indicates atoms below the ionic plane
- indicates atoms above the ionic plane

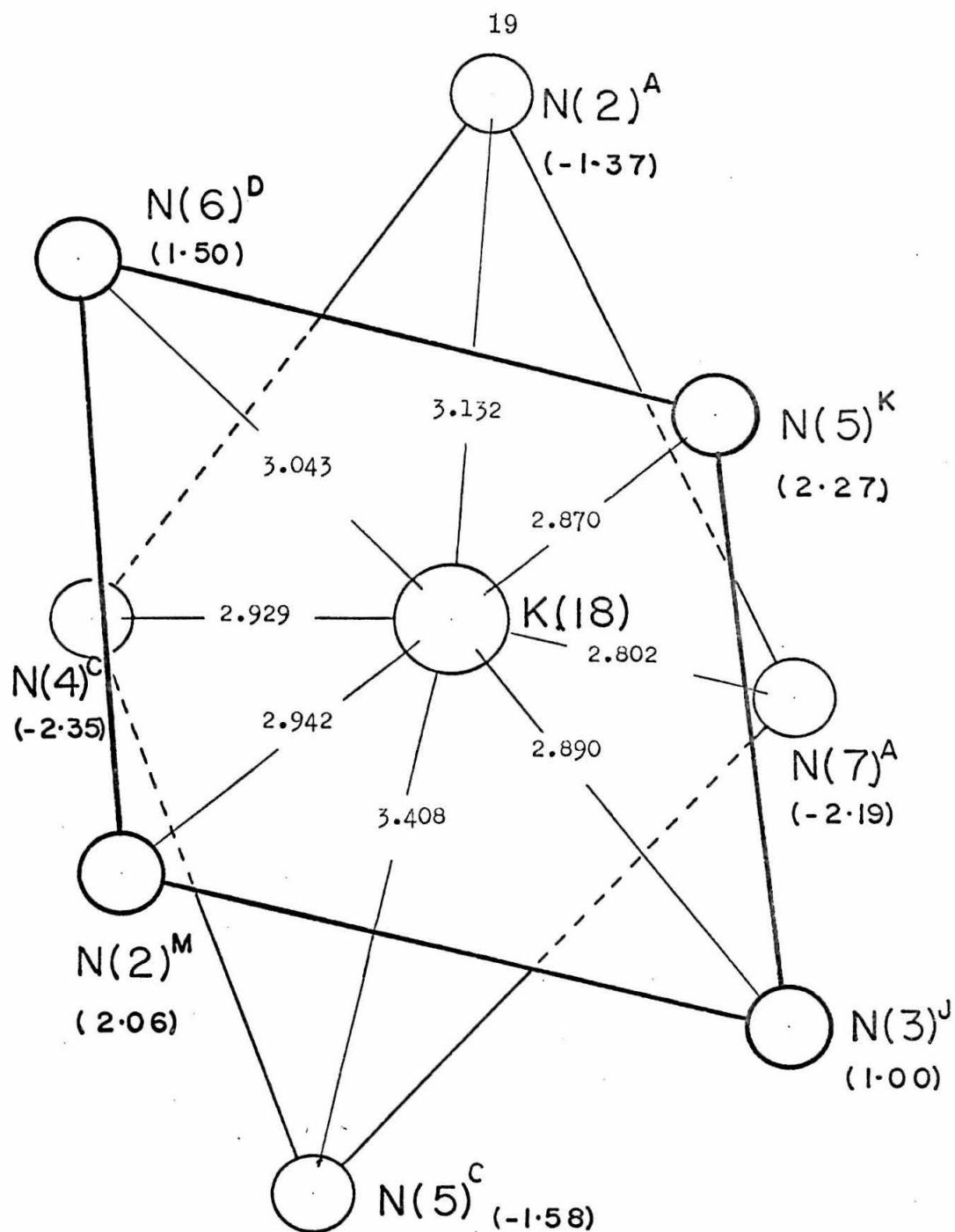


Figure 5

Coordination around a potassium ion, viewed along the b axis.
(Figures in parentheses show the heights in Å above the plane of
the potassium ion)

Table VI. Closest Interionic Bond Distances*

Atom	Atom	Dist.(Å)	Atom	Atom	Dist.(Å)
N(1) ^C	C(13)	3.540	C(12) ^C	N(7)	3.610
N(1) ^C	C(14)	3.798	C(12) ^C	C(14)	3.526
N(1) ^C	C(15)	3.621	C(13) ^C	N(6)	3.748
N(3) ^C	C(11)	3.623	C(14) ^C	N(6)	3.727
N(3) ^C	C(12)	3.723	C(16) ^C	C(14)	3.780
N(4) ^C	N(2)	3.532	C(16) ^C	C(15)	3.729
N(4) ^C	N(7)	3.500	C(17) ^C	N(7)	3.493
N(4) ^C	C(9)	3.680	C(17) ^C	C(14)	3.628
N(4) ^C	C(14)	3.744	N(5) ^E	N(3)	3.513
N(5) ^C	N(7)	3.465	N(5) ^E	N(4)	3.751
C(8) ^C	C(16)	3.623	N(6) ^E	N(4)	3.345
C(8) ^C	C(17)	3.747	N(6) ^E	N(5)	3.386
C(9) ^C	C(17)	3.729	N(6) ^E	C(12)	3.744
C(10) ^C	N(1)	3.773	C(15) ^E	N(4)	3.397
C(10) ^C	C(11)	3.673	C(17) ^E	N(4)	3.736
C(11) ^C	C(13)	3.567	N(2) ^D	N(3)	3.633
C(11) ^C	C(14)	3.758	N(6) ^D	N(2)	3.639
C(11) ^C	C(16)	3.576	N(7) ^D	N(2)	3.523
C(12) ^C	N(1)	3.636	N(7) ^D	N(3)	3.562
C(12) ^C	K ⁺ (18)	3.844	N(7) ^D	C(8)	3.313
C(17) ^C	K ⁺ (18)	4.121	N(7) ^D	C(9)	3.177

21
Table VI (continued)

Atom	Atom	Dist.(Å)	Atom	Atom	Dist.(Å)
N(7) ^D	C(10)	3.210	N(6) ^F	C(10)	3.351
C(13) ^D	N(2)	3.699	N(6) ^F	C(8)	3.613
C(14) ^D	N(2)	3.319	N(7) ^N	N(3)	3.616
C(14) ^D	C(9)	3.313	N(3) ^J	N(7)	3.616
C(15) ^D	N(2)	3.492	C(9)	K ⁺ (18)	4.039
C(15) ^D	K ⁺ (18)	3.807	C(14)	K ⁺ (18)	3.788
N(5) ^F	N(3)	3.474	C(17) ^K	K ⁺ (18)	3.837
N(6) ^F	N(2)	3.231	C(10) ^J	K ⁺ (18)	3.978
N(6) ^F	N(3)	3.523	C(9) ^M	K ⁺ (18)	3.670
N(6) ^F	C(9)	3.169			

* Absence of a superscript indicates an atom in the molecule at (x,y,z) with parameters listed in Table I. A superscript indicates a symmetry-related atom according to the following code: B, (x, -y, z+1/2); C, (x, -y, z-1/2); D, (x+1/2, -y+1/2, z+1/2); E, (x+1/2, -y-1/2, z+1/2); F, (x+1/2, y+1/2, z+1); G, (x-1/2, -y-1/2, z-1/2); H, (x-1/2, -y+1/2, z-1/2); I, (x-1/2, y-1/2, z-1); J, (x-1/2, y+1/2, z-1); K, (x, y+1, z); M, (x, -y+1, z-1/2); N, (x+1/2, y-1/2, z+1). Some bond distances not listed in the table can be found from the following equations: $U(u) \overset{B}{-} V(v) = V(v) \overset{C}{-} U(u)$; $U(u) \overset{G}{-} V(v) = V(v) \overset{E}{-} U(u)$; $U(u) \overset{H}{-} V(v) = V(v) \overset{D}{-} U(u)$; $U(u) \overset{F}{-} V(v) = V(v) \overset{I}{-} U(u)$; $U(u) \overset{N}{-} V(v) = V(v) \overset{J}{-} U(u)$, where $U(u) \overset{B}{-} V(v)$ indicates bond distance between atoms $U(u) \overset{B}$ and $V(v)$. etc. For example; when $U(u) \overset{N}{-} N(7) \overset{N}$, $V(v) = N(3)$, applying the last equation one gets $N(7) \overset{N}{-} N(3) = N(3) \overset{J}{-} N(7)$.

atoms N(7) and make the angle C(10)-C(8)-C(9) a little larger than 120° .

All the calculations except the standard deviations of the bond lengths and angles were carried out on the Caltech 7094 computer by the Caltech CRYRM System.

REFERENCES

1. E. R. Howell, D. C. Phillips, and D. Rogers, *Acta Cryst.* 3, 210 (1950).
2. International Tables for X-ray Crystallography Vol. III. Birmingham, Kynoch Press (1962).
3. M. J. Buerger, Crystal-Structure Analysis, John Wiley & Sons, Inc., New York (1960).
4. A. S. Parkes and R. E. Hughes, *Acta Cryst.* 16, 734 (1963).
5. K. Emerson and D. Britton, *Acta Cryst.* 17, 1134 (1964).
6. M. J. Cooper, *Acta Cryst.* 17, 1452 (1964).
7. Tables of Interatomic Distances, London: The Chemical Society (1958).
8. A. R. Luxmoore and M. R. Truter, *Acta Cryst.* 15, 1117 (1962).
9. M. J. Kornblau and R. E. Hughes, *Acta Cryst.* 17, 1033 (1964).
10. W. J. Takie and E. W. Hughes, unpublished research, California Institute of Technology (1957).
11. E. W. Hughes, *J. Am. Chem. Soc.* 62, 1258 (1940).
12. L. Pauling, The Nature of the Chemical Bond, Cornell University Press, Ithaca, New York, 3rd ed., 1960.

APPENDIX

Any reflection with a * on the right hand side of the observed value was given a zero weight in the least squares refinement. Any reflection with a minus sign in front of a small observed F value indicates that the reflection was too weak to observe and if the calculated $|F|$ value is less than the observed $|F|$ this reflection did not enter into the least squares refinement.

λ	F_{obs}	F_{cal}	α	λ	F_{obs}	F_{cal}	α	λ	F_{obs}	F_{cal}	α	λ	F_{obs}	F_{cal}	α	λ	F_{obs}	F_{cal}	α		
-14.0	0	1		-10.0	0	1		1	286	256	103	5	114	109	111	2	101	94	144		
0	189	195	355	0	179	183	327	4	140	123	13	6	90	92	269	0	632	608	2		
2	131	132	28	2	131	132	28	5	171	170	87	7	120	127	111	3	144	173	103		
4	98	102	73	4	83	98	27	6	92	81	107	8	54	56	260	2	116	117	171		
6	94	91	334	6	277	270	127	7	93	87	95	0	-8	10		0	-3	1			
8	126	130	325	8	104	102	2	8	85	82	16	0	91	91	182	0	632	608	2		
10	81	81	356	10	81	81	356	0	142	150	45	1	88	98	81	1	486	500	79		
-14.7	0	91	107	355	-10.2	0	215	216	18	1	111	117	52	2	71	79	156	2	1077	1047	352
-14.6	0	30	64	353	1	78	87	48	2	131	127	33	0	-5	1		4	400	374	353	
-14.8	0	50	53	118	2	157	158	24	3	175	140	109	0	623	639	1	5	262	245	217	
-13.1	0	61	61	164	3	144	154	110	4	89	78	103	1	317	345	32	6	301	284	329	
0	96	105	0	4	225	204	163	5	130	115	101	2	488	523	7	7	-374	41	244		
2	84	96	15	5	-46	33	153	6	154	158	23	3	282	256	251	8	99	96	315		
4	110	11	356	6	97	93	17	7	100	93	104	4	466	470	354	9	106	100	65		
6	52	54	30	7	150	155	76	0	-8	10		5	370	329	246	10	-854	106	319		
8	55	64	5	8	92	97	3	0	83	85	173	6	144	139	367	0	-3	3			
10	83	78	215	9	92	97	3	1	85	87	79	7	447	419	217	0	126	135	332		
-13.3	0	99	96	32	2	188	179	83	2	72	78	171	8	116	113	15	1	749	858	88	
-13.2	0	67	73	1	3	111	100	357	3	111	100	357	9	-48	39	119	2	757	758	352	
-13.5	0	54	70	92	4	60	64	56	4	140	155	316	10	90	88	355	3	161	155	99	
-13.7	0	84	87	73	5	162	177	83	0	407	429	99	0	-5	3		4	66	78	314	
-13.9	0	59	64	93	6	155	147	95	1	368	383	351	0	257	274	25	5	260	272	112	
-13.7	0	44	51	101	7	155	147	95	2	111	132	176	1	81	72	170	6	136	148	34	
-13.9	0	57	58	110	8	161	143	67	3	398	336	143	2	467	473	4	7	106	102	103	
-14.0	0	113	111	188	9	155	147	95	4	105	129	50	3	390	366	77	8	109	116	14	
-14.2	0	53	55	86	0	148	137	345	5	48	46	111	4	181	181	81	9	122	106	58	
-14.7	0	147	191	324	1	155	146	168	6	232	206	347	5	336	352	74	10	-65	75	338	
-14.8	0	80	86	304	2	163	163	5	7	68	66	63	6	219	220	21	0	-3	5		
-15.0	0	105	101	108	3	100	125	172	8	134	138	21	7	95	100	38	0	209	186	7	
-15.2	0	48	72	48	4	181	186	350	9	59	55	85	8	126	129	12	1	428	440	60	
-15.7	0	81	74	328	5	271	260	63	0	367	388	9	9	-50	16	94	2	102	96	13	
-15.2	0	152	171	14	6	172	146	95	1	146	171	135	0	117	147	47	3	210	342	90	
-15.7	0	103	113	340	7	98	87	202	2	329	318	345	1	254	247	129	4	179	163	330	
-15.9	0	103	108	313	8	161	143	67	3	114	124	85	2	387	371	6	6	53	69	5	
-16.0	0	133	133	132	9	108	118	75	4	105	129	50	3	219	228	79	7	-36	45	45	
-16.2	0	164	167	337	0	103	114	350	5	49	62	157	4	121	115	85	8	69	68	81	
-16.7	0	83	96	92	1	113	112	84	6	75	76	345	5	180	177	112	9	-45	65	4	
-16.9	0	119	124	352	2	180	180	334	7	68	66	63	6	136	157	28	10	-32	51	14	
-17.0	0	40	46	323	3	49	52	178	8	124	122	18	7	-47	4	67	0	89	93	40	
-17.2	0	76	70	125	4	52	32	319	9	20	80	205	8	124	122	18	1	347	366	74	
-17.7	0	41	47	1	5	99	103	313	0	-7	5		9	99	93	109	2	69	64	268	
-17.9	0	103	113	340	6	131	133	123	0	107	106	198	10	71	87	340	3	360	335	90	
-18.0	0	103	119	49	7	118	110	341	1	274	284	88	0	-5	7		4	170	161	313	
-18.2	0	103	108	313	8	161	143	67	2	88	80	306	1	138	157	98	5	150	137	130	
-18.7	0	133	133	132	9	108	118	75	3	168	181	92	1	432	459	103	6	141	129	295	
-18.9	0	164	167	337	0	103	114	350	4	129	122	345	2	175	147	17	7	77	77	89	
-19.0	0	83	96	92	1	113	112	84	5	75	76	345	3	292	279	97	8	-40	11	173	
-19.2	0	119	124	352	2	180	180	334	6	75	76	345	4	-34	26	89	0	138	156	89	
-19.7	0	41	47	1	3	49	52	178	7	114	120	95	5	191	181	102	1	108	112	168	
-19.9	0	103	113	340	4	96	91	311	8	-44	44	330	6	68	71	36	2	79	56	352	
-20.0	0	103	108	313	5	131	133	123	9	98	97	87	7	126	137	47	3	85	55	79	
-20.2	0	133	133	132	6	108	118	75	0	-7	7		8	-27	24	21	4	88	80	264	
-20.7	0	164	167	337	7	108	118	75	1	238	249	100	0	-5	9		5	151	158	103	
-20.9	0	83	96	92	8	113	112	84	2	70	80	205	1	110	122	92	6	70	66	232	
-21.0	0	119	124	352	9	49	52	178	3	115	103	110	2	132	119	267	0	-3	11		
-21.2	0	41	47	1	0	99	103	313	4	-39	12	175	3	86	86	67	1	87	99	91	
-21.7	0	103	113	340	1	131	133	123	5	132	101	75	4	155	145	209	2	134	138	178	
-21.9	0	103	108	313	2	118	110	341	6	70	114	65	5	136	108	113	0	-2	0		
-22.0	0	133	133	132	3	161	143	67	7	70	67	119	6	43	44	128	0	629	669	352	
-22.2	0	164	167	337	4	108	118	75	8	-7	9		0	-42	63	44	2	238	258	139	
-22.7	0	83	96	92	5	113	112	84	0	100	111	217	1	102	115	89	4	165	184	4	
-22.9	0	119	124	352	6	45	27	177	1	128	152	100	2	136	135	179	5	468	464	0	
-23.0	0	41	47	1	7	108	118	75	2	175	166	193	3	277	255	75	6	168	169	17	
-23.2	0	103	113	340	8	108	118	75	3	237	279	69	4	10	103	232	10	-45	55	17	
-23.7	0	164	167	337	9	69	66	91	4	121	106	167	0	139	103	232	0	352	390	28	
-23.9	0	83	96	92	0	96	91	311	5	194	183	87	1	308	319	34	0	176	71	201	
-24.0	0	119	124	352	1	131	133	123	6	53	56	112	6	339	343	25	2	613	631	1	
-24.2	0	41	47	1	2	133	134	292	7	51	68	147	7	135	132	36	3	512	498	64	
-24.7	0	103	113	340	3	161	143	67	8	-49	11	350	8	436	416	15	4	36	416	15	
-24.9	0	133	133	132	4	108	118	75	9	0	275	320	9	0	-894	104	349	5	85	103	329
-25.0	0	164	167	337	5	61	56	77	0	259	533	1	1	678	747	96	6	123	124	56	
-25.2	0	83	96	92	6	113	112	84	1	-4063	1074	339	2	463	484	358	7	-47	48	120	
-25.7	0	119	124	352	7	45	27	177	2	171	156	4	3	87	69	229	8	94	104	14	
-25.9	0	41	47	1	8	108	118	75	3	399	402	349	4	261	263	69	0	-2	8		
-26.0	0	103	113	340	9	66	55	189	4	-49	11	350	5	164	170	359	0	618	680	19	
-26.2	0	164	167	337	0	66	55	189	5	171	156	4	6	164	170	359	1	172	171	47	
-26.7	0	83	96	92	1	109	116	92	6	429	433	346	2	128	153	87	2	124	149	77	
-26.9	0	119	124	352	2	134	127	90	3	276	287	351	3	191	185	312	3	390	373	98	

PART II

Nuclear Magnetic Resonance Studies

of

Alkali Halide Solutions

INTRODUCTION

One of the most important and complex problems in the studies of electrolytic solutions is that concerning the details between the ion-ion and ion-solvent interactions. A considerable amount of work has been done in this area (1-16). One method of studying the problem is by looking at the nuclear magnetic resonance line width of the ions. The line width is related to the spin-spin relaxation time (T_2), which is to be distinguished from the spin-lattice relaxation time (T_1), which denotes the time scale at which a nonequilibrium spin distribution approaches thermal equilibrium via coupling with the lattice. Ordinarily, when the characteristic time modulating the molecular motions is short, T_1 and T_2 are equal and the line width is inversely proportional to the relaxation time (T_1 or T_2). There are several interactions which can cause the relaxation of a spin. However, when the nucleus possesses an electric quadrupole moment the relaxation process becomes simpler. The interaction of electric quadrupole moment with the surrounding electric field gradient is so strong that, ordinarily, it dominates all other relaxation processes and determines the observed line width.

The nuclei, ^{79}Br ($I = 3/2$), ^{81}Br ($I = 3/2$), and ^{127}I ($I = 5/2$) all have spin quantum numbers greater than $\frac{1}{2}$. They therefore possess electric quadrupole moments. Presumably, one can deduce some valuable information about the ion-ion and ion-solvent interactions via a study of the interaction of the quadrupole moment of

these nuclei with the electric field gradients surrounding these ions.

The general theory of quadrupole relaxation in liquids has been given by Abragam and Pound (17), who derived the following equation for the relaxation time:

$$T_1^{-1} = \frac{3}{40} \frac{4I(I+1) - 3}{I^2(2I-1)^2} \left(\frac{eQ}{\hbar} \right)^2 \left\langle \left(\frac{d^2V}{dz^2} \right)^2 \right\rangle \tau_c \quad (1)$$

where eQ is the quadrupole moment of the nucleus,

$\left\langle \left(\frac{d^2V}{dz^2} \right)^2 \right\rangle$ is the mean square electric field gradient at the nucleus,

and τ_c the correlation time describing the molecular motions that modulate the electric field gradient tensor. Both

$\left\langle \left(\frac{d^2V}{dz^2} \right)^2 \right\rangle$ and τ_c may change when the nature of the solution is

changed. Theoretical calculation of these two quantities are difficult and subject to very gross uncertainties. Experimental results indicate that, in general, when the concentration of electrolytic solution increases, the line width becomes broader. The origin of this broadening effect is still not completely clear. Several models, however, have been developed in an attempt to explain this line-broadening. Valiev and Khabibullin (18) first assumed that the halide ions do not form stable complexes with the dipolar solvent molecules, i. e., the dipolar solvent molecules are subjected to unhindered translational and rotational diffusion. With this model, they are able to calculate the contributions of both the translational and rotational diffusion of dipole solvent molecules on the halide ion

line widths. The following expression was obtained:

$$T_1^{-1} = \frac{216}{875} \pi^2 \left(\frac{eQ(1+\gamma)}{\hbar} \right)^2 \frac{d^2}{(2a)^3} \frac{N}{V} \frac{\eta}{kT} \quad (2)$$

where d is the dipole moment of the solvent, a is the distance between the ions and the solvent molecules, η the viscosity of the solutions, and N , V , k , T , γ are the Avogadro's number, volume, Boltzman constant, temperature, and the Sternheimer antishielding constant respectively. This model was partially supported by the experimental results of Itoh and Yamagata (19). Itoh and Yamagata studied the dependence of T_1^{-1} on temperature and viscosity for I^- ions in aqueous solutions of NaI and KI. They found that the change in T_1^{-1} with temperature (at constant concentration) followed closely the temperature dependence of η/T . This is in complete agreement with equation 2. Hertz (14) later suggested that at dilute solutions, the field gradient arises principally from the solvent dipoles. At higher concentrations, however, the ion-ion interaction is presumed to become important. The broadening of line width was interpreted as an indication of these ion-ion interactions. The complete expression of line width as derived by Hertz is given by:

$$\Delta H = C \frac{16\pi}{5\gamma\sqrt{3}} \frac{e(1+\gamma')PQ}{\hbar}^2 \frac{d^2 C_{H_2O}}{\gamma_O} + \sum V_i Z_i^2 \frac{e^2 c \tau_{cs}}{2a^3} \quad (3)$$

where γ is the gyromagnetic ratio

P is the polarization factor and it is equal to $\frac{2\epsilon + 3}{5\epsilon}$

ϵ is the dielectric constant

$Z_i e$ is the charge of the i^{th} ion

V_i is the stoichiometric number corresponding to the i^{th} ion

$C = 1.0$ for ^{79}Br and ^{81}Br resonance

$C = 0.24$ for ^{127}I resonance

The right hand side of equation 3 contains essentially two terms. The first term is quite similar to the one derived by Valiev and Khabibullin (18), except that the constant is different. The second term, as suggested by Hertz, arises from the ion-ion interaction. This interaction is related to the number of ions in the solution as well as the distance between the two interacting ions. Hertz assumed that the increasing line width with increasing salt concentration is due to the change in the concentration, c , instead of the distance, a . He assumed that there is a value ξ such that $\tau_c / \tau_{\text{CH}_2\text{O}} \geq \xi$ and ξ is always a constant for all concentrations. The "minimum approach distance" between halide ions and the cations were calculated based on these assumptions.

Several interesting points arise from Hertz's model. First, the minimum approach distance, a , should be less than the value $3\sqrt{V/N}$ where $3\sqrt{V/N}$ is the distance between two ions when there are N ions which are equally spaced in a volume V . However, for several salts, such as NH_4Br , NH_4I , and KBr at some concentration, the value of a is greater than $3\sqrt{V/N}$. Secondly, the basic assumption

in Hertz's model can be summarized as follows:

- (a) The halide ions do not form stable complexes with the solvent dipoles, i. e., the dipolar solvent can move freely.
- (b) The broadening of the line width with increasing salt concentration is due to an increase in the number of interactions instead of the change in the correlation time.

In Richards and York's (7, 8) studies of alkali bromide and alkali iodide solutions, they found that the line width is related to the viscosity of the solution. They concluded that the ion-ion interaction between cations and halide ions is almost negligible when the cations are highly hydrated. This indicates that for sodium and lithium halides, as well as alkali earth halide solutions, the main contribution to the line width is from the change in the viscosity (or the correlation time) instead of the change in the field gradient surrounding the halide ions. Eisenstadt and Friedman (12), on the other hand, strongly objected to Richards and York's conclusion. They claimed that the specific ion-ion interaction is as large as for Ba^{++} as for Cs^+ , for Sr^{++} as well as for Rb^+ .

The main difference between Hertz's (14) and Richards' (8) model is in the interpretation of the broadening of the line width when the salt concentration is increased. For cesium halide solutions, both Hertz and Richards agree that ion-ion interaction exists. For other salts, however, Hertz suggested that the broadening of the

line width is due to the change of the field gradient surrounding the halide ions, whereas Richards suggested that the broadening effect is due to the change of the viscosity or the correlation time. It is clear that, in view of these controversies, further studies are desirable before this problem can be settled.

Both Richards and Hertz are working on a system where only one alkali or alkaline earth halide salt exists in the aqueous solution. In order to study the cation-halide ion interaction it is necessary to have the cation concentration as high as possible. In Hertz and Richards' system, the only way to increase the cation concentration is to increase the salt concentration. However, the viscosity of the solution also increases, approximately, linearly with salt concentration. Hence it is not easy to separate out the ion-ion interaction and the viscosity contribution to the line width if both contributions are proportional to the salt concentration. One can, however, compare the line width of solutions containing different cations at constant viscosity. For this reason we have studied the halide magnetic resonance (^{81}Br and ^{127}I) as a function of solution viscosity for solutions containing a fixed concentration of NH_4Br or NH_4I , and to which numerous salts such as LiCl , NaClO_4 , and MgCl_2 have been added. If ion-ion interaction is unimportant, then the halide line-widths would be independent of the nature of the cation when the results are compared at constant viscosity. Any dependence of the resonance widths on the nature of the cation at constant solution viscosity must therefore reflect ion-ion interaction.

The importance of determining whether or not the specific ion-ion interaction in aqueous solution does occur does not need to be overemphasized. Equally important, however, are the interactions which occur between ion and solvent. In the earlier study by Richards and York (7) an attempt was made to obtain some information on the ion-solvent interaction from line width studies but no detailed information was obtained. The interaction between the halide ions and the solvent molecules is still unknown. There are two possible types of interactions which may occur.

(1) The dipolar solvent molecules interact individually with the halide ions. In this case no specific ion-solvent complex is formed. The observed line width is dependent on the interactions between the halide ion and the surrounding solvent molecules. Since the halide ions possess a quadrupole moment, the observed line width is mainly dependent on the quadrupole-dipole interaction (8). When a solute such as methanol, acetonitrile, or acetone is added to the aqueous solution, these solute molecules have a chance to interact with the halide ions. Since this solute-ion interaction may not be equal to the water-halide ion interaction, the line width may change. The amount of change in the line width is dependent on the difference between the magnitude of the solute-halide ion and the water halide ion interactions. As mentioned above, since the quadrupole-dipole interaction dominates the relaxation process, it is expected that the effect of various organic solutes on the line width will be proportional to the square of the dipole moment of the solute. The dipole moments

of water, methanol, acetonitrile, and acetone are: 1.87, 1.71, 3.45, and 2.78 D respectively. It is expected that the effect of these organic solutes on the line width of the halide ion resonances should be in the order: acetonitrile > acetone > methanol, and in the case of methanol the line width should be sharper, since the dipole moment of methanol is smaller than water.

(2) The halide ion and the solvent molecules may form some specific complex. If this is the case, the halide ion line width is no longer entirely dependent on the individual solvent-halide ion interaction. It is dependent on the type and symmetry as well as the correlation time of the complex that is formed. When a small amount of organic solute such as methanol, acetonitrile, and acetone is added to the aqueous solution, the solute molecules may replace one of the water molecules in the first coordination sphere of the water-halide ion complex and form a new type of complex. This new complex has a lower symmetry than the water-halide ion complex. The mean square field gradient and, consequently, the line width is increased. The change in the line width is dependent on how much the symmetry of the complex is changed as well as the change in the correlation time of the new complex. The mean square field gradient of the new complex may be related to the dipole moment of the solute. However, it is not necessarily proportional to the dipole moment of the solute. The size of the solute molecule may have a larger effect on the halide ion line width, since the larger the solute molecule the more it will distort the symmetry of the solute-water-halide complex.

In the present work, a study has been made on the ion-ion interaction as well as on the ion-solvent interaction in order to ascertain in a more definitive manner the principal factors responsible for the halide ion line widths in aqueous solutions.

EXPERIMENTAL

Nuclear resonance measurements were carried out with a Varian 4200 B variable frequency spectrometer, using a 12" magnet. The resonance frequencies for ^{81}Br and ^{127}I were measured by a frequency counter. They are:

13.260 Mcps for ^{81}Br resonance for the studies of
aqueous solutions

8.051 Mcps for ^{81}Br resonance for the studies of
aqueous solutions with added organic solutes
(methanol, acetonitrile, and acetone)

8.051 Mcps for all ^{127}I resonance

The viscosity was measured with an Ostwald viscometer. The density was measured with a 2-ml densitometer. The probe temperature was in the range of $25 \pm 1.5^\circ \text{C}$. The added solutes used in the studies were methanol, acetonitrile and acetone. These solutes were distilled before use through a fractional distillation column to remove impurities. Since the line width is not sensitive to those impurities in the salts, the salts bought from the stock room were used without further treatment. The following reagent grade chemicals were used:

NaCl , NaI , NH_4Cl , LiCl , KBr , KI , MgCl_2 , KClO_4
(from Baker and Adamson)

NaClO_4 (from G. Frederick Smith Co.)

NH_4Br , NH_4I (from Mallinckrodt Chemical Works)

A trace of sodium thiosulphate was added to each alkali iodide solution to ensure the absence of free iodine which would produce line broadening by an exchange process (15).

RESULTS

 ^{81}Br resonances

Several series solutions contain mixed electrolytes: NaBr and NaClO_4 ; NaBr and MgCl_2 ; NH_4Br and LiCl ; NH_4Br and CsCl ; and NH_4Br and KCl were prepared. In each series the concentration of Br^- is kept at 1.5 moles/Kg H_2O , whereas the concentration of other electrolyte changes. The ^{81}Br resonance line width and the viscosity were measured for each solution. The results are shown in Table I-V. A plot of line width vs. viscosity for the first three series was shown in Fig. 1.

In order to study the ion-solvent interactions, three series of solutions were prepared. In each series, the concentration of Br^- in all the solutions was kept at 0.427 moles NaBr per 4.81 moles water-organic solute mixture whereas the water to organic solute ratio changes. The organic solutes used in our studies are methanol, acetonitrile, and acetone. The results are shown in Tables VI-VIII. A line width/viscosity vs. organic solute concentration plot is shown in Fig. 2.

 ^{127}I resonance

Similarly, several series solutions contain mixed electrolytes: NH_4I and LiCl , NH_4I and NaClO_4 , NH_4I and KCl , and NH_4I and CsCl were prepared. In each series, the concentration of ^{127}I was kept at 1.5 moles/Kg H_2O , whereas the concentration of other electrolytes

Table I. Line width of Br^{81} in an aqueous solution
which contains 1.5 molal NH_4Br and various
concentrations of LiCl

Concentration of LiCl moles/Kg H_2O	Viscosity in units of $\eta_{\text{H}_2\text{O}}$	Br^{81} line width (in gauss)
0	0.99	0.30
2.5	1.27	0.41
4.9	1.67	0.51
7.3	2.30	0.73
9.8	3.24	1.12
13.2	5.15	1.78
16.0	8.50	2.86
18.3	10.8	3.82

Table II. Line width of Br^{81} in an aqueous solution
which contains 1.5 molal NaBr and various
concentrations of NaClO_4

Concentration of NaClO_4 moles/Kg H_2O	Viscosity in units of $\eta \text{ H}_2\text{O}$	Br^{81} line width (in gauss)
0	1.10	0.31
2.8	1.28	0.41
5.6	1.54	0.52
8.4	2.24	0.76
9.8	2.76	1.04
11.2	3.18	1.14
12.6	4.20	1.52
14.0	5.55	1.98
15.4	7.35	2.47
16.8	9.60	3.12

Table III. Line width of Br^{81} in an aqueous solution which contains 1.5 molal NaBr and various concentrations of MgCl_2

Concentration of MgCl_2 (in moles/Kg H_2O)	Viscosity in units of $\eta_{\text{H}_2\text{O}}$	Line width (in gauss)
0	1.10	0.31
0.84	1.37	0.43
1.68	1.67	0.52
2.50	2.04	0.69
3.36	2.48	0.91
4.20	3.20	1.18
5.05	4.15	1.58

Table IV. Line width of Br^{81} in an aqueous solution which contains 1.5 molal NH_4Br and various concentrations of KCl

Concentrations of KCl in moles/ $\text{Kg H}_2\text{O}$	Viscosity in units of $\eta_{\text{H}_2\text{O}}$	Line width in gauss
0	0.95	0.30
0.77	0.96	0.31
1.54	0.97	0.32
2.30	0.99	0.34
3.08	1.02	0.34
3.84	1.06	0.38
4.61	1.09	0.39

Table V. Line width of Br^{81} in an aqueous solution
which contains 1.5 molal NH_4Br and various
concentrations of CsCl

Concentration of CsCl in moles / Kg H_2O	Viscosity in units of $\eta_{\text{H}_2\text{O}}$	Line width in gauss
0	0.95	0.30
1.3	0.95	0.40
2.6	0.96	0.49
3.9	1.01	0.56
5.2	1.05	0.65
6.3	1.09	0.79

Figure 1. Br^{81} line width for various aqueous solutions

- Aqueous solution contains 1.5 molal NH_4Br and various concentrations of LiCl
- X Aqueous solution contains 1.5 molal NaBr and various concentrations of NaClO_4
- O Aqueous solution contains 1.5 molal NaBr and various concentrations of MgCl_2

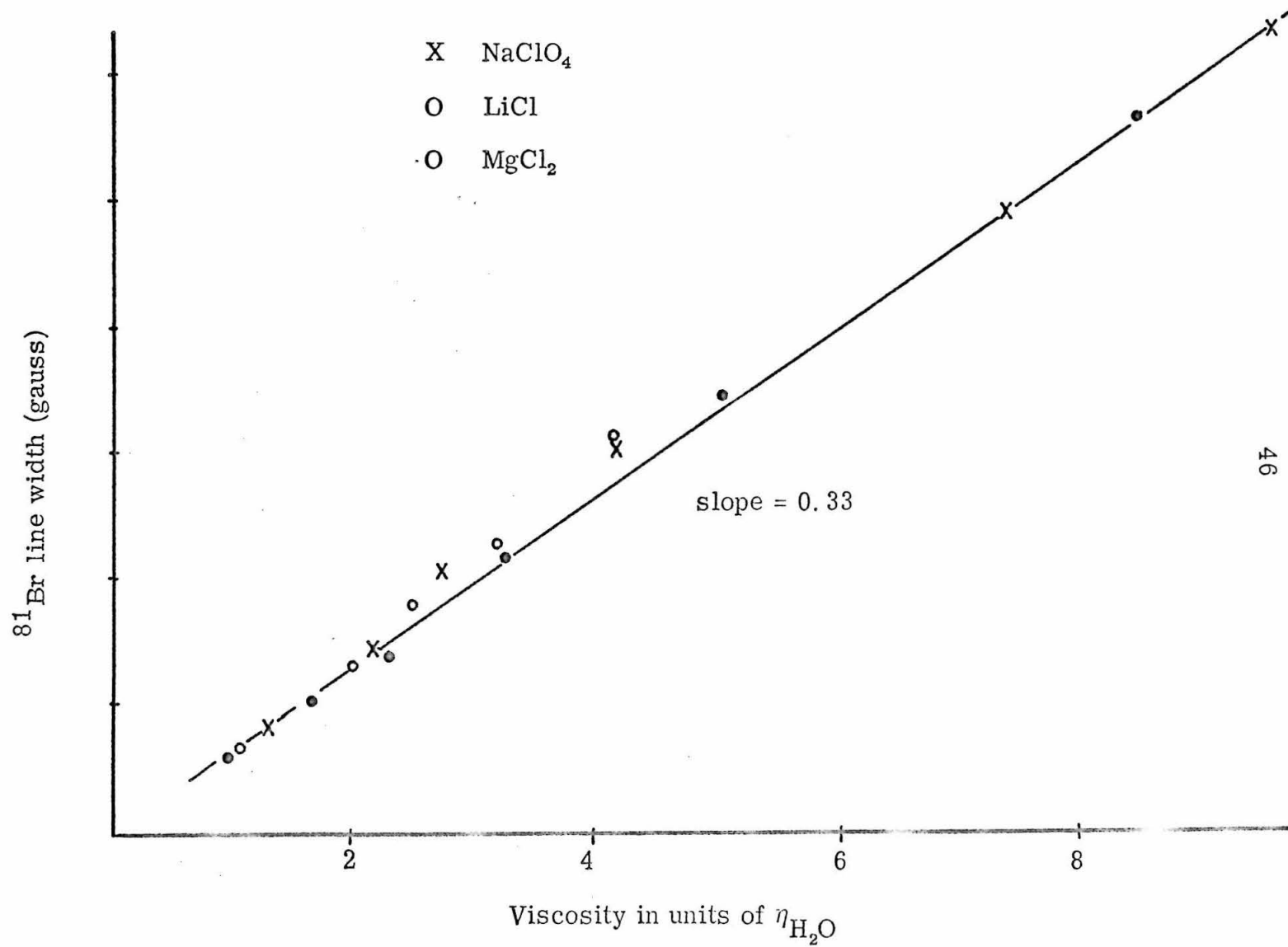


Table VI. Line width of ^{81}Br in solutions which
 contain 8.9 moles NaBr/100 moles
 $\text{CH}_3\text{CN}-\text{H}_2\text{O}$ mixture

ΔH (in gauss)	η (in units of $\eta_{\text{H}_2\text{O}}$)	$\frac{\text{moles CH}_3\text{CN}}{100 \text{ moles H}_2\text{O}}$	$\Delta H/\eta$
0.364	1.48	0	0.245
0.418	1.52	0.8	0.275
0.486	1.56	1.59	0.311
0.557	1.58	2.38	0.352
0.601	1.60	3.18	0.375
0.660	1.63	3.98	0.404
0.764	1.66	4.78	0.460
0.852	1.69	5.57	0.504
0.945	1.72	6.37	0.549
1.01	1.74	7.16	0.580
1.08	1.77	7.98	0.610
1.25	1.79	8.87	0.698
1.35	1.82	9.57	0.741
1.43	1.84	10.35	0.777

Table VII. Line width of ^{81}Br in solutions which
 contain 8.9 moles $\text{NaBr}/100$ moles
 $(\text{CH}_3)_2\text{CO}-\text{H}_2\text{O}$ mixture

ΔH	η	$\frac{\text{moles } \text{CH}_3\text{COCH}_3}{100 \text{ moles } \text{H}_2\text{O}}$	$\Delta H/\eta$
0.344	1.52	0	0.226
0.475	1.57	0.80	0.303
0.519	1.62	1.59	0.320
0.700	1.70	2.38	0.411
0.775	1.77	3.18	0.437
1.01	1.84	3.98	0.548
1.25	1.91	4.78	0.654
1.43	2.00	5.57	0.715
1.49	2.05	6.37	0.726
1.63	2.12	7.16	0.768
2.03	2.18	7.98	0.931
2.30	2.25	8.87	1.022
2.64	2.30	9.57	1.147

Table VIII. Line width of ^{81}Br in solutions which
 contain 8.9 moles $\text{NaBr}/100$ moles
 $\text{CH}_3\text{OH}-\text{H}_2\text{O}$ mixture

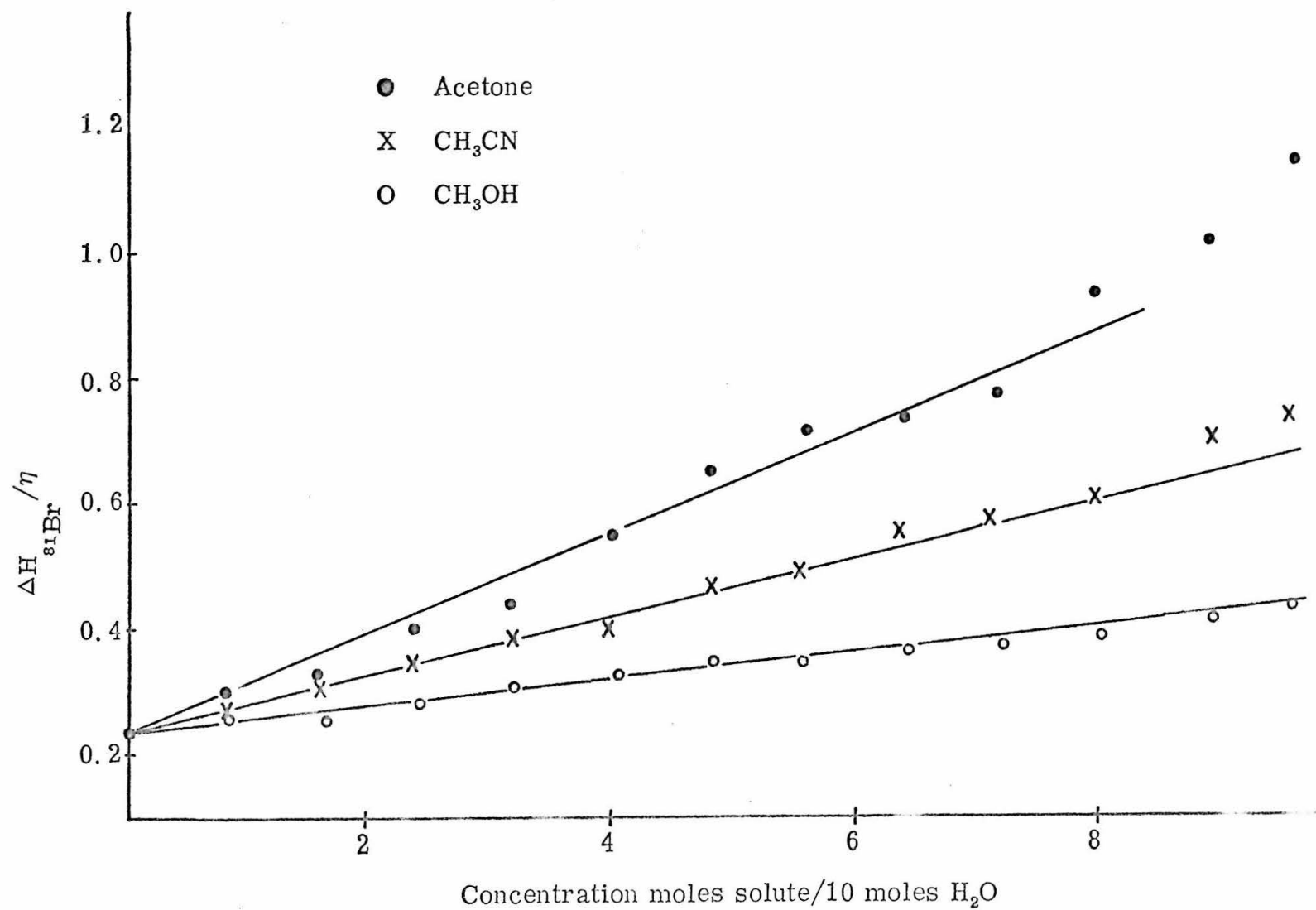
ΔH	η	$\frac{\text{moles CH}_3\text{OH}}{100 \text{ moles H}_2\text{O}}$	$\Delta H/\eta$
0.38	1.46	0	0.231
0.40	1.50	0.8	0.266
0.40	1.54	1.59	0.259
0.45	1.58	2.38	0.284
0.495	1.61	3.18	0.307
0.519	1.65	3.98	0.314
0.580	1.69	4.78	0.343
0.606	1.72	5.57	0.352
0.645	1.76	6.37	0.366
0.680	1.80	7.16	0.377
0.730	1.84	7.98	0.397
0.787	1.87	8.87	0.420
0.824	1.91	9.57	0.431
0.861	1.95	10.35	0.441

Figure 2. Br^{81} line width/viscosity vs. concentration plot

● $(\text{CH}_3)_2\text{CO}$

X CH_3CN

O CH_3OH



changes. The ^{127}I line width and the viscosity were measured for each solution. The results were shown in Tables IX-XII. A plot of line width vs. viscosity for the first three series is shown in Fig. 3.

In order to study the ion-solvent interactions, three series of solutions were prepared. The concentration of I^- in all the solutions was kept at 6 moles NH_4I per Kg H_2O . To each series, the organic solute to water ratio was changed. The organic solute used in the studies are methanol, acetonitrile, and acetone. The results are shown in Table XIII-XV. The line width/viscosity vs. organic solute concentration plot was shown in Fig. 4.

Table IX. Line width of ^{127}I in an aqueous solution
which contains 1.5 molal NH_4Br and various
concentrations of LiCl

C	η	ΔH
0	0.98	1.24
2.9	1.21	1.47
5.7	1.59	1.95
8.7	2.16	2.75
11.5	3.07	4.03
14.4	4.75	6.5
17.2	7.71	9.6
18.7	9.75	11.8

Table X. Line width of ^{127}I in an aqueous solution which contains 1.5 molal NH_4I and various concentrations of NaClO_4

ΔH	η	C
1.25	1.01	0
1.57	1.27	2.8
2.18	1.64	5.7
3.2	2.29	8.6
5.0	3.46	11.4
7.8	5.86	14.3
13.2	10.2	17.2

Table XI. Line width of ^{127}I in an aqueous solution which contains 1.5 molal NH_4I and various concentrations of KCl

ΔH	η	C
1.23	0.98	0
1.23	1.00	0.70
1.23	1.01	1.41
1.23	1.03	2.11
1.29	1.09	3.52
1.30	1.12	4.22
1.41	1.14	4.57

Table XII. Line width of ^{127}I in an aqueous solution
which contains 1.5 molal NH_4I and various
concentrations of CsCl

ΔH	η	C
1.23	0.98	0
1.48	0.98	1.47
1.63	1.01	2.94
2.01	1.09	4.78

Figure 3. ^{127}I line width for various aqueous solutions

- X Aqueous solution contains 1.5 molal NH_4I and various concentrations of LiCl
- Aqueous solution contains 1.5 molal NaI and various concentrations of NaClO_4

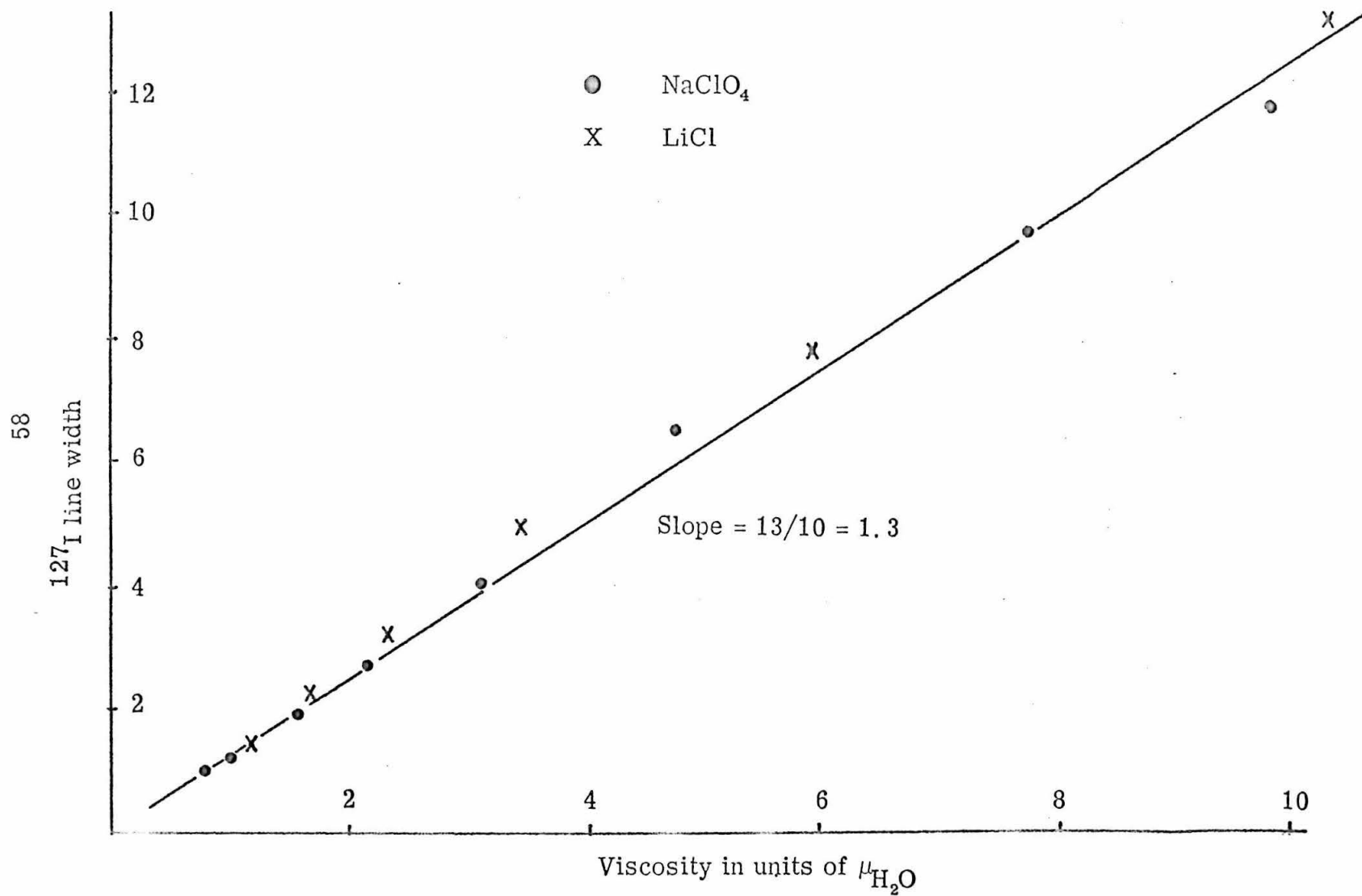


Table XIII. Line width of ^{127}I in CH_3CN , H_2O ,
 NaI mixture. $C_{\text{NaI}} = 6 \text{ moles NaI/Kg H}_2\text{O}$

ΔH	η	$\frac{\text{moles CH}_3\text{CN}}{100 \text{ moles H}_2\text{O}}$	$\Delta\text{H}/\eta$
1.43	1.00	0	1.43
1.83	1.03	1.74	1.78
2.09	1.05	3.48	1.99
2.52	1.07	5.22	2.36
3.28	1.09	6.95	3.07
3.60	1.12	8.70	3.21
4.10	1.14	10.4	3.59

Table XIV. Line width of ^{127}I in CH_3OH , H_2O , NaI mixture. $C_{\text{NaI}} = 6 \text{ moles NaI/Kg H}_2\text{O}$

ΔH	η	$\frac{\text{moles CH}_3\text{OH}}{100 \text{ moles H}_2\text{O}}$	$\Delta\text{H}/\eta$
1.43	0.99	0	1.43
1.94	1.01	2.23	1.92
2.02	1.06	4.47	1.90
2.21	1.10	6.70	2.01
2.52	1.18	11.2	2.37
3.22	1.23	13.4	2.62

Table XV. Line width of ^{127}I in $(\text{CH}_3)_2\text{CO}$, H_2O , NaI solution. $C_{\text{NaI}} = 6 \text{ moles NaI/Kg H}_2\text{O}$

ΔH	η	$\frac{\text{moles } (\text{CH}_3)_2\text{CO}}{100 \text{ moles H}_2\text{O}}$	$\Delta\text{H}/\eta$
1.43	1.00	0	1.43
1.94	1.04	1.25	1.87
2.46	1.07	2.50	2.30
3.04	1.10	3.75	2.76
3.70	1.17	5.00	3.16
4.37	1.21	6.25	3.61
5.15	1.28	7.5	4.02

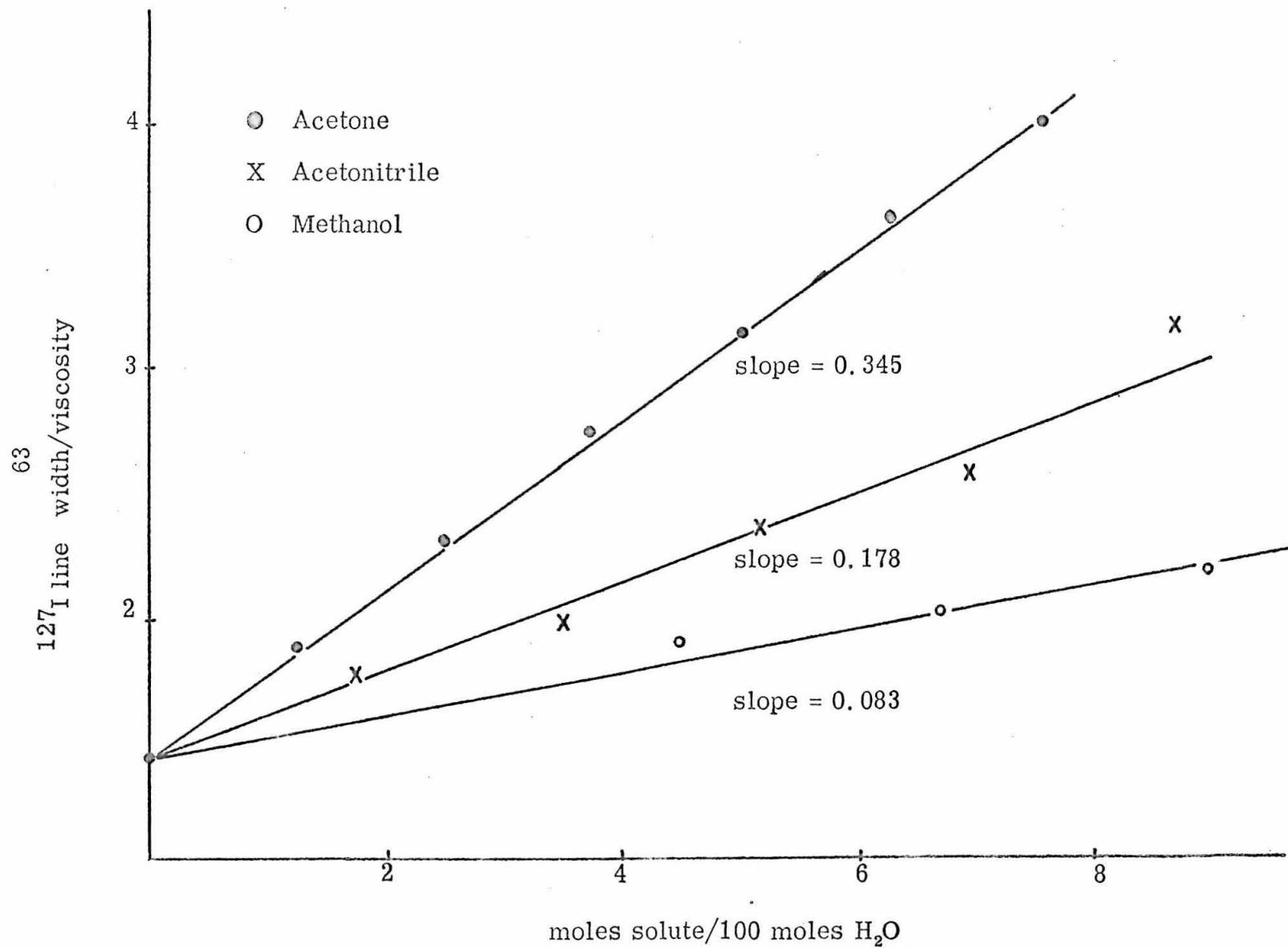
Figure 4

$\frac{^{127}\text{I line width}}{\text{viscosity}}$ vs. solvent concentration plot

● $(\text{CH}_3)_2\text{CO}$

X CH_3CN

O CH_3OH



DISCUSSION

As discussed in the introduction, many attempts have been made to interpret the broadening of nuclear magnetic resonance line width of halide ions with increasing salt concentration in terms of ion-ion and ion-solvent interactions. The results are not very successful.

The general relationship between line width, field gradient surrounding the halide ions, and the correlation time was shown in equation 1. Both correlation time and the mean square field gradient was very difficult to calculate and subject to very high uncertainty.

The correlation time is the time which describes the motion of molecules or ions. The major contribution of this is by the translational and the rotational diffusion of the solvent molecules. Since both translational and rotational diffusional is proportional to the viscosity, it is quite reasonable to say that the correlation time is proportional to the viscosity. It is generally accepted that the correlation time can be approximated as:

$$\tau_c = C \eta / T$$

where C , η , T are the constant, the viscosity, and the temperature respectively.

If the correlation time can be well represented by $C\eta/T$ then the problem becomes simpler, since both viscosity and temperature are a measurable quantity.

The most well-known models for the interpretation of halide ion line width broadening phenomena were proposed by Hertz (14), and Richards and York (7). Hertz suggested that the broadening effect is mainly caused by the change of the mean field gradient surrounding the halide ions by a cation-halide ion interaction. Richards and York, on the other hand proposed that the broadening effect is mainly coming from the change of the viscosity of the solution. Since viscosity is closely related to the correlation time, Richards' proposal mainly means that the change of line width is coming from the change of correlation time instead of the field gradient surrounding the halide ions.

An ^{81}Br line width vs. viscosity plot for several compounds is shown in Fig. 1. A similar plot for ^{127}I line width is shown in Fig. 3. For lithium, sodium, and alkali earth salts, the points are almost fallen in one straight line. Furthermore, this line passes through the origin. This is in complete agreement with equation 2. From this experimental result, it suggests:

- i. When LiCl , NaClO_4 , as well as MgCl_2 are added to the aqueous alkali halide solution, the change of the mean square field gradient surrounding the halide ions is negligible. The change of halide ion line width is mainly come from the viscosity (or correlation time) effect.
- ii. When cesium salt is added to the solution, both correlation time and mean field gradient are changed.

iii. The mean square field gradient is given by:

$$\left\langle \left(\frac{\partial^2 V}{\partial^2 X} \right)^2 \right\rangle = \text{constant} \times \frac{\Delta H}{\eta}$$

The most acceptable model of the structure of aqueous electrolyte solutions was proposed by Frank et al. (21). Frank suggested that there are several coordination spheres surrounding an ion. Since the relaxation of halide ions is mainly by means of the quadrupole dipole interaction and the magnitude of this interaction is inversely proportional to r^5 , only these molecules (or ions) which are entering the closest sphere have significant contribution upon the line width. This means only the first coordination sphere needs to be considered in the calculation of the halide ion line width. The structure of this first coordination sphere has not been discussed in much detail. Several investigators have shown that halide ions do not form stable complexes with surrounding water molecules (22). Based on this assumption, both Valiev and Khabibullin (18) and Hertz (14) had derived an expression for the halide ion line width in aqueous solution. The agreement between the calculated and the observed line width is not very satisfactory. From infrared studies, Chan and Iwamasa (1) had shown that halide ions and water molecules do form some type of complex. It is doubtful whether this noncomplex model is still applicable in the calculation of halide ions line width in the solutions. There are several comments about this model and the way Valiev and Khabibullin (18) proved their model.

1. Itoh and Yamagata (19) studied the dependence of T_1^{-1} on temperature and viscosity for I^- ions in aqueous solutions of NaI and KI. They found that the change in T_1^{-1} with temperature followed closely the temperature dependence of η/T . Valiev and Khabibullin (18) suggested that this is a good support of their model. This is not true. From equation 1, the general expression for halide ion line width in the solution can be simplified as:

$$T_1^{-1} = A \left\langle \left(\frac{\partial^2 V}{\partial^2 Z^2} \right)^2 \right\rangle \cdot \tau_c \quad (1b)$$

Valiev and Khabibullin's work is mainly concerned with the calculation of mean square field gradient

$$\left\langle \left(\frac{\partial^2 V}{\partial Z^2} \right)^2 \right\rangle.$$

It has nothing to do with the value τ_c . Since

$$\tau_c = \frac{4\pi \eta a^3}{kT} = A' \eta / T \quad (4)$$

It is clear that Itoh and Yamagata's (19) results do not have any relation with Valiev and Khabibullin's model. However, it does demonstrate that η/T is a very good approximation for the correlation time.

2. In our studies, the line width vs. viscosity plot for several electrolytes is linear, even if the cation concentration is as

high as 18 moles/Kg H_2O . The mean distance between halide ion and cation is about 4.1 \AA at the concentration. It is questionable whether at such a high concentration the water molecules and the cations are still able to move freely at the surrounding of halide ions.

3. As discussed in the introduction, if no specific kind of complex is formed between halide ions and the solvent molecules, one would expect that the effect of organic solute on the line width of halide ions resonance would be in the order of acetonitrile > acetone > methanol water. Furthermore, since the dipole moment of methanol is smaller than water, the halide ion line width should be sharper when methanol is added to the aqueous solution. A $\Delta H/\eta$ vs. concentration plot for several organic solutes are shown in Fig. 2 and Fig. 4. At low concentration the plot is linear. The slope of these straight lines is an indication of the ability of these solutes to change the mean field gradient surrounding the halide ion in the solution. For simplicity we shall name this ability as "broadening ability" in our later discussion. The broadening abilities of several organic solutes and water upon ^{81}Br and ^{127}I were listed in Table XVI. For convenience, the dipole moment and dipole moment square are also listed in Table XVI.

Table XVI. The broadening ability of various organic solvents upon the halide ions.

ion solute	^{81}Br	^{127}I	dipole moment d	d_2	^{127}I ^{81}Br
acetone	0.0785	0.34	2.78	7.7	4.3
aceto- nitrile	0.042	0.178	3.45	11.9	4.2
methanol	0.021	0.083	1.71	2.9	4.0
water	~ 0	~ 0	1.87	3.3	

From Table 16, it is quite clear that the broadening ability of these organic solutes upon the halide ions (^{81}Br and ^{127}I) line width is in the order of acetone > acetonitrile > methanol > water. This order is quite different from the order one would expect if all solvent molecules are allowed to move freely and react individually with the halide ions. (If all solvent molecules are allowed to move freely and interact individually, then according to equation 2 and equation 3 the broadening ability should be proportional to the square of the dipole moment of the organic solvent, i. e., acetonitrile > acetone > water > methanol.)

4. The solubility of alkali halide in various solvents is generally in the order: $\text{H}_2\text{O} > \text{CH}_3\text{OH} > \text{CH}_3\text{CN} > \text{CH}_3\text{COCH}_3$. If the solubility has any relation with the strength of the bonding between the ions and the solvent molecules, it is expected that the bonds formed between halide ions and solvents mentioned above should also be in the order as shown above. It seems reasonable that the stronger the bond the longer the correlation time. This implies that if only the correlation time is concerned, the effect of various organic solvents upon the halide ion line width in solutions should be in the order of water > methanol > acetonitrile > acetone. This is also contrary to the experimental results.

5. It is well-known that the bond strength between halide ions and water molecules are in the order of $\text{Cl}^- > \text{Br}^- > \text{I}^-$. It seems reasonable to assume that the bond strength between halide ions and methanol, acetonitrile, and acetone is also in this order. If one assumes such a model that halide ions do not form stable complex with these solvent molecules, the iodide ions should be a better example of this model than the bromide ion. This indicates that the broadening ability of various dipole solvents in the case of iodine should be more closely proportional to the dipole moment square of these organic solvents than the case of bromine. From Table XVI, this is not true either. $0.34:0.178:0.083$ compares with $7.1:11.9:2.9$ as badly as $0.0785:0.042:0.021$ compares with $7.7:11.9:2.9$. For these reasons, it is clear that the noncomplex model is not very satisfactory. Actually this model does not need to be over-emphasized. Equally important, however, is the possibility that halide ion may also form some type of complex with the solvent molecules or the cations surrounding it. We shall discuss our result base on this model in our later discussion.

In equation 1, the two possible variables which correspond to the halide ion line width are the mean field gradient surrounding the halide ions and the correlation time. Since the interaction between

the halide ions and the surrounding solvent molecules (or cations) is approximately proportional to R^{-5} (14, 19), only these solvent molecules or cations which can enter into the first closest coordination sphere have an effect upon the line width. The contribution from second and farther coordination spheres are negligible. For this reason it is suggested:

1. The mean field gradient is mainly dependent on the structure of the complex surrounding the halide ion.
2. The correlation time is the duration time of this complex (diffusing away one of the components of the complex or the tumbling of the whole complex).
3. The relation:

$$\frac{\text{mean square field gradient}}{\Delta H/\eta} = \text{constant}$$

still holds, since both diffusion of the solvent molecules and the tumbling of the whole complex are still proportional to the viscosity.

When LiCl , NaClO_4 , as well as MgCl_2 are added to the solution, Li^+ , Na^+ , and Mg^{++} are so strongly hydrated that they do not have a chance to enter the first coordination sphere of the halide ion. However, they do change the viscosity of the solution. This explains why the mean square field gradient surrounding the halide ion is unchanged and the line width vs. viscosity plot is linear.

X-ray diffraction studies (2, 3) indicated that when KOH is dissolved in water the tetrahedral water structure is almost unchanged. However, when these salts such as LiCl, NaCl are dissolved in water the tetrahedral structure is no longer in existence. It seems that these cations such as Cs^+ , K^+ can replace one of the water molecules and keep the water structure unchanged. It is expected that these cations will work just like water molecules and can replace one of the water molecules in the water-halide ion complex. If this is the case, halide ion line width is expected to become broader when Cs^+ is added to the solution, since the symmetry of this new cation-halide-water complex is lower than the original water-halide ion complex. This is exactly the result we have observed.

When organic solvent, such as methanol, acetonitrile and acetone is added to the aqueous solution, this organic solvent has a tendency to replace one of the water molecules in the water-halide complex and form a new type of complex. Since this new complex has a lower symmetry than the original one, it is expected that the line width will be broader. The change of the line width is mainly dependent on how much the complex is distorted from the complex which has zero mean square field gradient. In view of this, the size of these organic solvents may be more important than the dipole moment. The observed "broadening ability" for several solvents are in the order: $\text{CH}_3\text{COCH}_3 > \text{CH}_3\text{CH} > \text{CH}_3\text{OH} > \text{H}_2\text{O}$. This is in agreement with our assumption, i. e., the larger the size of

organic solvent, the more it will distort the complex from the totally symmetric complex.

REFERENCES

1. R. I. Iwamasa, Ph.D. Thesis, Chemistry, California Institute of Technology, 1967.
2. G. W. Brady and J. T. Krause, J. Chem. Phys. 27, 304 (1957).
3. G. W. Brady, *ibid.* 28, 464 (1958).
4. J. L. Kavanau, Water and Solute-Water Interactions, Holden-Day, Inc., 1964.
5. R. E. Glick, W. E. Stewart, and K. C. Tewari, J. Chem. Phys. 45, 4049 (1966).
6. M. St. J. Arnold and K. J. Packer, Molecular Physics 10, 141 (1966).
7. R. E. Richards and B. A. York, *ibid.* 6, 289 (1963).
8. C. Deverell, D. J. Frost, and R. E. Richards, *ibid.* 9, 565 (1965).
9. C. Deverell and R. E. Richards, *ibid.* 10, 551 (1966).
10. A. Fratiello and D. P. Miller, *ibid.* 11, 37 (1966).
11. W. L. Masterton and L. M. Berka, J. Phys. Chem. 70, 1924 (1966).
12. M. Eisenstadt and H. L. Friedman, J. Chem. Phys. 44, 1407 (1966).
13. E. R. Malinowski, P. S. Knapp, and B. Feuer, *ibid.* 45, 4274 (1966).
14. H. G. Hertz, Z. Elektrochem 65, 20 (1960).

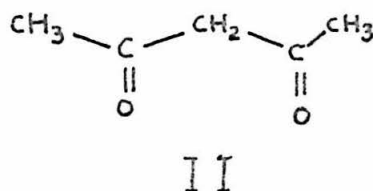
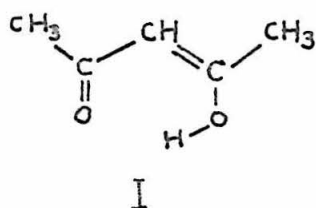
15. H. G. Hertz and M. D. Zeidler, Berchte der Bunsengesellschaft 68, 821 (1964).
16. H. G. Hertz and M. D. Zeidler, *ibid.* 67, Nr. 8, 774 (1963).
17. A. Abragam and R. V. Pound, Phys. Rev. 92, 943 (1953).
18. K. A. Valiev and B. M. Khabibullin, Russ. J. Phys. Chem. 35, 1118 (1961).
19. I. Itoh and Y. Yamagata, J. Phys. Soc. Japan 13, 1182 (1959).
20. M. Eisenstadt and H. L. Friedman, J. Chem. Phys. 46, 2182 (1967).
21. H. S. Frank and W. Y. Wen, Disc. Faraday Soc. 24, 133 (1957).
22. R. Fowler and E. Guggenheim, Statistical Thermodynamics (Translated into Russian), Inostr. Lit., Moscow, p. 391, 1949.

PART III

Elucidation of the Intramolecular Hydrogen-Bond in
Acetylacetone by the Deuterium Isotope Effect on
the Chemical Shift of the Bridge Hydrogen

INTRODUCTION

It is well-known that 2,4-pentanedione (acetylacetone) exists in both the enol (I) and the keto (II) forms, and the interchange between



these two tautomers of this molecule is slow (1). In fact, this exchange is so slow that both tautomers exhibit distinct NMR signals in the PMR spectrum of this compound (1). Proton magnetic resonance studies of acetylacetone have been investigated by several groups of investigators (1-8).

The nature of the intramolecular hydrogen bond in the enol tautomer is, of course, of great interest. Presumably both IR and NMR spectroscopy can be used to elucidate this intramolecular hydrogen bond. There is a little question that the intramolecular hydrogen bond is strong. The OH stretching vibration in the IR spectrum appears (9,10) around 2700 cm^{-1} ; this would indicate a strong hydrogen bond. Additional evidence has come from the PMR studies (8). The position of the bridge hydrogen occurs at approximately 15 ppm downfield from TMS, and as shown by Reeves (1) the position of this resonance is independent of both the concentration and the solvent provided the solvent is not too basic. For example, the chemical shift of the OH proton relative to the enol CH_3 group is

almost unchanged when the solution is diluted with such solvents as cyclohexane and acetic acid. Thus, the intramolecular hydrogen bond is sufficiently strong that the enol tautomer exists primarily in the form of monomers (8).

The object of this research is to obtain some information about the potential function for this intramolecular hydrogen bond. The best approach clearly is to study the energy levels of the OH stretching vibration by IR spectroscopy. This turns out to be more readily said than done. As we shall show later, even the OH.....O stretch in the vicinity of 2700 cm^{-1} is extremely complicated and the spectrum is not readily interpretable. The chemical shift of the bridge hydrogen is a sensitive probe of the average electron density at the proton. However, the measured shift is, in general, only a vibrational average over the zero point vibrational motion, and unless such vibrational averages are known for several vibrational states, it is not possible to infer much information about the potential well. The deuterium isotope effect on the chemical shift of the bridge hydrogen may, in certain cases, provide some information about the nature of the potential function provided the isotope effect is large enough to be measurable.

Deuterium isotope effects on hydrogen chemical shifts are small, typically less than 0.05 ppm (see Table I), and can be readily accounted for by difference in the zero point vibrational amplitudes between the normal and unsubstituted molecules. It is clear that the isotope effect will depend upon the anharmonicity of the potential well.

Table I. Some Typical Deuterium Isotope Effect^a

	H	D
Chloroform and acetone	5.92	5.91
Water and acetone	2.84	2.87
Benzene and acetone	5.14	5.08
Benzene and water	1.75	1.74
Chloroform and water	2.56	2.61
Chloroform and benzene	0.82	0.86

^aP. Diehl and T. Leipert, *Helv. Chim. Acta*, 47, 545 (1964).

However, there exists no theory to predict both the direction and magnitude of this isotope effect. The intramolecular hydrogen bond in acetylacetone is strong. The O—O distance is, for example, only $\sim 2.5 \text{ \AA}$. Thus, we expect the potential function describing the motion of the bridge hydrogen to be extremely anharmonic. It is, then, conceivable that the hydrogen-bond shift would exhibit an unusual isotope effect. With this concept in mind, we have measured the deuterium isotope effect on the chemical shift of the bridge hydrogen in acetylacetone and several other related molecules. This part of the thesis also summarizes the results of several other experiments directed toward a more detailed description of the nature of the intramolecular hydrogen bond in the enol form (or forms) of the acetylacetone. We have, for example, also studied the temperature dependence of the chemical shift of this bridge hydrogen. We shall show that the results of these experiments together with a more careful examination of the IR spectra in the region of the OH, OD stretch and the C—O and C=O stretch enable us to make some definite conclusions regarding the nature of the intramolecular hydrogen bond in acetylacetone.

EXPERIMENTAL

Materials

CCl_4 and acetylacetone were obtained from Matheson Coleman & Bell, D_2O from Columbia Organic Chemical Company, Inc., and 3-methylpentanedione-2,4 from K and K Laboratories, Inc., CD_3COOD , CD_3OH were purchased from Merck Sharp and Dohme of Canada Limited, Co., and CH_3COOH from Van Waters and Rogers, Inc. A sample of CH_3OD was kindly supplied by J. H. Nelson.

Preparation

The partially deuterated acetylacetone was prepared by adding D_2O to acetylacetone, warming up the mixture until it became homogeneous, and then separating the partially deuterated acetylacetone from water by fractional distillation. Partially deuterated 3-methylpentanedione-2,4 was prepared in a similar way.

In the partially deuterated 3-methylpentanedione-2,4 an unassigned resonance was observed at 3.41 ppm downfield from keto methyl group in PMR spectrum and 3.55 ppm downfield from CD_3 group in the deuteron magnetic resonance spectrum. This resonance is probably due to some impurity which we were not able to remove by normal fractional distillation. Since it does not affect our results, no further attempts were made to remove this impurity.

Instrumentation

All the proton magnetic resonance measurements were made using a Varian HA 100 spectrometer. The deuteron magnetic resonance measurements were carried out on a Varian DP 60 spectrometer operating at the frequency of 6.5358 Mcps. In order to improve the signal to noise ratio and to facilitate more accurate measurements of the chemical shifts, the deuteron resonance spectra of partially deuterated acetylacetone and 3-methylpentanedione-2,4 were taken employing the dispersion mode. The deuteron chemical shifts were measured using the standard sideband technique. The deuteron resonance spectra of the other compounds were taken using the absorption mode. All the deuteron resonance spectra were obtained at the probe temperature of 27.5° C.

The temperature dependence of the bridge hydrogen of partially deuterated acetylacetone was carried out on the HA 100 spectrometer operating in the frequency lock mode. The separation of the two ethylene glycol peaks was used to determine the probe temperature. For each temperature, two spectra were taken: one locked at the enol methyl group, the other locked at the keto methyl group. After the spectra were taken, the probe temperature was remeasured to ensure that the probe temperature remained constant during the measurements.

All IR spectra were taken on the Beckman IR-7 spectrophotometer employing double beam operation. A set of nearly matched 0.1 mm sodium chloride cells was used.

RESULTS AND DISCUSSIONS

Deuterium isotope effect

The deuterium magnetic resonance spectra of partially deuterated acetylacetone and partially deuterated 3-methylpentane-dione-2,4 are shown in Fig. 1 and Fig. 2 respectively. The chemical shifts of these two compounds are summarized in Table II and Table III. For comparison, the corresponding proton chemical shifts are also listed in Table II and Table III. It is interesting to note that while the deuterium isotope effect is small for a hydrogen bonded to carbon, of the order of 0.05 ppm, it is extremely large for the bridge hydrogen in the enol tautomers. The magnitude of these isotope effects is of the order of 0.65 ppm and the resonances are shifted to higher fields in the deuterated molecules.

In order to ascertain the origin of this unusually large isotope effect on the chemical shift of the bridge hydrogen, we have measured the deuterium isotope effect for other related compounds. If the isotope effect arises merely from the difference in the vibrational amplitude of the zero point energy, then the results indicate that the deuterium isotope effect is a strong function of the anharmonicity of the potential well and that the potential function describing the vibration of the bridge hydrogen is extremely anharmonic. The later conclusion is probably not unexpected since the intramolecular hydrogen bond is strong. If this is the correct interpretation of the deuterium isotope effect, then it will be appropriate to make similar

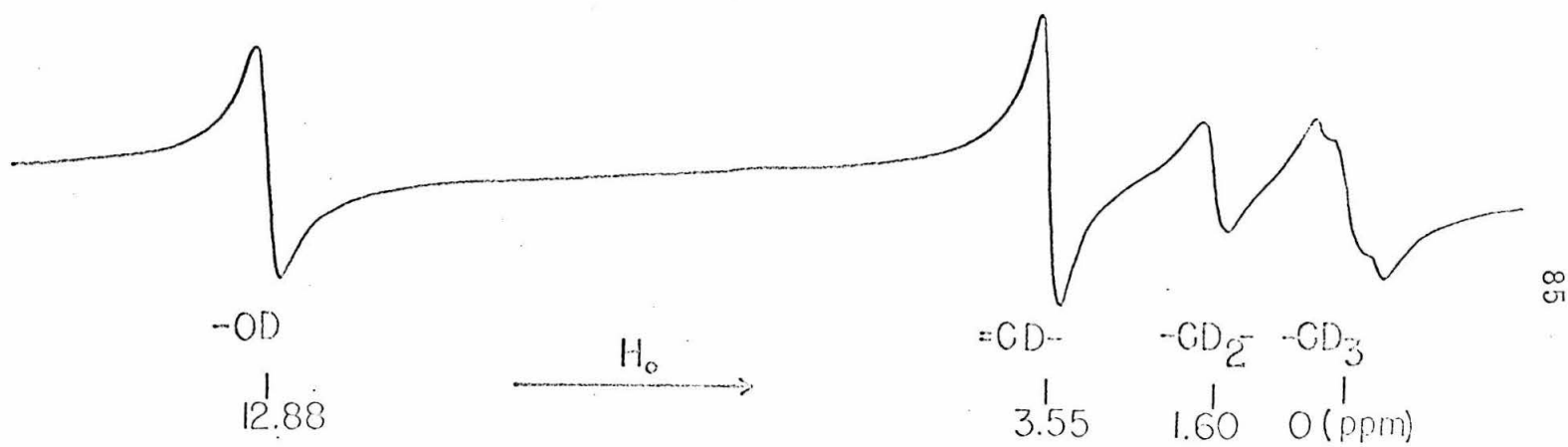


Figure 1. The deuterium magnetic resonance spectrum of partially deuterated acetylacetone.

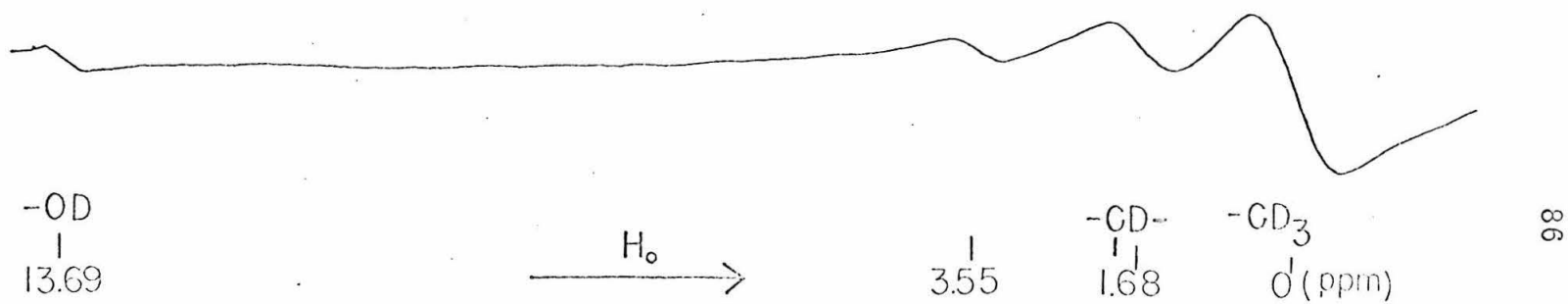


Figure 2. The deuterium magnetic resonance spectrum of partially deuterated 3-methylpentanedione-2,4.

Table II. The Proton and Deuteron Chemical Shifts
of Partially Deuterated Acetylacetone

Group	Chemical Shift ^a	Group	Chemical Shift ^a
CH ₃ (enol)	0	CD ₃ (enol) ^b	0
CH ₃ (keto)	-0.16	CD ₃ (keto)	
-CH ₂ -	-1.58	-CD ₂ -	-1.60 ± 0.03
=CH-	-3.54	=CD-	-3.55 ± 0.03
-OH	-13.56	-OD	-12.90 ± 0.04

^aChemical shift in ppm.

^bNot resolved.

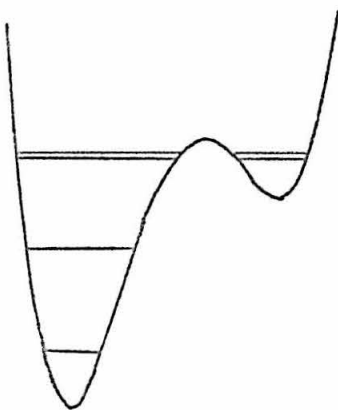
Table III. The Proton and Deuteron Chemical Shift of
Partially Deuterated 3-Methylpentanedione-2, 4

Group	Chemical Shift ^a	Group	Chemical Shift ^a
CH ₃ (keto)	0	CD ₃	0
—C(CH ₃)H—	1.64	—C(CH ₃)D—	-1.68 ± 0.03
-	3.41	-	3.55 ± 0.05
OH	14.32	OD	13.69 ± 0.13

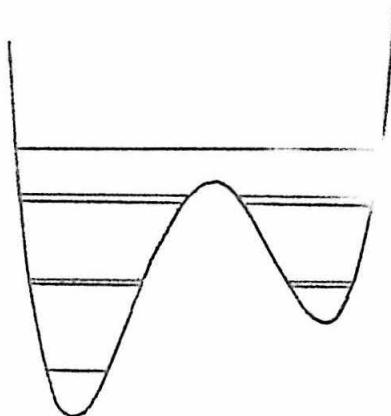
^aChemical shift in ppm.

measurements on other compounds for which the potential functions have been well-characterized.

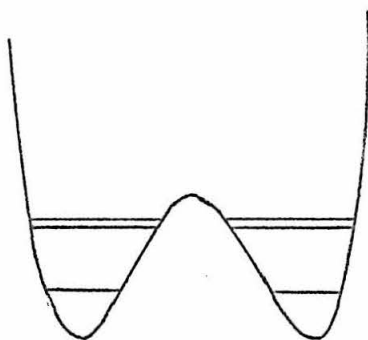
The hydrogen bond potential function for the $\text{O}-\text{H}\cdots\cdots\text{O}$ system has been subjected to numerous investigations (10,12,13). As expected, the potential function is a strong function of the relative acidity of the donor and the basicity of the acceptor of the hydrogen bond. Recently, Chan and Fung (10) carried out a systematic investigation of the energy levels of the hydrogen bond system. These workers examined the IR and near IR spectra of H_2O , HOD , HCOOD , DCOOH , HCOOH , CH_3COOD , CD_3COOD , CH_3OH , and CH_3COOH hydrogen-(or deuterium)-bonded to such bases as acetonitrile, acetone, dioxane, tetrahydrofuran, and dimethylsulfoxide. From the determination of these energy levels they obtained some rather definite information about the anharmonicity of the potential well. For example, the potential function for methanol and water hydrogen bonded to the various solvents was shown to be:



The corresponding potential function for the stronger carboxylic acid solvent complexes were of the following form:



These workers also determined the potential function for the hydrogen bond in the biacetic acid anion. Here, as expected, the potential function is symmetrical double minimum. The potential function of biacetic acid anion is shown as follows:

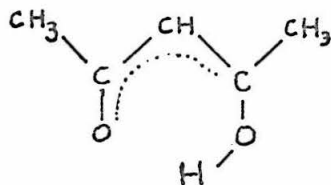


It is clear that the hydrogen bonds in the above systems are all extremely anharmonic. It will be ideal if similar deuterium isotope experiments can be carried out for these systems. However, due to low sensitivity of detection, this was not possible. For this reason, we have chosen instead to examine the deuterium isotope effect for two

systems which we feel are reasonable approximations to the above better characterized systems.

The deuterium magnetic resonance spectra of acetic acid and methanol are shown in Fig. 3 and Fig. 4, respectively. The proton and deuteron chemical shifts for these two compounds are listed in Table IV. As shown in Table IV, the isotope effect for acetic acid and methanol is small. We therefore conclude that the anharmonicity of the potential function is not the primary cause of the large isotope effect observed in acetylacetone and 3-methylpentanedione-2,4.

The potential function for the intramolecular hydrogen bond in acetylacetone is probably not drastically different from those which have been proposed for some of the systems mentioned above. In acetylacetone and its derivative, conjugation of the π system should play an important role in determining this potential function. For example, if the electronic structure is such that there is no conjugation of one of the lone pairs on the terminal oxygens, i. e., if the lone pair is strongly localized at one of the oxygen atoms, then from chemical knowledge we would write the structure of the enol form of acetylacetone as:



Structure I

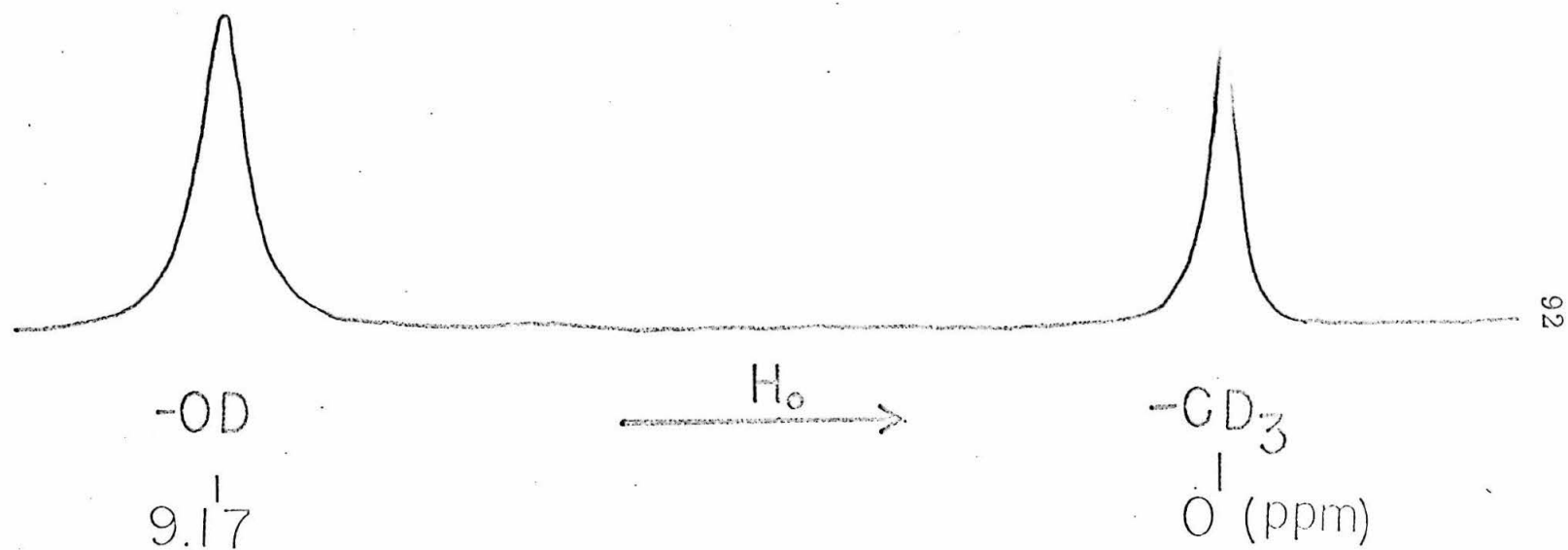


Figure 3. The deuterium magnetic resonance spectrum of a mixture of CH_3COOH and CD_3COOD (10% CH_3COOH).

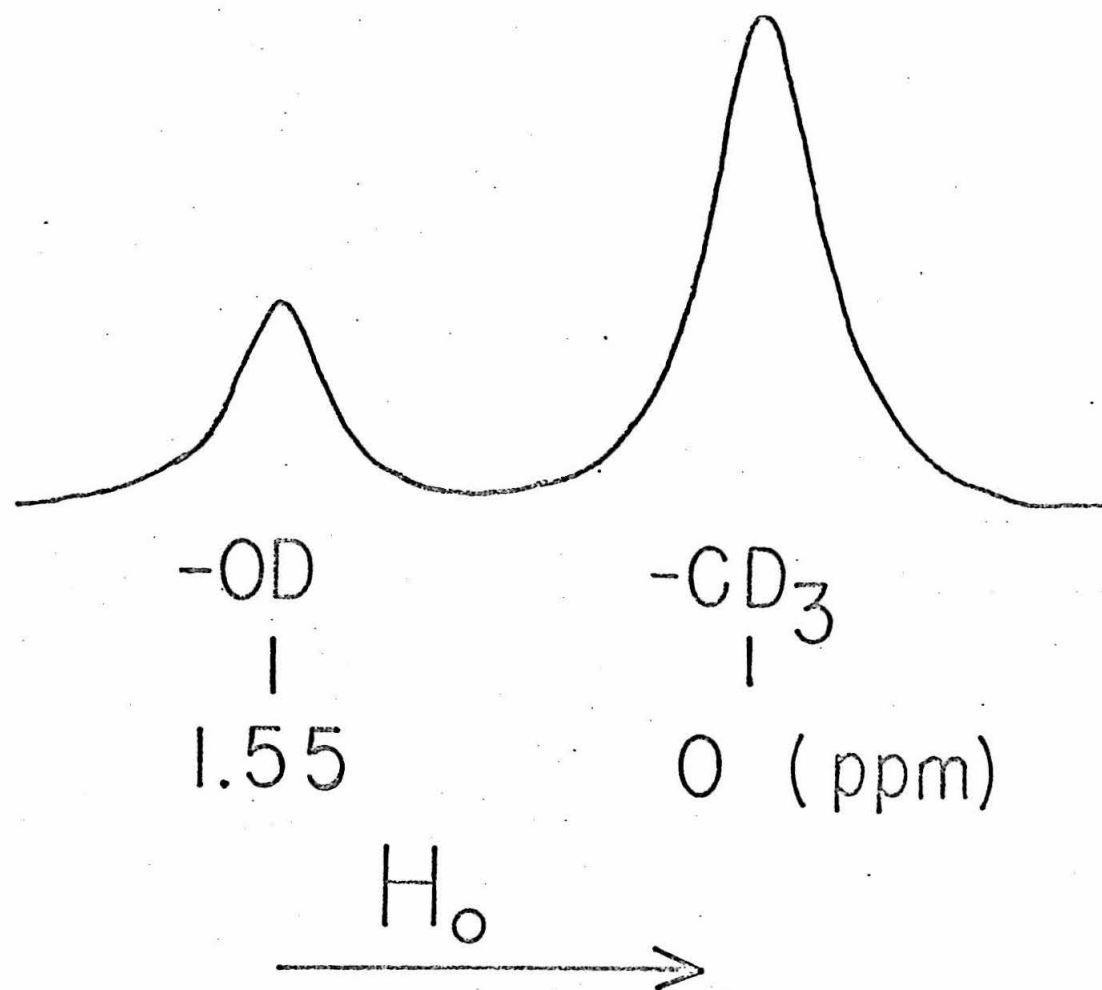


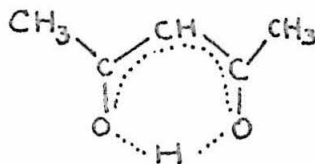
Figure 4. The deuterium magnetic resonance spectrum of a mixture of CH_3OD and CD_3OH (45% CD_3OH).

Table IV. The Proton and Deuteron Chemical Shifts
of Methanol and Acetic Acid

	proton ^a	deuteron ^a
Acetic acid	9.238	9.165 ± 0.04
Methanol	1.54	1.545 ± 0.03

^a Chemical shift in ppm.

In this case, the two oxygen donors and accepters are not equivalent and the potential function should be like that of an alcohol hydrogen-bonded to a ketone. However, if the electrons are completely delocalized, then the two oxygen atoms will be equivalent, in which case one would characterize the structure of the enol form of acetylacetone as follows:



Structure II

In this case the potential function will be similar to the symmetric double minimum suggested by Chan and Fung (10) for the biacetate anion.

It is important to note that these structures are not resonance structures, since the geometry of the $O \cdots H \cdots O$ bond is different in these two structures. In structure I the $H-O-C$ angle is probably $\sim 110^\circ$, whereas in structure II the $O \cdots H \cdots O$ linkage is approximately colinear. These structures, therefore, correspond to distinct electronic states, since the motion of the hydrogen between the two structures is long compared with the time scale of the electronic motion.

From these considerations, we feel we could rule out the possibility that the isotope effect arises from the change in the zero point vibrational amplitude in structure I. However, we cannot rule out

structure II completely. Theoretical calculations indicate that the ground level for symmetric double minimum potential wells is almost doubly degenerate when the potential barrier is very high. As the potential barrier becomes lower, the anharmonicity of the potential function increases and as a consequence, the degeneracy is removed. Therefore, we have to consider inversion doubling and changes in the energies of the inversion states with isotope substitution. It is a good approximation to assume in this case that only the ground inversion doublet is thermally populated at room temperature. Thus, if the average chemical shift in the two inversion states is somewhat different in the two lowest inversion states, which implies of course that the chemical shift is strongly depended on the vibrational amplitude, a large isotope effect will be expected. However, if this is the case, then the chemical shift would be temperature dependent and lowering the temperature would have the same effect as the isotopic substitution. We shall now show that the temperature studies enable us to rule out this possibility.

Temperature studies

Lowering the temperature will populate the lower energy states. Since the measured chemical shift is an average over all the vibrational states, lowering the temperature should have a similar effect upon the chemical shift as the deuterium substitution. The effect of temperature upon the bridge hydrogen chemical shift in acetylacetone is shown in Table V. As shown in Table V, a tempera-

Table V. The Proton Chemical Shifts of Partially
Deuterated Acetylacetone at Various
Temperatures

Temperature	Ethylene glycol	OH	CH	CH ₂	CH ₃ (keto)	CH ₃ (enol)
-14.0° C	200.1 ^a 199.9	1372.9 1355.2	355.5 -	164.1 146.8	0.0	0.0
- 5.5	191.8 191.6	1368.8 1352.6	355.3 338.7	163.2 146.1	0.0	0.0
7.0	179.2 179.0	1365.1 1347.1	355.2 338.4	162.3 145.5	0.0	0.0
16.2	170.3 169.5	1360.8 1444.2	354.9 338.3	164.4 144.7	0.0	0.0
24.5	160.9 160.7	1356.4 1339.6	354.8 338.3	160.9 144.2	0.0	0.0
34.5	152.6 151.4	1351.6 1334.5	354.6 338.2	160.5 144.1	0.0	0.0
43.8	142.5 142.5	1347.5 1330.6	354.7 337.9	159.9 143.5	0.0	0.0
54.3	132.4 132.1	1342.5 1326.5	354.1 338.0	159.4 143.0	0.0	0.0
64.0	122.7 122.9	1337.6 1322.4	354.2 337.9	159.1 142.5	0.0	0.0
73.2	113.6 113.5	1334.0 1318.8	354.1 337.6	158.7 142.0	0.0	0.0
82.7	104.2 104.3	1330.3 1314.8	354.1 337.5	157.9 141.7	0.0	0.0
93.0	93.9 93.6	1326.5 1310.0	353.7 337.4	157.7 141.4	0.0	0.0

Table V (continued)

Temperature	Ethylene glycol	OH	CH	CH ₂	CH ₃ (keto)	CH ₃ (enol)
102.7	84.6	1321.8	353.8	154.4		0.0
	84.3	1306.5	337.3	140.7	0.0	
112.5	75.3	1318.7	353.6	150.7		0.0
	74.3	1302.5	337.3	140.7	0.0	
122.5	64.3	1314.7	353.4	156.6		0.0

ture effect is indeed observed. However, the temperature effect is opposite in direction to the deuterium isotope effect. (Lowering the temperature has a downfield shift effect, whereas the deuterium isotope effect observed is upfield.) This result is quite different from what one would expect, if the isotope effect arises from the difference in the zero point vibrational amplitude, since both lowering the temperature and the deuterium isotope substitution tend to emphasize the same part of the potential well, and therefore should lead to changes in the same direction. On the basis of this observation, we can therefore rule out the second possibility raised in the previous section.

However, the existence of the temperature effect is interesting. It suggests that there are at least two states which are populated at room temperature and the chemical shifts of the bridge hydrogen is quite different in these states. The above discussion, however, enables us to eliminate the possibility that the other state corresponds to the upper inversion level of structure II. Thus, these states must either be those of another species, or the potential function for the intramolecular hydrogen bond is considerably more complicated than we have assumed it to be. Physical and chemical intuition indicate that the latter is probably more unlikely.

IR studies

It is clear from the previous section that there are at least two energy states which are thermally populated at room temperature and which are associated with the motion of the bridge hydrogen. The

chemical shift moves downfield with decreasing temperature; this would indicate that the proton is less shielded magnetically for the lower energy states. However, deuterium substitution apparently increases the population of the upper state. As we concluded in the previous section, these results tend to suggest that the enol form of acetylacetone exists in two or more forms. The species which immediately come to mind are the intra- and inter-molecular hydrogen bonded molecules. However, there appears to be sufficient evidence to rule out any appreciable concentration of intermolecular hydrogen-bonded complexes. The intramolecular hydrogen-bond is strong, and both the IR and the PMR data, as we have indicated before, are independent of concentration and solvent provided the solvent is not too basic. The question is then, whether there may be two or more intramolecular hydrogen bond species which are electronically different. We have already indicated two possible structures for the hydrogen bond in the enol tautomer. There is, of course, no a priori reason why these two structures cannot coexist as distinct tautomers.

Nuclear magnetic resonance by virtue of its slow time scale of observation cannot usually distinguish species which are rapidly exchanging. In fact, when the exchange rate between various species is fast, the measured chemical shift is an average of all these species. Hence, it is very difficult to deduce much information about each species from the NRM results. IR spectroscopy, on the other hand, by virtue of its considerably faster time scale of observation is often a more powerful method for deciding structure questions. For this

reason, we have decided to reexamine the IR spectra of acetylacetone. The IR spectra of acetylacetone and several derivatives have been investigated by several groups of investigators (9, 14).

The IR spectra of partially deuterated acetylacetone in the region of OH and OD stretch are shown in Fig. 5 and Fig. 6 respectively. The IR spectrum was determined to be concentration independent and was also invariant upon dilution in other solvent. As shown in Fig. 5 and Fig. 6 the OH stretch in the vicinity of 2700 cm^{-1} and OD stretch in the vicinity of 2000 cm^{-1} regions are quite complicated. The band around 2700 cm^{-1} is extremely broad; in fact it appears to consist of a superposition of several bands. This feature, which was reproducible in all of our spectra, has apparently never been discussed in the literature prior to the present work. The OD band at 2000 cm^{-1} exhibits no evidence of fine structure and was somewhat narrower than the corresponding band of the normal molecule.

It is difficult to deduce definite information from these spectra. However, it also appears that these data are not inconsistent with the existence of two or more enol tautomers, since the spectra are indeed more complicated than one would expect.

The IR spectrum of acetylacetone in the region of C—O and C=O stretch was shown in Fig. 7. Band a ($\nu = 1727\text{ cm}^{-1}$) and band b ($\nu = 1707\text{ cm}^{-1}$) were previously assigned by Mecke and Funck (9) to the symmetric and antisymmetric keto C=O stretch. Band d ($\nu = 1455\text{ cm}^{-1}$) was assigned to the C—O stretch of the enol form. Band e was assigned to be a superposition of two unresolved bands: one at

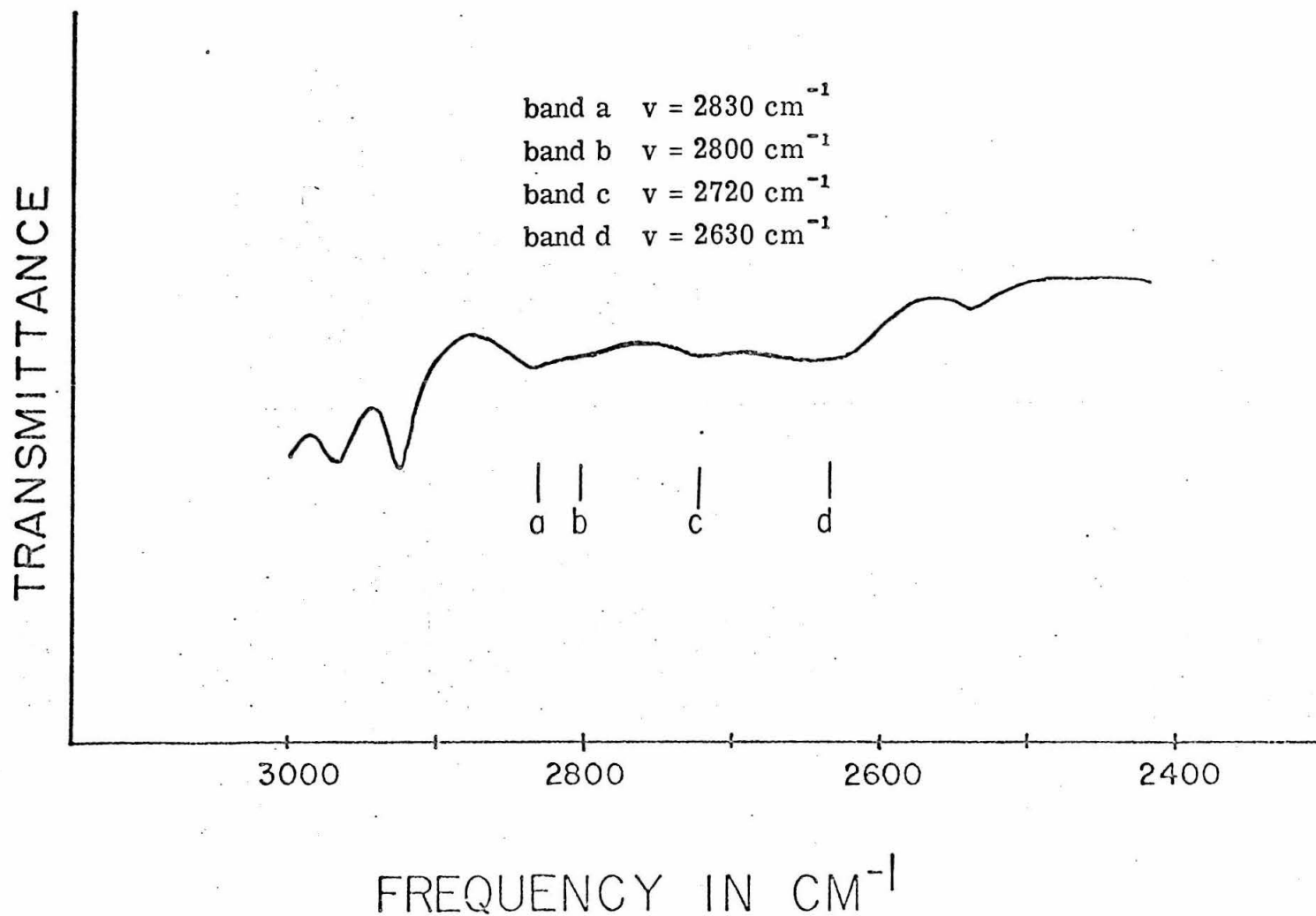


Figure 5. The IR absorption spectrum of acetylacetone at OH stretching vibration region.

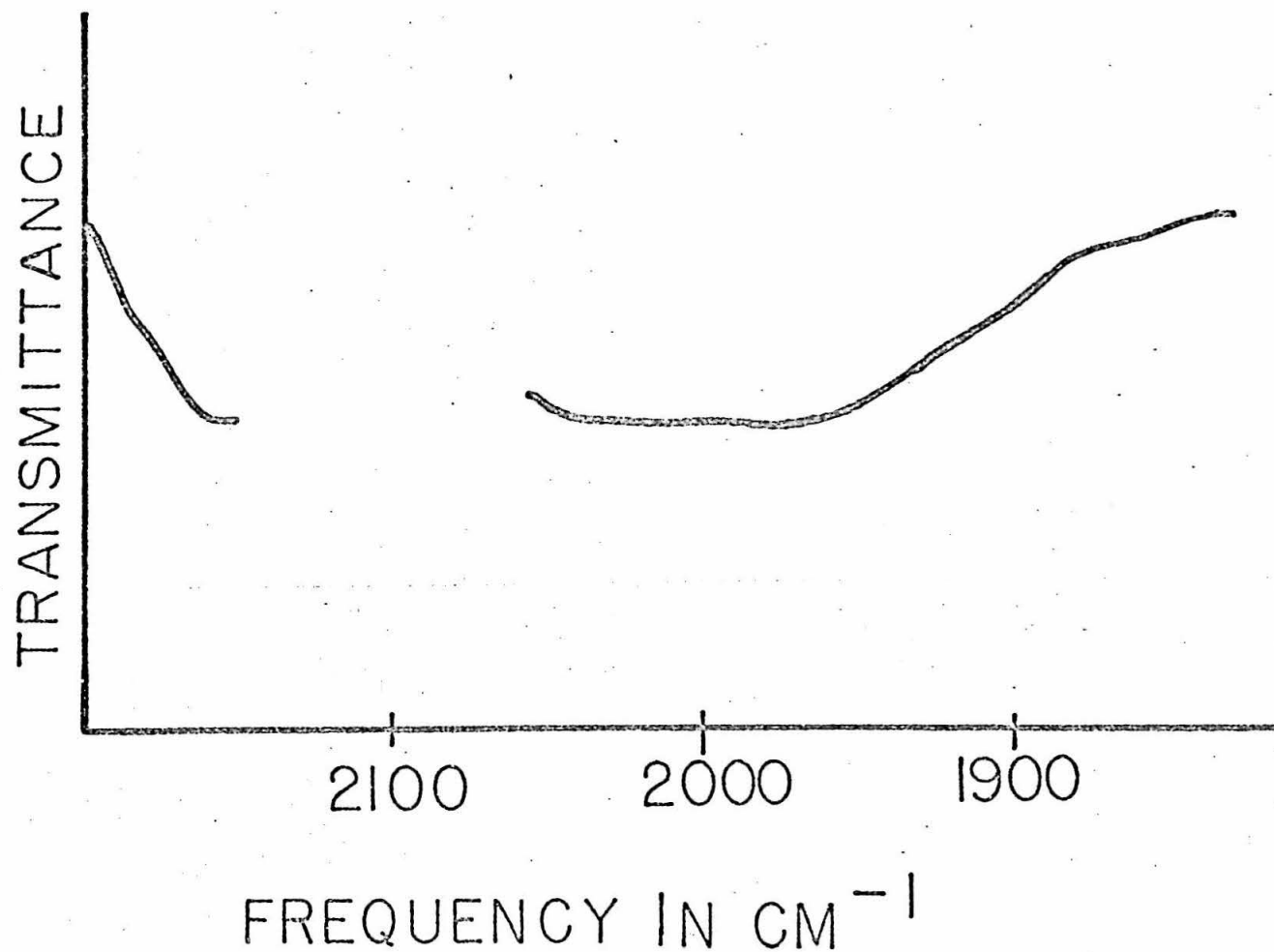


Figure 6. The IR absorption spectrum of partially deuterated acetylacetone at OD stretching vibration region

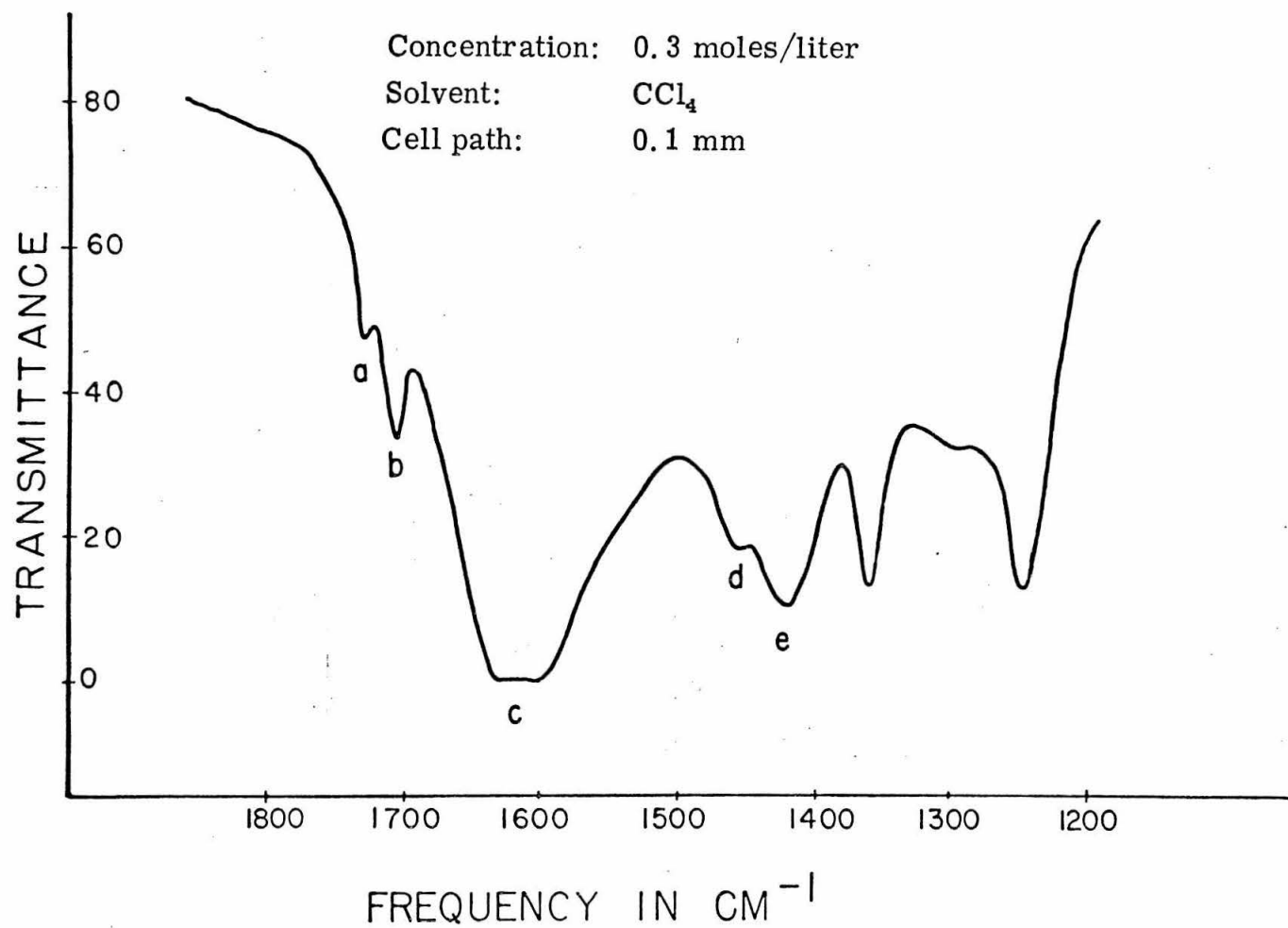


Figure 7. The IR absorption spectrum of acetylacetone at $\nu = 0$ stretching vibration region.

$\nu = 1419 \text{ cm}^{-1}$ for the C—OH bending mode of the enol tautomer and the other at $\nu = 1420 \text{ cm}^{-1}$ for the CH_3 bending mode in the keto tautomer. There is a shoulder at $\sim 1545 \text{ cm}^{-1}$, this band probably corresponds to the C=C stretching vibration of the enol tautomer. The strong band c ($\nu = 1616 \text{ cm}^{-1}$) was assigned to the stretching vibration of the C=O in the enol form. Thus, there is the strong IR evidence for the existence of an enol tautomer with electronic structure I. The assignments of these bands seems clear cut enough and beyond question. It may be recalled, however, that the existence of this structure alone would not account for both the temperature dependence and deuterium isotope effect.

We now wish to comment on the band at 1616 cm^{-1} . As we mentioned previously this band has been assigned by other workers to the C=O stretching vibration of the enol tautomer. There are some difficulties connected with this assignment: First, the band appears to be unusually broad. Secondly, we feel that it is also unusually intense. Thirdly, one might argue that this band should appear at a somewhat higher frequency. Even though the hydrogen bond is strong, the C=O group in the enol form, as depicted by structure I, is still to a good approximation that of a strong alcohol hydrogen-bonded to a ketone. Thus, it is possible that the broad band at 1616 cm^{-1} is a superposition of a number of bands. In fact, we propose that this broad band consists of superposition of three bands; the C=O stretch of the structure I, and the symmetric and antisymmetric stretch of C=O in structure II. The C=O stretching

frequency for the structure I, we feel, is located on the higher frequency side of this unresolved band, while we assigned the remainder to the two C=O stretching vibrations of structure II. The center of the C=O stretching vibration in enol tautomer II should appear at a lower frequency than the C=O stretch in the enol structure I. This follows because we expected the C \cdots O bond in structure II to be between a double and a single bond, if the electronic structure of this species is that indicated in structure II.

Summary

In summary, the deuterium isotope effect on the chemical shift of the bridge hydrogen and the temperature dependence of bridge hydrogen chemical shift suggest that there are two enol structures for acetylacetone. The basic difference between these tautomers is in the electronic structure of the π system. Apparently the OH \cdots O bond plays an important role in determining the electronic structure of the π system.

The temperature studies indicate that structure II is the lower energy structure, since the proton chemical shift of the bridge hydrogen is expected to be the least shielded in this tautomer. The deuterium isotope effect indicates that the difference in the zero point energies between these two structures is decreased upon deuterium substitution. This is, of course, expected when the potential function for structure I is symmetrically double minimum while that for structure II is asymmetric. Because of the central barrier in the

potential function of structure II, the change in the zero point energy with deuterium substitution here is expected to be less than that in the asymmetrical form. To a good approximation, we can ignore the higher vibrational states of the OH (or OD) stretch in both forms, since these higher vibration levels lie $\geq 2000 \text{ cm}^{-1}$ higher. However, the energy difference between the two enol forms is apparently only of the order of kT .

MODEL

In this section, we shall attempt to place the above results on a somewhat more quantitative basis. We propose the following model: We assume that there are only two enol structures. The vibrational potential function for structure I is asymmetric, while that for structure II is symmetrical double minimum. For the normal molecule, we shall denote their zero-point energy difference by ΔE_H^0 , and for the deuterated molecule, we shall denote the difference in their zero point energies by ΔE_D^0 . A schematic representation of energy levels is given in Fig. 8. We shall assume an equilibrium between these two structures. This equilibrium will be rapid on NMR (or PMR) time scale; however, it will be slow on the IR time scale. It is clear from the previous discussion that the equilibrium constant, K , will be isotope dependent. In fact, we shall show that the deuterium isotope effect is merely a reflection of the change in the free energy difference between the two enol tautomers in the normal and deuterated molecules.

If we ignore the higher vibrational states of both structures, then there will be two "ground" vibrational energy states for structure II and for structure I. The two vibrational states for structure II are the well-known symmetric and antisymmetric vibrational states. It should be pointed out, however, that only half of the possible rotational-nuclear-spin states are allowed by Pauli principle in these two vibrational states. For structure I there is only one



Figure 8. The symmetric and asymmetric potential functions and energy levels.

vibrational state of interest. Here, of course, all the nuclear spin states are symmetry allowed. There is, of course, another way of looking at the problem. We can, for example, include in the discussion that there are two structures I; e.g., the one depicted in Fig. 8a and its mirror image. The reason why we can ignore one of these is that we assume that the potential barrier to go from one to another is very high and the resonance between two wells has no effect on the energy. Clearly, if resonance is included in the treatment of the problem, the Hamiltonian has C_{2v} symmetry, and again, we have to bring in nuclear spin statistics. In this representation, the energy levels are doubly degenerate and only half of the rotational and nuclear spin states of the symmetric and antisymmetric states are allowed. In any case, the above discussion clearly indicates that there is no entropy difference between these two structures I and II, if we ignore the minor differences in the structure of these two molecules. Then,

$$\Delta F^0 = \Delta H^0 = \Delta E^0$$

and

$$K = e^{-\Delta F^0/kT} = e^{-\Delta E^0/kT}$$

The exchange-averaged chemical shift can be expressed as

$$\delta_{\text{obs}} = \delta_1 P_1 + \delta_2 P_2 \quad (1)$$

where P_1 and P_2 are the mole fraction of structure I and structure II respectively, and δ_1 and δ_2 are the chemical shifts for structure I and structure II respectively. Equation 1 can be rewritten as:

$$\delta_{\text{obs}} = \delta_1 \frac{1}{1 + e^{\Delta E/kT}} + \delta_2 \frac{e^{\Delta E/kT}}{1 + e^{\Delta E/kT}} \quad (2)$$

For the normal compound $\Delta F^0 = \Delta E_H^0$ and for deuterated compound $\Delta F^0 = \Delta E_D^0$.

We shall use this model to show that the temperature dependence of bridge hydrogen chemical shift, the deuterium isotope effect, and the IR results are all consistent with one another, thus, suggesting that our model may not be very far from reality. We shall first extract a Δ_H^0 from the temperature measurements of the bridge hydrogen chemical shift. On the bases of the IR data, we shall estimate $\Delta E_H^0 - \Delta E_D^0$, from which ΔE_D^0 will be obtained when combined with ΔE_H^0 . The deuterium isotope effect can then be calculated and can be compared with experiment.

Estimation of ΔE_H^0 from temperature dependence of the bridge hydrogen chemical shift

According to our model

$$\delta_{\text{obs}}^H = \delta_1^H \frac{1}{1 + e^{\Delta E_H^0/kT}} + \delta_2^H \frac{1}{1 + e^{\Delta E_H^0/kT}} \quad (3)$$

There are three unknowns, δ_1^H , δ_2^H , and ΔE_H^0 , and two measurable quantities, δ_{obs}^H and T in equation 2. If one measures three sets of δ_{obs}^H and T and plugs these values into equation 2, then theoretically all δ_1^H , δ_2^H , and ΔE_H^0 can be solved since there are three

simultaneous equations and only three unknown parameters. Fifteen sets of data were collected for this purpose. Theoretically, it is possible to fit these three unknown parameters from these 15 sets of data. However, this turns out to be more readily said than done. Instead of trying to fit all these three unknown parameters at once, the following procedure was applied:

- (1) Pick a particular value of ΔE_H^0 .
- (2) Plug this value into equation 3.
- (3) Do a least square fitting for values δ_1^H and δ_2^H .
- (4) Calculate the standard deviation, σ .
- (5) Pick another value of ΔE_H^0 .
- (6) Repeat procedures 2-5.
- (7) Make a σ vs. ΔE_H plot.

The σ vs. ΔE_H^0 plot is shown in Fig. 9. There is a minimum at $\Delta E = 673 \text{ k (} 467 \text{ cm}^{-1}\text{)}$. The set of parameters which gave the best fit between the measured and calculated chemical shifts were: $\Delta E_H^0 = 467 \text{ cm}^{-1}$, $\delta_1^H = 7.30 \text{ ppm}$, $\delta_2^H = 14.21 \text{ ppm}$. The observed and the calculated chemical shifts for this set of parameters are shown in Table VI.

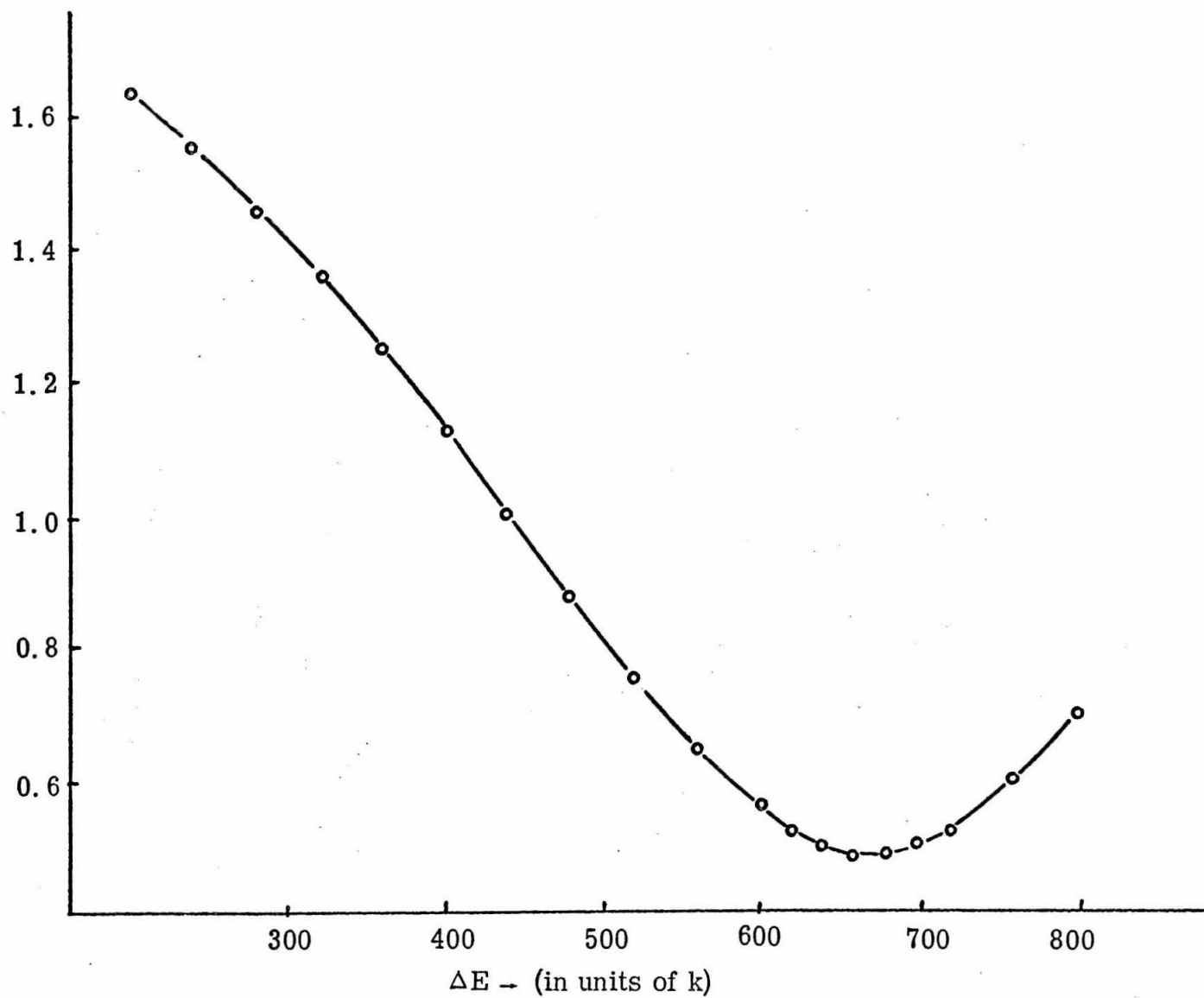


Figure 9. The standard deviation vs. ΔE plot

Table VI. The chemical shift of OH proton in acetylacetone (refer to enol CH_3 group) at various temperatures.

$$\delta_1 = 1421.4, \delta_2 = 730, \Delta E = 672 \text{ k}$$

Temperature °C	δ_{obs}	δ_{cal}	$\delta_{\text{obs}} - \delta_{\text{cal}}$
122.5	1314.7	1314.5	-0.19
112.5	1318.7	1318.4	-0.27
102.7	1322.3	1322.3	-0.04
93.0	1326.5	1325.3	-0.19
82.7	1330.3	1330.6	0.28
73.2	1334.0	1334.6	0.59
64.0	1338.4	1338.5	0.13
54.3	1342.5	1342.7	0.24
43.8	1347.0	1347.4	0.36
34.5	1351.3	1351.5	0.19
24.5	1356.4	1356.0	-0.42
16.2	1360.8	1359.7	-0.08
7.0	1364.7	1363.9	-0.83
-5.5	1368.8	1369.5	0.71
-14.0	1372.9	1373.3	0.43

Standard deviation 0.487 Cps.

Potential function for the two enol structures and the estimation of isotope effect on the zero point energy.

The two potential functions for the two enol form structures of acetylacetone have been shown in Fig. 8. In this section we shall calculate the energy levels of these two potential functions from the data obtained from the IR spectra in the OH and OD stretching vibration regions.

As shown before, the potential function for structure II can be approximated by

$$V(x) = ax^4 - \frac{1}{2} kx^2 \quad (4)$$

where x is the vibration coordinate. Using the linear transformation

$$X = \left(\frac{8\mu a'}{\hbar^2} \right)^{\frac{1}{6}} x$$

Chan et al. (15) were able to rewrite equation 4 as following:

$$\begin{aligned} V(x) &= \left(\frac{a\hbar^4}{b4M^2} \right)^{\frac{1}{3}} (X^4 - \eta X^2) \\ &= A(X^4 - \eta X^2) \end{aligned} \quad (5)$$

where

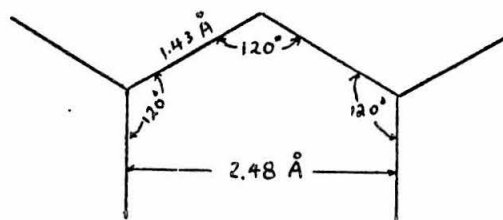
$$\eta = \frac{k^3 \mu}{a^2 \hbar^2}$$

and μ is the reduced mass.

As shown in Fig. 5 and Fig. 6, the IR spectra in the OH and OD stretching vibration regions are very complicated. There may

be four bands in the OH stretching vibration region. Only two of these four bands are to be ascribed to the 1→4 and 2→3 transitions. One or two of these four bands may arise from the 0→1 transition for structure I. There are 6 possible combinations from these 4 bands; 2830 cm^{-1} and 2800 cm^{-1} , 2830 cm^{-1} and 2720 cm^{-1} , 2830 cm^{-1} and 2630 cm^{-1} , 2800 cm^{-1} and 2720 cm^{-1} , 2800 cm^{-1} and 2630 cm^{-1} , and 2700 cm^{-1} and 2630 cm^{-1} . Only one of these combinations may be due to the 1→4 and 2→3 transitions.

Theoretical calculations indicate that the closer the $0\cdots 0$ distance in the system, the lower the energy barrier (10), i. e., the shorter the $0\cdots 0$ distance the larger the separation between the 1→4 transition band and the 2→3 transition band. Chan and Fung (10) in their studies of biacetic anion indicated that the distance between the two minima is 0.82 Å. The separation between the 1→4 and 2→3 transition bands here was 90 cm^{-1} . Assuming OH distance in biacetic acid anion is 0.9 Å, then the $0\cdots 0$ distance in biacetate anion is $2 \times 0.9 + 0.82 = 2.62\text{ Å}$. The $0\cdots 0$ distance in acetylacetone calculated from the following model is $1.43 \times \sqrt{3} = 2.48\text{ Å}$.



This value is much less than the $0\cdots 0$ distance in the biacetate anion. It is, therefore, expected that the separation between the 1→4 and

and 2-3 transitions is larger than 90 cm^{-1} . On this basis, we only considered the following four pairs in our calculations. They are: 2830 cm^{-1} and 2630 cm^{-1} , 2830 cm^{-1} and 2720 cm^{-1} , 2800 cm^{-1} and 2630 cm^{-1} , and 2800 cm^{-1} and 2720 cm^{-1} .

The calculation of energy levels for the potential function as shown in equation (5) has been treated by Chan et al. (15). In general, the separation between the 1-4 and 2-3 transition bands is dependant upon the value η . A band separation vs. η plot is shown in Fig. 10. Fig. 10a indicates the case that the 1-4 transition band is at 2830 cm^{-1} , whereas Fig. 10b indicates the case when the 1-4 transition is assigned to be 2800 cm^{-1} . From Fig 10, the parameters A and η are obtained. The potential functions for the four pairs are:

$$V(x) = 171.7(x^4 - 11.05x^2) \text{ for the } 2830 \text{ and } 2630 \text{ pair}$$

$$V(x) = 168.2(x^4 - 11.26x^2) \text{ for the } 2800 \text{ and } 2630 \text{ pair}$$

$$V(x) = 165.2(x^4 - 11.80x^2) \text{ for the } 2830 \text{ and } 2720 \text{ pair}$$

$$V(x) = 160.9(x^4 - 12.10x^2) \text{ for the } 2800 \text{ and } 2700 \text{ pair}$$

The first four energy levels corresponding to these potential functions are listed in Table VII.

For the calculation of the potential function and the corresponding energy levels of the deuterated acetylacetone the following relations were applied:

$$\frac{A_D}{A_H} = \left(\frac{\mu_H}{\mu_D} \right)^{\frac{2}{3}}$$

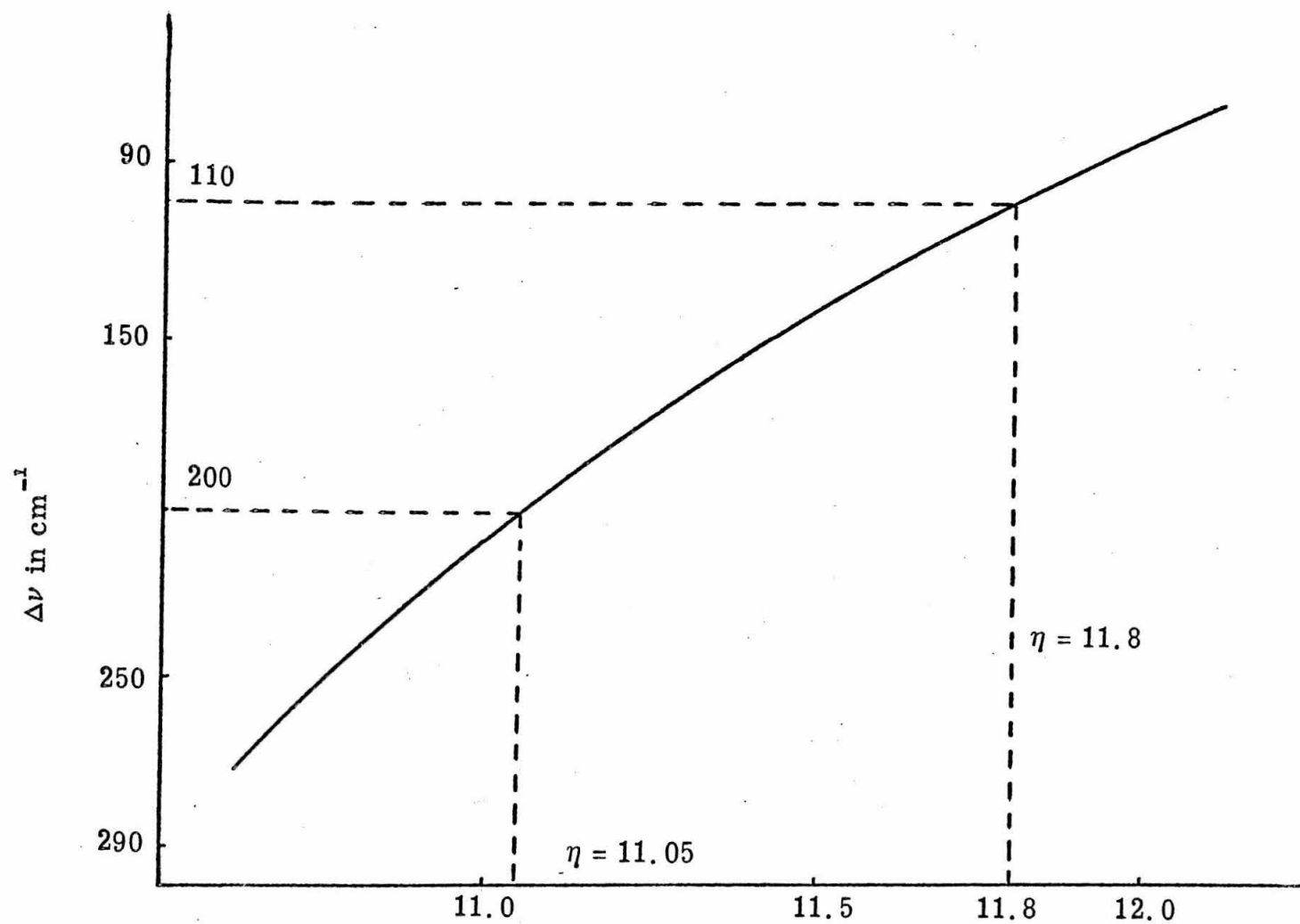


Figure 10a. The band separation with respect to the 2830 cm^{-1} bond

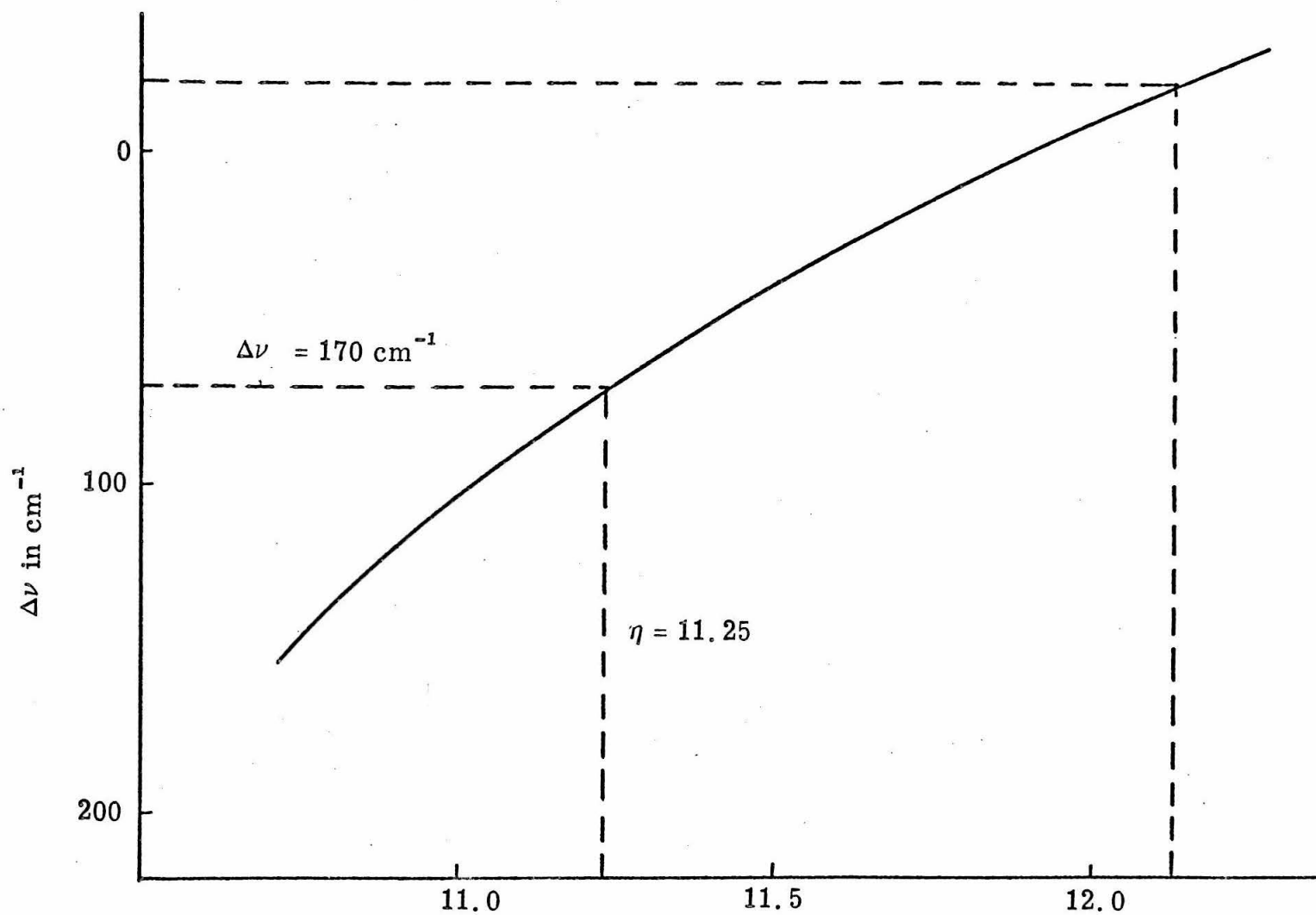


Figure 10b. The bond separation with respect to $280^\circ \text{ cm}^{-1}$ bond

TABLE VII

η	11.05	11.25	11.8	12.15
E(0)	-3698	3795	4208	4365
E(1)	-3695	3791	4207	4364
E(2)	-1064	1160	1484	1645
E(3)	- 869	994	1378	1565
a	171.7	168.2	165.2	160.9
0-3	2830	2800	2830	2800
1-2	2630	2630	2720	2720

TABLE VIII

E(0)	-4134	4226	4646	4798
E(1)	-4134	4226	4646	4798
E(2)	-2077	2184	2570	2741
E(3)	-2068	2178	2569	2741
A	108.19	105.97	104.1	101.37
0-3	2066	2050	2077	2057
1-2	2057	2042	2076	2056

TABLE IX

E(0)	-4010	4134	4480	4666
E(1)	-4010	4134	4480	4666
E(2)	-2015	2137	2479	2665
E(3)	-2006	2131	2478	2665
A	104.94	103.67	100.28	98.57
0-3	2004	2003	2002	2001
1-2	1998	1997	1998	2001

$$\frac{\eta_D}{\eta_H} = \left(\frac{\mu_D}{\mu_H} \right)^{\frac{1}{3}}$$

where μ_D and μ_H are the reduced masses of the deuterium and the proton respectively. The values of A_D and η_D calculated from these relations and the first four energy levels based on these A_D and η_D values are listed in Table VIII. In all these calculations, $\mu_D/\mu_H = 2.0$ was assumed. The observed OD stretching vibration frequency is $\sim 2000 \text{ cm}^{-1}$ (see Fig. 8). As shown in Table VIII, the calculated 1 \rightarrow 4 and 2 \rightarrow 3 transitions are always a little high. For this reason, A_D was adjusted so that the 1 \rightarrow 4 and 2 \rightarrow 3 transitions for the deuterated molecule fall at 2000 cm^{-1} . The energy levels calculated from these new values are shown in Table IX.

From the zero point energies for the normal molecule and the deuterated molecule, we can calculate the zero point energy difference between the normal and the deuterated molecule. For structure II, we denote this energy difference as ΔE_{II} . From Table VII and Table IX, the following ΔE_{II} values were obtained:

$$\Delta E_{II} = 312 \text{ cm}^{-1} \text{ for the 2830 and 2630 pair}$$

$$\Delta E_{II} = 339 \text{ cm}^{-1} \text{ for the 2800 and 2630 pair}$$

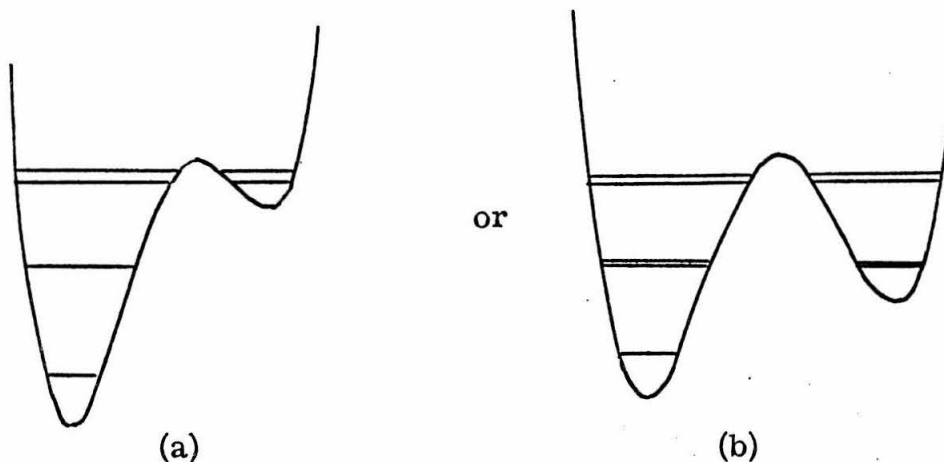
$$\Delta E_{II} = 272 \text{ cm}^{-1} \text{ for the 2830 and 2720 pair}$$

$$\Delta E_{II} = 301 \text{ cm}^{-1} \text{ for the 2800 and 2720 pair}$$

Since no further information is available, any one of these four values is possible. However, these values do not vary too much. We shall

assume $\Delta E_{\text{II}} \cong 300 \text{ cm}^{-1}$ in our later calculations.

The potential function for the asymmetric form can generally be approximated as



Structure a is quite similar to the potential function for methanol hydrogen bonded to most solvents, whereas structure b is quite similar to the stronger carboxylic acid-solvent hydrogen bonded complexes. In the former case there is only one band in the fundamental OH stretching vibration region while in the later case there are generally two bands in the fundamental OH stretching vibration region. However, for the ground vibrational state it is adequate to assume in both cases that the isotope shift is given by:

$$\frac{\nu_{\text{H}}}{\nu_{\text{D}}} = \sqrt{\frac{\mu_{\text{D}}}{\mu_{\text{H}}}} = 1.414$$

If we denote the energy difference between the zero point energy of normal and deuterated molecules as ΔE_{I} , then from Fig. 8a it is

clear that

$$\Delta E_I = \frac{1}{2} (\nu_H - \nu_D) = \frac{1}{2} \left(\nu_H - \frac{1}{1.414} \nu_H \right) = 0.146 \nu_H$$

If the fundamental frequency for the OH stretch, ν_H is $\sim 3000 \text{ cm}^{-1}$, then

$$\Delta E_I = 0.146 \times 3000 \approx 440 \text{ cm}^{-1}$$

The isotope effect is therefore

$$\begin{aligned} \Delta E_I - \Delta E_{II} &\approx 440 \text{ cm}^{-1} - 300 \text{ cm}^{-1} \approx 140 \text{ cm}^{-1} \quad (6) \\ &= \Delta E_H^0 - \Delta E_D^0 \end{aligned}$$

Calculation of the deuterium chemical shift

From equation 2, the deuterium chemical shift is given by:

$$\delta_{\text{obs}}^D = \delta_1^D \frac{1}{1 + e^{\Delta E_D^0/kT}} + \delta_2^D \frac{e^{\Delta E_D^0/kT}}{1 + e^{\Delta E_D^0/kT}} \quad (7)$$

We shall assume that

$$\delta_1^D \approx \delta_1^H = 7.30 \text{ ppm} \quad (8)$$

$$\delta_2^D \approx \delta_2^H = 14.21 \text{ ppm} \quad (9)$$

since the changes in the chemical shift due to the changes in the vibrational amplitude are usually less than 0.05 ppm. Since

$$\Delta E_H^0 + \Delta E_D^0 = \Delta E_I - \Delta E_{II} \approx 140 \text{ cm}^{-1}$$

and $\Delta E_H^0 = 476 \text{ cm}^{-1},$

therefore,

$$\Delta E_D^0 = 476 \text{ cm}^{-1} - 140 \text{ cm}^{-1} \approx 336 \text{ cm}^{-1}$$

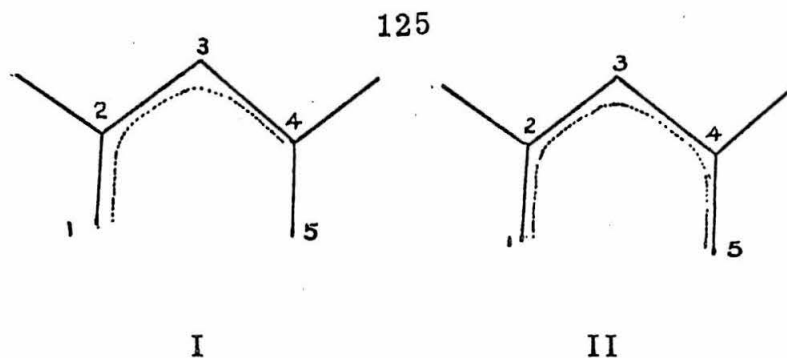
From equations 7-10, the chemical shift of the bridge deuterium at 27.3° C in deuterated acetylacetone is then

$$\begin{aligned} \delta_{\text{cal}}^D &= \frac{7.3}{1 + e^{336/207}} + \frac{14.214}{1 + e^{336/207}} \\ &= 12.99 \text{ ppm}, \end{aligned}$$

in good agreement with the observed chemical shift of 12.90 ppm.

Molecular Orbital Calculations

It has been shown that there are two different electronic structures of the enol form of acetylacetone. The basic difference between these two structures is in the electronic structure of the π system. In structure I, one of the oxygen lone pairs is localized at the hydrogen bonded oxygen, whereas in structure II these two electrons are also delocalized into the π -system of the acetylacetone molecule. The electronic structure for these two forms are shown as follows:



It seems that structure I might be energetically unfavorable. However, one should be reminded that the Coulomb energy for oxygen atom is larger than that of carbon atom. The gain of this Coulomb energy may be large enough to compensate the loss due to the delocalization energy. A calculation of energy difference for these two electronic structures would therefore be appropriate. In this section, we present a simple HMO calculation for these two structures.

Structure I

Point group: C_1

Basic assumptions:

$$\alpha_1 = \alpha_5 = \alpha_C + 2\beta$$

$$\beta_{ij} = S_{ij}\beta = \beta \text{ if } i \text{ and } j \text{ are neighboring atoms,}$$

$$\text{except } \beta_{4,5} = 0.$$

Energy levels:

$$\text{energy} = \alpha + \beta x$$

$$x = -2.496, -1.220, -0.220, \text{ and } 1.496.$$

Eigenvectors:

$$x = -2.496 \quad \psi_A = 0.873\phi_1 + 0.433\phi_2 + 0.208\phi_3 + 0.083\phi_4$$

$$x = -1.220 \quad \psi_B = 0.354\phi_1 - 0.276\phi_2 - 0.691\phi_3 - 0.566\phi_4$$

$$x = -0.220 \quad \phi_C = 0.294\phi_1 - 0.652\phi_2 - 0.153\phi_3 + 0.683\phi_4$$

Total π electron energy:

$$4\alpha + 2(2.496 + 1.220) = 4\alpha + 7.432\beta$$

Total energy for 6 electrons = total π electron energy

+ localized electron energy

$$= 6\alpha + 11.432\beta$$

Structure II

Point group: C_2

Basic assumptions:

$$\alpha_1 = \alpha_5 = \alpha_c + 2\beta$$

$$\beta_{ij} = S_{ij}\beta = \beta, \text{ if } i \text{ and } j \text{ are neighboring atoms.}$$

Energy levels:

$$\text{Energy} = \alpha + \beta x$$

$$x = -2.562, -2.414, -1.000, 0.414 \text{ and } 1.44.$$

Eigenvectors:

$$x = -2.562 \quad \psi_A = 0.595\phi_1 + 0.334\phi_2 + 0.261\phi_3 + 0.334\phi_4 + 0.595\phi_5$$

$$x = -2.414 \quad \psi_B = 0.653\phi_1 + 0.271\phi_2 - 0.271\phi_4 - 0.653\phi_5$$

$$x = -1.000 \quad \phi_C = 0.354\phi_1 - 0.354\phi_2 - 0.707\phi_3 - 0.354\phi_4 - 0.354\phi_5$$

$$x = 0.414 \quad \phi_D = 0.271\phi_1 - 0.653\phi_2 + 0.653\phi_4 - 0.271\phi_5$$

Number of electrons: 6

Number of atoms considered: 6

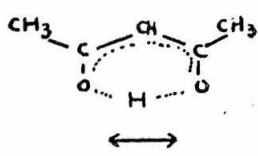
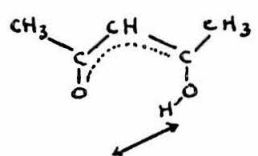
Total π electron energy:

$$6x + 2(2.562 + 2.414 + 1.00) = 6\alpha + 11.952\beta$$

It is very interesting to note that the total energy for the two structures is almost the same. From these calculations, it is not surprising that the two structures co-exist.

CONCLUSIONS

The intramolecular hydrogen bond in acetylacetone has been studied in detail. Our results suggest that there are two electronic structures for the enol form of acetylacetone. The difference between these two structures presumably arises from differences in the π -electronic distribution. Some properties of these two structures are shown in the following table.

Structure	Structure II	Structure I
		
Vibrational coord.		
Symmetry	C_{2v}	m
Zero point energy of normal acetylacetone	0	467 cm^{-1}
<hr style="border-top: 1px dashed black;"/>		
Relative population at room temperature	90.5%	9.5%
Zero point energy of deuterated acetylacetone	0	300 cm^{-1}
<hr style="border-top: 1px dashed black;"/>		
Relative population at room temperature	80.8%	19.2%
<hr style="border-top: 1px solid black;"/>		
The chemical shift of the bridge hydrogen at room temperature (ppm downfield from the enol form methyl group)	14.21	7.30

REFERENCES

1. L. W. Reeves, Can. J. Chem. 35, 1351 (1957).
2. W. G. Schneider and L. W. Reeves, Annals, N. Y. Acad. Sci., 70, 858 (1958).
3. H. S. Jarrett, M. S. Sadler, and J. N. Shoolery, J. Chem. Phys. 21, 2092 (1953).
4. B. N. Bhar, Arkiv Kemi 10, 223 (1956).
5. B. N. Bhar, and G. Lindström, J. Chem. Phys. 23, 1958 (1955).
6. B. N. Bhar, W. Forsling, and G. Lindström, Arkiv Fys. 10, 59 (1956).
7. F. J. B. Calleja, Compt. Rend. 249, 1102 (1959).
8. J. W. Emsley, J. Feeney, and L. H. Sutcliffe, High Resolution Nuclear Magnetic Resonance Spectroscopy, Pergamon Press, 1965.
9. R. Mecke and E. Funck, Zeit. Electrochemie 60, 1124 (1956).
10. S. I. Chan and B. M. Fung, to be published.
11. P. Diehl and T. Leipert, Helv. Chim. Acta 47, 545 (1964).
12. D. Hadži (ed). Hydrogen Bonding, Pergamon Press (1959).
13. G. C. Pimentel and A. L. McClellan, The Hydrogen Bond, W. H. Freeman and Co. (1960).
14. C. Y. Liang, E. J. Schimitschek, D. H. Stephens, and J. A. Trias, J. Chem. Phys. 46, 1588 (1967).

15. S. I. Chan, D. Stelman, and L. E. Thompson, J. Chem. Phys. 41, 2828 (1964).

PROPOSITIONS

Proposition I

It is proposed that for organic molecular crystals there may be a relationship between the thermal energy gap derived from the conductivity measurements and the energy gap between the highest occupied molecular orbital and the lowest unoccupied molecular orbital calculated from the HMO theory.

Proposition II

A very interesting property about the spacing of the energy levels in the HMO calculations was found. It can be proved mathematically that for a conjugated organic compound, (1) the average spacing of energy levels becomes smaller when the number of molecular orbitals is increased, and (2) the average spacing of energy levels becomes larger when the number of rings in the system is increased.

Proposition III

It is proposed that:

(1) The amounts of ionic character of AB type (B the halogen atom) molecules with electronegativity X_A (atom A) and X_B (atom B) are given by

$$m(X_A - X_B) + b$$

where m and b are constants and depend upon the cation only.

(2) The amount of ionic character of alkali metal halides are given by

$$(0.97X_A - 0.72)(X_B - X_A) - 2.27 X_A + 2.24$$

Proposition IV

An empirical equation similar to Badger's formula for the calculation of bond bending force constants is proposed. It is found that the value δ/l_1l_2 (where δ is the bond bending force constant and l_1 and l_2 are the length of the two edges of the angle) is directly proportional to the electronegativity and inversely proportional to the covalent radius of the central atom.

Proposition V

It is proposed that the equation $\log K = \log K_0 + aP + bP^2$ (where K and K_0 are the reaction rates at pressure P and 1 atm, a and b are constants) will probably give a better relationship between pressure and the reaction rate than the equation proposed by Benson and Berson.

PROPOSITION I

It has been found for a long time that certain types of organic crystals exhibit a weak form of semiconductivity. This continues to be actively and successfully explored (1). More recently, some quite spectacular conductivity has been found in some of the charge transfer complexes of the TCNQ types (2). The conductivity of these types of compounds approaches that of some of the metals. The present state of organic semiconductors is comparable to that of inorganic research in the 1930's. The greatest barrier toward advancement in this field lies in the lack of understanding of the mechanism by which conduction occurs in organic substances.

The most acceptable conducting mechanism in molecular crystal was proposed by Eley (3). This model is explained schematically in Fig. 1. Eley's model is quite similar to the band model in the inorganic solid.

From band theory of solid it is clear that the smaller the gap between the highest occupied orbital and the lowest unoccupied orbital the easier the solid will conduct current. Therefore, the conductivity and the energy gap are quite related.

In free electron gas models the energy gap of n electron system (3) is

$$\frac{h^2}{8ma^2} (n + 1) \quad \text{for an open path, length } a \quad (1)$$

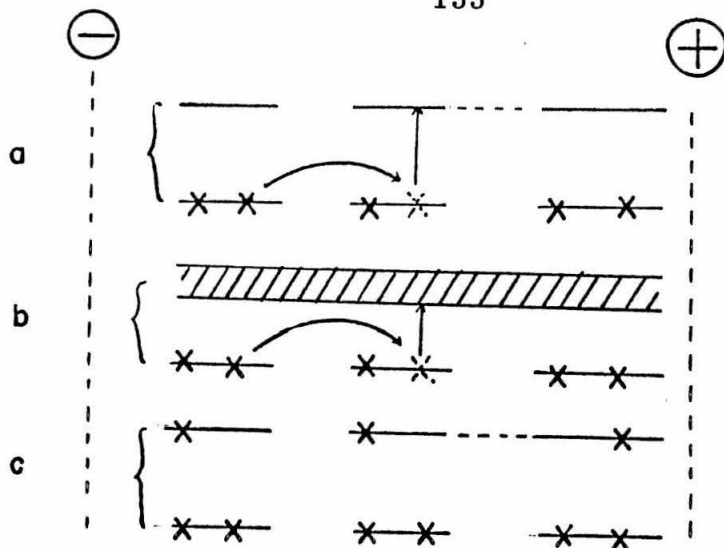


Figure 1. An electron can only move into an energy level which already contains less than two electrons. In fig. 1a an electron denoted by a cross received energy $\Delta\epsilon$ to excite it to an upper $(n/2 + 1)$ th level from which it can pass (dotted arrow) to the next molecule. The empty space set free in the lower $(n/2)$ th level is taken up by an electron from the next molecule. In fig. 1b the interaction between the excited $(n/2 + 1)$ th states in the neighboring molecules broadens the upper level into a band, hence lowering the energy gap $\Delta\epsilon$. In 1c, a solid free radical, the electron can pass directly (dotted line) into the corresponding level of the next molecule (3).

$$\frac{h^2}{4ma^2} n \quad \text{for a close circular path of circumference } a \quad (2)$$

Eley (3) assumed that for ordinary $n\pi$ -electron system the energy gap is between these values calculated from equation 1 and equation 2. A correlation of the thermal energy gap determined by conductivity measurements and the number of π electrons is shown in Fig. 2. Beyond this correlation there is apparently no further attempt made to calculate the thermal energy gap theoretically (2).

Hückel molecular orbital theory has been well developed. There are many applications of this method. The applicability of this method to the area of organic semiconductors has not been explored. It seems very desirable to correlate the thermal energy gap determined from the conductivity measurements and the energy gap calculated from the molecular orbital theory.

This proposition is an attempt to study the thermal energy gap for various molecular crystals from HMO point of view. Unfortunately, there are only few compounds where both the HMO calculation and the thermal energy gap measurements were carried out. Data of eight compounds are collected. They are shown in Table I. From Table I it is clear that the agreement between the energy gap calculated from the HMO theory and the conductivity measurement is very good. The agreement may be better if other factors are considered. However, this made the calculation more complicated. At present it seems a simple replacement of the electron gas model with the simple HMO calculation is ideal. More calculation of HMO

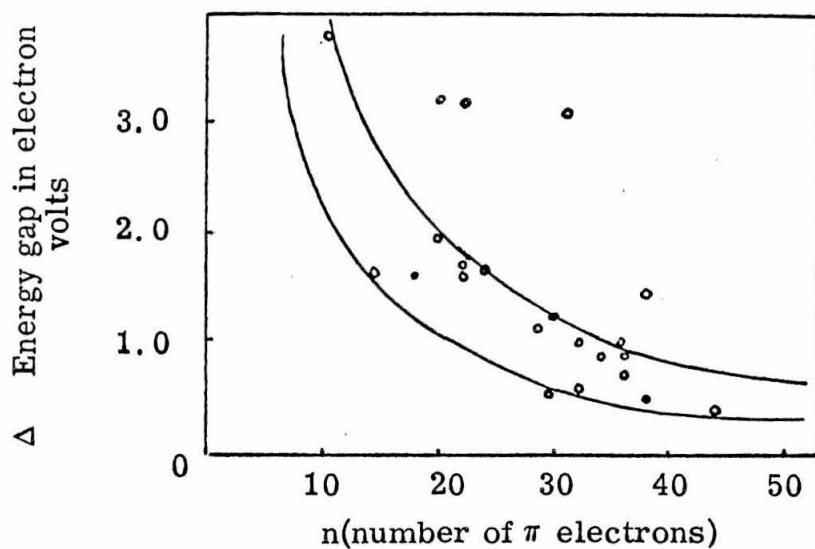


Figure 2. A correlation of thermal energy-gap determined by conductivity measurements and the calculated values on electron gas theory.
 Lower curve: for an open conjugation path;
 Upper curve: for a closed conjugation path or ring (3).

TABLE I

Compound	Energy gap calculated from the HMO theory ^a	Thermal energy gap ^b derived from the conductivity measurements
Perylene	1.75 ^c	1.9-2.0 ^c
Pyrene	2.25	2.02-2.4
Pyrunthrene	1.30	1.07
Anthanthrene	1.45	1.67
Pentacene	1.1	1.5
Meso-naphtho- dianthrene	0.9	1.2-1.48
Ovalene	1.6	1.13-2.0
Coronene	2.5	2.3

^areference 4 and reference 5 ($\beta \sim 2.5$ ev)

^breference 2

^cin units of ev

for heterogeneous molecules seems desirable. The results of these calculations may prove to be very fruitful. It is believed that a more detailed study of the relationship between the HMO results and the value derived from the conductivity measurements may give some very valuable information about the conducting mechanism in the metal free molecule crystals.

REFERENCES

1. N. W. Tschoegl, A. Rembaum, Research Proposal to the NASA, 1967.
2. F. Gutmann and L. E. Lyons, Organic Semiconductors, John Wiley & Sons, Inc., New York, 1967.
3. D. D. Eley and G. D. Parfitt, Trans. Faraday Soc. 51, 1529
4. A. Streitwieser, Jr. and J. I. Brauman, Supplemental Tables of Molecular Orbital Calculations, Pergamon Press, Inc., 1965.
5. A. Streitwieser, Jr., Molecular Orbital Theory, John Wiley & Sons, Inc., p. 208-217, 1961.

PROPOSITION II

As shown in proposition IV, it seems very probable that one can deduce some very valuable information about the thermo energy gap from the spacing between the lowest unoccupied molecular orbital and the highest occupied molecular orbital. The purpose of this proposition is to find some general information about these spacings from the Hückel molecular orbital calculations. As it will be shown later, it can be proved mathematically that for a conjugate organic compound

- (1) The average spacing of energy levels calculated from the HMO calculations becomes smaller when the number of molecular orbitals is increased.
- (2) The average spacing of energy levels becomes larger when the number of rings in the system is increased.

From these two conclusions, it is suggested that if the band theory is applicable in the organic semiconductors, the long open chain polymers will probably give better electric conductivity than others.

In HMO calculations, if there are n orbitals the polynomial expanded from the secular determinant generally has the form:

$$x^n + a_1x^{n-1} + a_2x^{n-2} + a_3x^{n-3} \dots$$

The highest order in the polynomial is n and the coefficient of the x^n term is 1. In general it is very tedious to expand the secular

determinant. Several methods have been developed in an effort to simplify this computational problem (1-5). Heilbronner (1) has shown how the secular polynomials for a complex system may be derived from those of component parts. If K_n , K_{n-1} , and K_{n-2} are the secular polynomial for chain of n , $n-1$, and $n-2$ atoms respectively, then

$$K_n = x K_{n-1} - K_{n-2} \quad (1)$$

and if R_n is the polynomial for a ring of n atoms, then

$$R_n = K_n - K_{n-2} - 2(-1)^n \quad (2)$$

It will show later some very interesting properties about the energy levels that can be derived from these two recruiting equations.

The secular polynomial of a chain of n atoms

In general one can express the secular polynomial in the following way:

$$K_n = x^n + a_1 x^{n-1} + a_2 x^{n-2} + a_3 x^{n-3} + \dots \quad (3)$$

for the case of $n = 2$, and $n = 3$

$$K_2 = x^2 - 1 \quad (4)$$

$$K_3 = x^3 - 2x \quad (5)$$

It is very interesting to note from equations 4 and 5 that in the secular polynomials a_1 is always zero and a_2 is always equal to $n-1$. As we

shall show, this is also true for the case of K_n .

$$\text{If } K_{n-2} = x^{n-2} - (n-2)x^{n-4} + \dots \quad (6)$$

$$K_{n-1} = x^{n-1} - (n-1)x^{n-3} + \dots \quad (7)$$

then from equation 1 it can be proved that:

$$\begin{aligned} K_n &= xK_{n-1} - K_{n-2} \\ &= x[x^{n-1} - (n-1)x^{n-3}] - x^{n-2} \dots \\ &= x^n - (n-1)x^{n-2} \dots \end{aligned} \quad (8)$$

Thus we have proved that the secular polynomial of a chain of n atoms is $x^n - (n-1)x^{n-2} + \dots$

The secular polynomial of a system which has n atoms and m rings

From equation 2, it is clearly seen that any time a ring is formed the coefficient of x^{n-2} in the secular polynomial decreases by 1. Therefore, the secular polynomial of a system which has n atoms and m rings is

$$R_n^m = x^n - (n-1+m)x^{n-2} \dots$$

The average spacing of the energy levels

If one denotes the root of the following equation

$$K_n = x^n + a_1x^{n-1} + a_2x^{n-2} \dots = 0$$

as $x_1, x_2, x_3, \dots, x_i, \dots, x_n$, then

$$\sum_i x_i = a_1$$

$$\sum_{\substack{i,j \\ i \neq j}} x_i x_j = a_2$$

Since $a_1 = 0$

therefore $\sum x_i = 0$

$$x_j \sum x_i = 0$$

$$\sum_{i,j} x_i x_j = 0$$

$$\sum_i x_i^2 + \sum_{\substack{i,j \\ i \neq j}} x_i x_j = 0$$

therefore $\sum_i x_i^2 = - \sum_{\substack{i,j \\ i \neq j}} x_i x_j = -a_2$

$$= (n-1-M) \quad (8)$$

where n is the number of atoms in the system and m is the number of rings in the system.

It is well-known that x_i is also the i^{th} energy level in the molecular orbitals calculations. The average spacing of energy levels can generally be approximated by

$$\sum_i x_i^2 / n^2,$$

that is, the average spacing $\propto \frac{\sum x_i^2}{n^2}$

$$\propto \frac{(n - 1 + R)}{n^2} \quad (10)$$

From equation 10 it is concluded that the average spacing will be the smallest for these open-chain polymers.

REFERENCES

1. E. Heilbronner, *Helv. Chim. Acta* 36, 170 (1953).
2. I. Samuel, *Compt. rend.* 238, 2422 (1954).
3. T. H. Goodwin and V. Vand, *J. Chem. Soc.* 1683, 1955.
4. H. H. Günthard and H. Primas, *Helv. Chim. Acta*, 39, 1645 (1956).
5. A. Streitwieser, Jr., *Molecular Orbital Theory*, John Wiley & Sons, Inc., 1961.

PROPOSITION III

It is proposed that:

- (1) The amounts of ionic character* of AB type (B the halogen) molecules with electronegativity X_A (atom A) and X_B (atom B) are given by⁺

$$m(X_A - X_B) + b \quad (1)$$

where m and b are constants and depend upon the cation only.

- (2) The amounts of ionic character of alkali halides are given by⁺

$$(0.97X_A - 0.72)(X_B - X_A) - 2.27X_A + 2.24 \quad (2)$$

Pauling (1) related the ionic character of a single bond between two atoms A and B with electronegativity X_A , X_B , respectively by the equation

$$\text{Amount of ionic character} = 1 - \exp[-0.25(X_A - X_B)^2] \quad (3)$$

According to this equation H^F has 60% ionic character, but the value calculated from dipole moment is 45%. Hannay and Smyth (2) proposed the equation

$$\% \text{ ionic character} = 16(X_A - X_B) + 3.5(X_A - X_B)^2$$

which holds for hydrogen halides only. Oskan E. Polansky and

G. Derflinger (3) proposed another equation

$$\text{Amount of ionic character} = \frac{X_A - X_B}{X_A + X_B} \quad (4)$$

The amounts of ionic character of alkali halides and hydrogen halides calculated from equation 3 are listed under column I_3 in Table I.

The amounts of ionic character of alkali halides and hydrogen halides calculated from equation 4 are listed under I_4 in Table I. Experimental values of dipole moment and amount of ionic character calculated from these dipole moments* are listed in Table I under columns 2 and 5 respectively. Comparing the values between columns 5 and I_3 , 5 and I_4 in Table I indicates that both equation 3 and 4 are not satisfactory.

Figure 1⁺⁺ shows a plot of percentage ionic character vs. ΔX (difference in electronegativity) for various alkali halides and hydrogen halides. If one connects all the points for the same cation together, a straight line is always obtained. Based on this, equation 1 is proposed. The parameters m and b for each cation were calculated by a least squares method. The amounts of ionic character of compounds calculated from equation 1 are listed in Table I under the column I_1 . The agreement is excellent (average error 0.6%).

The second object of this proposition is to try to find a simple general equation which gives the amounts of ionic character of any alkali halides from the electronegativity of the two atoms involved. Such an equation is found (equation 2). The amounts of ionic character

TABLE I

Compound	Obs. dipole moment		d in Å	ΔX	% ionic	I ₁	I ₂	I ₃	I ₄
LiF			1.452	3.0	90.8 ⁺⁺	90.5	93		
LiCl			2.013	2.0		66.0	68		
LiBr	6.19	0.15	2.170	1.8	59.5	60.6	61	55	47
LiI	6.25	0.20	2.392	1.5	54.5	53.5	55	44	43
NaF			1.799	3.1			89		
NaCl	8.5	0.4	2.361	2.1	75.0		73	66	54
NaBr			2.502	1.9			70		
NaI			2.712	1.6			65		
KF	8.62		2.105	3.2	85.2	85.2	82	92	67
KCl	10.0 ^{**}		2.667	2.2	78.4	78.6	77	70	58
KBr	10.60 ^{***}		2.821	2.0	77.8	77.4	75	63	56
KI	11.05		3.048	1.7	75.5	75.5	74	51	52
CsF	7.87		2.345	3.3	69.9	70.0	72	94	70
CsCl	14.40		2.906	2.4	74.5	73.9	75	75	62
CsBr			3.072	2.1		71.3	77		
CsI	12.1		3.315	1.8	76.0	76.0	78	55	56
HF	1.91 [*]		0.926 ⁺	1.9	43.0	43.2		59	30
HCl	1.08 [*]		1.284 ⁺	0.9	17.5	17.2		19	18
HBr	0.79 [*]		1.423 ⁺	0.7	11.6	12.1		12	14
HI	0.38 [*]		1.615 ⁺	0.4	4.9	4.4		4	9

Data taken from reference 5 unless specified.

** Take average value of 9.53 (reference 7) and 10.48 (reference 5)

*** Take average value of 10.8 (reference 7) and 10.4 (reference 5)

*, +, and ++ indicate data are taken from reference 4, 6, and 1 respectively.

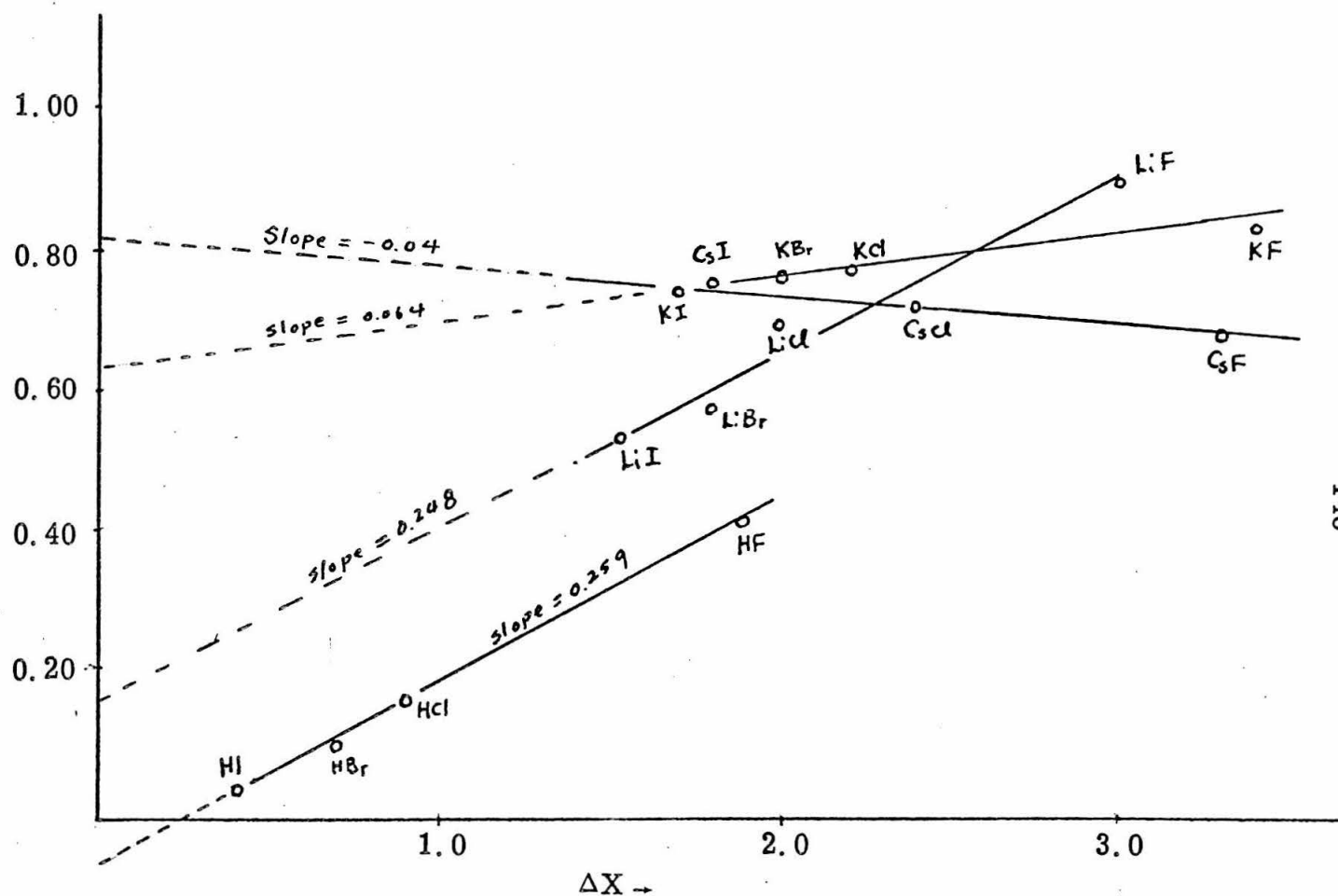


Figure 1. Curves relating the amount of ionic character of a bond to the electronegativity difference of the two atoms. Experimental points, based upon observed values of the electric dipole moment of diatomic molecules, are shown for 15 compounds.

of alkali halides calculated by this equation are listed in Table I under the column I_2 .

*The amount of ionic character (y), bond length (d), dipole moment (μ), and the charge of an electron (e) are related by the following equation (1).

$$\mu = y e d$$

⁺These equations obviously hold only in the range where experimental points exist and can not be extrapolated to all ΔX values.

⁺⁺In Fig. 1 the straight lines are extrapolated to $\Delta X = 0$. The purpose of this is only to show the intercepts and the slopes of the experimental straight lines. It does not imply that equations 1 and 2 hold when $\Delta X = 0$.

REFERENCES

1. L. Pauling, The Nature of the Chemical Bond, Cornell University Press, Ithaca, New York, 3rd ed., 1960.
2. N. B. Hannay, and C. P. Smyth, J. Am. Chem. Soc. 68, 171, (1946).
3. O. E. Polansky, and G. Derflinger, Theoret. Chem. Acta 1 (4), 308-15 (1963).
4. A. F. Wells, Structure Inorganic Chemistry, Oxford University Press, London, p. 254, 1962.
5. A. Honog, M. Mandel, M. L. Stitch, and C. H. Townes, Phys. Rev. 96, 629 (1954).
6. T. L. Comell, The Strengths of Chemical Bonds, Academic Press, 1954.
7. L. A. Murray, Jr., W. H. Rodebush, and M. E. Bixler, J. Chem. Phys. 4, 372 (1936).

PROPOSITION IV

According to the valence force theory the internal potential energy of a molecule can be calculated approximately by the equation

$$2v = \sum_i k_i Q_i^2 + \sum_j \delta_j \alpha_j^2 \quad i, j = 1, 2, 3 \dots$$

where Q_i is the change of the i th bond length and α_j the change of the j th bond angle, k_i and δ_j are the stretching and bending force constants of the i th bond length and j th bond angle respectively. The bond stretching force constants can be calculated from the well-known Badger formula (1). There is as yet no way to predict the bond bending force constants.

Some values of $\delta/l_1 l_2$ (where δ is the bond bending force constant, l_1, l_2 are the length of the two edges of the angle) are listed in Table I. A simple equation similar to Badger's formula for the bond bending force constants cannot be obtained. But if we define a parameter y_A for each atom by the equation

$$y_A = \frac{X_A}{r_A^2}$$

where

X_A = the electronegativity of atom A

r_A = the covalent radius of appropriate
multiplicity for atom A

then some quite interesting relations between y values are found.

TABLE I

Atom	$y^{\#}$	Bond	Compound	$\left(\frac{\delta^*}{l_1 l_2}\right)_{\text{exp}}$	$\left(\frac{\delta}{l_1 l_2}\right)_{\text{cal}}$
-F	4.7	H-C-H	CH ₄	0.46	0.47
-Cl	3.0	F-C-F	CF ₄	0.71	0.71
-Br	2.6	Cl-C-Cl	CCl ₄	0.33	0.29
-I	2.2	Br-C-Br	CBr ₄	0.24	0.22
-O	4.0	H-C-F	CH ₃ F	0.57	0.58
=O	4.5	H-C-Cl	CH ₃ Cl	0.36	0.37
-S	2.5	H-C-Br	CH ₃ Br	0.30	0.32
=S	2.7	H-C-I	CH ₃ I	0.23	0.26
-N	3.6				
=N	3.8	H-C≡N	HCN	0.20	0.23
≡N	4.1	Cl-C≡N	ClCN	0.20	0.18
-H	3.8	Br-C≡N	BrCN	0.17	0.16
-C	2.9	I-C≡N	ICN	0.12	0.13
=C	3.1	P-C≡N			0.12
≡C	3.1	As-C≡N			0.11
-As	1.8	Se-C≡N			0.13
-P	2.0	S-C≡N			0.13
-B	2.2				
-Se	2.3	F-B-F	BF ₃	0.37	0.39
		Cl-B-Cl	BCl ₃	0.16	0.16
		Br-B-Br	BBr ₃	0.13	0.12
		H-O-H	H ₂ O	0.69	
		H-S-H	H ₂ S	0.43	
		H-N-H	NH ₃	0.4-0.5	
		H-P-H	PH ₃	0.33	
		F-O-F	F ₂ O	0.69	
		Cl-O-Cl	Cl ₂ O	0.41	
		O-C-O	C ₂ O	0.57	
		S=C=S	CS ₂	0.23	

Table I footnotes

Values of x and r are taken from reference 7.

*Data are taken from reference 8.

- (i) Qualitatively, if $y_A > y_{A'}$, then the values of $\delta/l_1 l_2$ for bonds $A \sim B \sim C$ and $B \sim A \sim C$ are greater than the values of bonds $A' \sim B \sim C$ and $B \sim A' \sim C$ respectively. (The symbol \sim indicates single, double, or triple bond.) The y values of 13 elements and bond bending force constants for 27 bonds are listed in Table I.
- (ii) Quantitatively, the ratio of the bond bending force constants for similar types of bond $A' - B - C$ and $A' - B - C'$ or $A' - B \equiv C$ and $A' - B \equiv C$ is approximately equal to

$$\frac{y_A y_C}{y_{A'} y_{C'}}$$

that is,
$$\frac{\delta_{ABC}}{l_1 l_2} = y_A y_C \cdot C_B$$

where C_B is a constant. Some $\delta/l_1 l_2$ values calculated from equation 1 are listed in Table I under the column

$$\left(\frac{\delta}{l_1 l_2} \right)_{\text{cal}}$$

According to statements i and ii above, it is predicted that all these bond $A - C \equiv N$ where A is As, P, Se, or S have a low value of bond bending force constant, i. e., those bonds are easily bent. X-ray diffraction data show that this is true. ⁺

Another application of equation 1 is that one can use it to get some information of the crystal structure. For example, $\text{Se}(\text{SeCN})_2$ and $\text{Se}(\text{SCN})_2$ are isomorphic. Since the y value of S and Se are approximately equal and the bond $\text{Se}-\text{C}\equiv\text{N}$ is bent 16° (2) it is predicted that the bond $\text{S}-\text{C}\equiv\text{N}$ in the structure $\text{Se}(\text{SCN})_2$ will be bent. Careful studies of the model of Ohlberg and Vaughan for $\text{Se}(\text{SCN})_2$ (3) show that the van der Waals distances between N and S and N and Se are too short⁺⁺ and bending of the bond $\text{S}-\text{C}\equiv\text{N}$, as suggested, will lengthen the above two van der Waals distances and reduce the repulsive forces between N and S and Se and N.

⁺The following values of the bond angle A C N have been obtained by the x-ray diffraction method. $\text{As}-\text{C}\equiv\text{N}=170^\circ$ in $\text{As}(\text{CN})_3$ (4), $\text{P}-\text{C}\equiv\text{N}=172^\circ$ in $\text{P}(\text{CN})_3$ (5), $\text{Se}-\text{C}\equiv\text{N}=164^\circ$ in $\text{Se}(\text{SCN})_2$ (2), $\text{S}-\text{C}\equiv\text{N}=163^\circ$ in $[\text{Hg}(\text{SCN})_4][\text{Cu}(\text{en})_2]$ (6).

⁺⁺According to the model of Ohlberg and Vaughan the observed van der Waals distances between N and S and N and Se are 2.89 and 3.03 Å respectively. The van der Waals radii of Se, S, and N as given by Pauling (7) are 2.0, 1.85, and 1.5 Å respectively which correspond to the van der Waals bond distances between N and S and N and Se 3.35 and 3.5 Å respectively.

REFERENCES

1. R. M. Badger, J. Chem. Phys. 3, 710 (1935).
2. O. Aksness and O. Foss, Acta Chem. Scand. 8, No. 10, 1187 (1954).
3. S. M. Ohlberg and P. A. Vaughan, J. Am. Chem. Soc. 76, 2649 (1954).
4. K. Emerson and B. Britton, Acta Cryst. 16, 113 (1963).
5. K. Emerson and B. Britton, Acta Cryst. 17, 1134 (1964).
6. H. Scouloudi, Acta Cryst. 6, 651 (1953).
7. L. Pauling, The Nature of the Chemical Bond, Cornell University Press, Ithaca, New York, 3rd ed., 1960.
8. E. B. Wilson, Jr., J. C. Decius, and P. C. Cross, Molecular Vibrations, McGraw-Hill Book Co. Inc., 1955.

PROPOSITION V

It is proposed that the equation $\log K = \log K_0 + aP + bP^2$ (where K and K_0 are the reaction rates at pressure P and 1 atm., a and b are constants) will probably give a better relationship between pressure and the reaction rate than the equation proposed by Benson and Berson (1) (equation 1 below).

Benson and Berson proposed that the reaction rate and the pressure can be related by the following equation:

$$\frac{\log K/K_0}{P} = A + DP^{0.523} \quad (1)$$

where A and D are constants.

A plot of $\frac{\log K/K_0}{P}$ vs. $P^{0.523}$ for the decomposition of azo-bis-isobutyronitrile in the solvent toluene in the presence of iodine at 62.5° is shown in Fig. 1. A similar plot of the Diel-Alder dimerization of isoprene in bulk at 60° is shown in Fig. 2. Both figures show that equation 1 is not satisfactory.

A brief description of Benson and Berson's work is as following: Assuming that the Tait equation holds (2),

$$V_u^P = V_u^0 \left[1 - C_u \log \left(1 + \frac{P}{B_u} \right) \right] \quad (2)$$

where u can be 1, 2, \dots and t (1 implies reactant 1, 2 implies reactant 2, \dots and t implies the transition state), c_u and B_u are constants

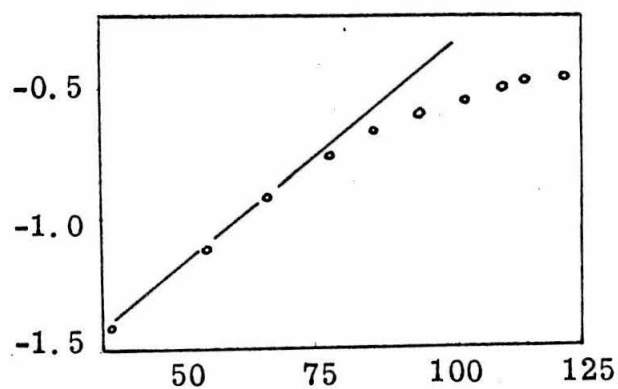


Figure 1. Decomposition of azo-bis-isobutyronitrile in solvent toluene in the presence of iodine at 62.5° (1).

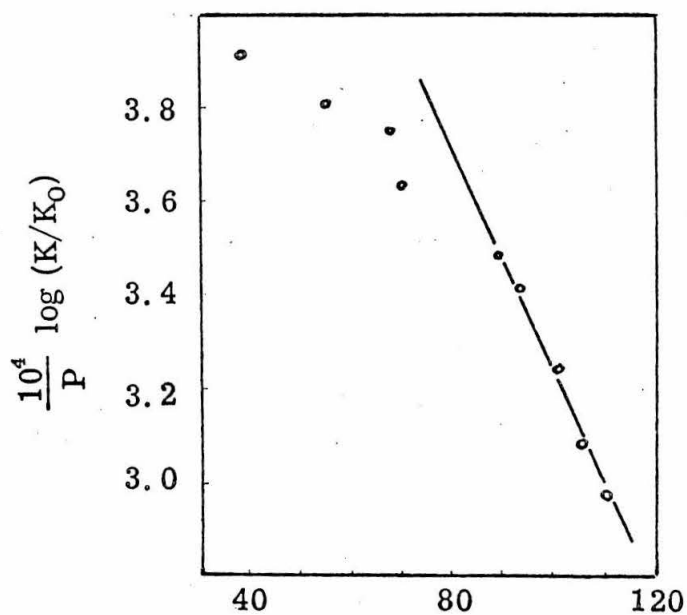


Figure 2. Diels-Alder dimerization of isoprene in bulk at 60° (3).

for non-ionic system

$$-RT \left(\frac{\delta \ln K}{\delta P} \right)_T = \Delta V^\ddagger = V_t^P - \sum_r V_r^P \quad (3)$$

where V_u^P = partial molar volume of component u at pressure P

V_u^0 = partial molar volume of component u at 1 atm.

Equations 2 and 3 can then be combined to give

$$-RT \left(\frac{\delta \ln K}{\delta P} \right)_T = (V_t^0 - \sum V_r^0) - \frac{C_t V_t^0}{2.3} \ln \left(1 + \frac{P}{B_t} \right) + \sum_r \left[\frac{C_r V_r}{2.3} \ln \left(1 + \frac{P}{B_r} \right) \right] \quad (4)$$

Integration of 4 gives (assuming all the constants C_u are the same and are independent of the pressure)

$$\frac{\log K^P/K^0}{P} = \frac{-\Delta V^{\ddagger 0}}{2.3 RT} - \frac{C}{2.3 RT} \left[\sum_r V_r^0 T(X_r) - T_t^0 T(X_t) \right] \quad (5)$$

$$T(x_u) = \left(\frac{1}{X_u} + 1 \right) \log(1 + x_u) - 0.4343 \quad (6)$$

$$X_u = P/B_u$$

In the range $2 < X < 16$, $T(X)$ can be approximated by the following equation:

$$T(X) = 0.2 X^{0.523} + 0.008 \quad (7)$$

Equations 5 and 7 can then be combined to give equation 1

$$\begin{aligned} \frac{\log K^P/K^0}{P} &= -\frac{\Delta V_0^\#}{2.3} (1 - 0.008 C) \\ &\quad - \left\{ \frac{r}{2.3RT} \left[V_1^0 B_1^{2.523} + V_2^0 B_2^{0.323} - V_t B_t^{0.323} \right] \right\} P^{0.523} \quad (8) \\ &= A + DP^{0.523} \quad (1) \end{aligned}$$

The validity of equation 7 is based upon the value X , not P . Table I in Benson and Berson's work shows that constant B is very sensitive to the temperature and its values cover a range from 160 Kg/cm² to 1340 Kg/cm². A serious error will be introduced when the values of B , say B_1 , B_2 , and B_t , are not approximately equal. The following table shows that if a system has three components 1, 2 and t with $B_1 = 300$ Kg/cm², $B_2 = 500$ Kg/cm² and $B_t = 1000$ Kg/cm² then the region of pressure in which equation 7 is applicable to all three components is 2000-4800 Kg/cm². It is not the region 1000-16000 Kg/cm² as proposed by Berson and Benson. Therefore, the range of pressure to which equation 1 is applicable is severely restricted.

Component	B	Value of P when X=2	Value of P when X=16	Range of P to which eq. 7 is applicable
1	300	600	4800	600-4800
2	500	1000	8000	1000-8000
t	1000	2000	16000	2000-16000

Besides, even in this region each component in equation 9 may have an error of 0-6%. The sum of them may go up to as high as 18%.

There are also two possible errors in the derivation of equation 1. The Tait equation may not be accurate enough and the constants C_u in the Tait equation may not be equal. Since so many possible errors occur in equation 1, it is better to choose a simple equation in the form of $\log K = \log K_0 + aP + bP^2$ to substitute for it. A plot of $\log K$ vs. $0.62 + 0.647 P - 0.02 P^2$ for the Diels-Alder dimerization of isoprene at 60° is shown in Fig. 3. The fitting is much better.

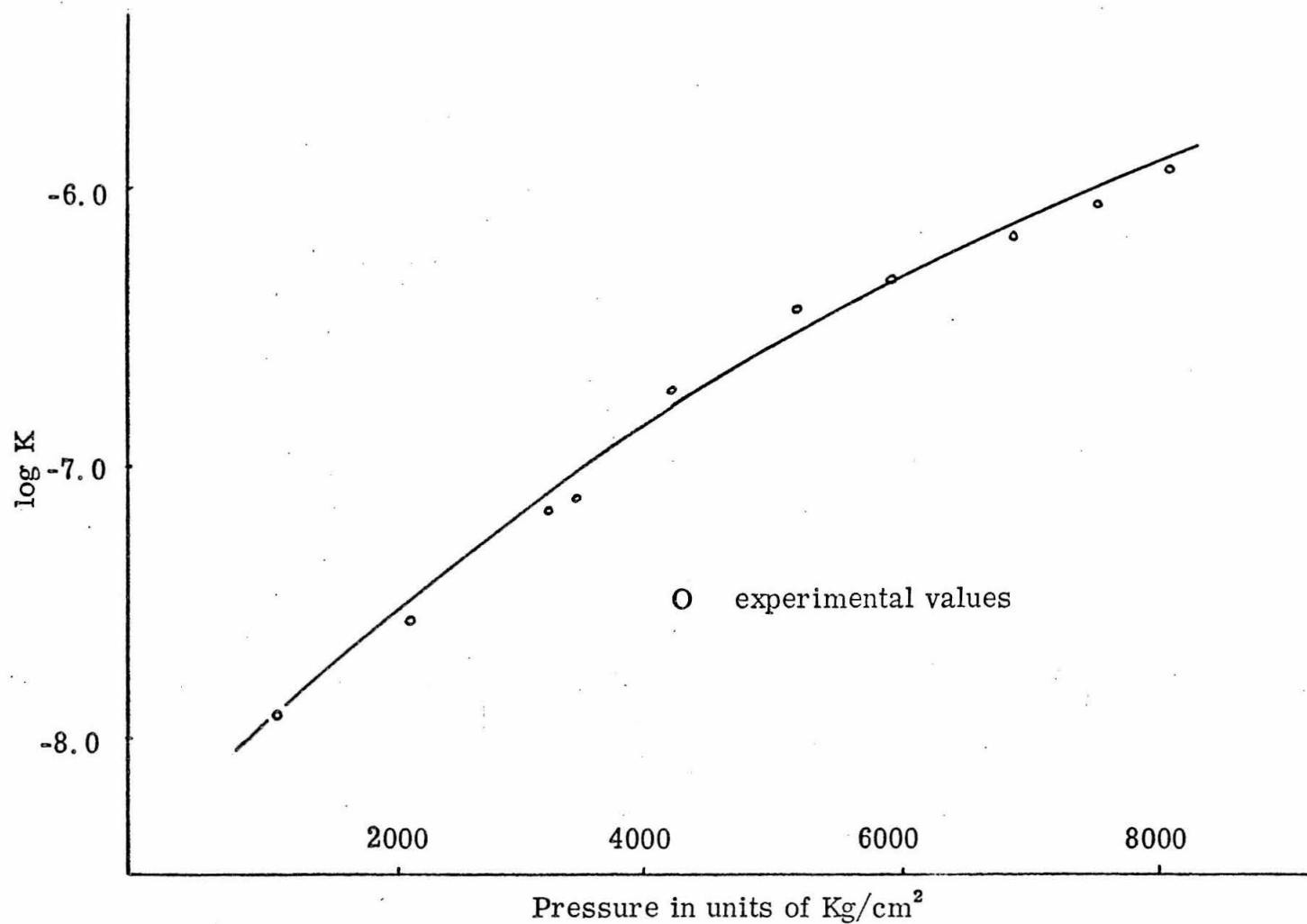


Figure 3. Diels-Alder dimerization of isoprene in bulk at 60°
(Data are taken from reference 3)

REFERENCES

1. S. W. Benson and J. A. Berson, J. Am. Chem. Soc. 84, 152 (1961).
2. H. S. Harned and B. B. Owen, The Physical Chemistry of Electrolytic Solutions, 3rd ed., Reinhold Publishing Corp., New York, N. Y., p. 379, 1958.
3. C. Walling and J. Peisach, J. Am. Chem. Soc. 80, 5819 (1958).